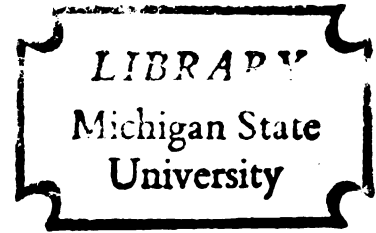


PART I
EFFECT OF PHONON AND ELECTRON-ELECTRON
INDUCED INTERBAND TRANSITIONS ON THE
THERMOPOWER OF THE
TRANSITION METALS

PART II
LATTICE DYNAMICS OF CRYSTALS WITH
MOLECULAR IMPURITY CENTERS

Thesis for the Degree of Ph. D.
MICHIGAN STATE UNIVERSITY

Hans Rudolf Fankhauser
1969



This is to certify that the
thesis entitled
EFFECT OF PHONON AND ELECTRON-ELECTRON INDUCED INTERBAND
TRANSITIONS ON THE THERMOPOWER OF THE TRANSITION METALS
LATTICE DYNAMICS OF CRYSTALS WITH MOLECULAR IMPURITY CENTERS
presented by

Hans Rudolf Fankhauser

has been accepted towards fulfillment
of the requirements for

Ph.D. degree in Physics


Major professor

Date July 28, 1969

ABSTRACT

PART I

EFFECT OF PHONON AND ELECTRON-ELECTRON INDUCED INTERBAND TRANSITIONS ON THE THERMOPOWER OF THE TRANSITION METALS

PART II

LATTICE DYNAMICS OF CRYSTALS WITH MOLECULAR IMPURITY CENTERS

By

Hans Rudolf Fankhauser

Part I:

Using a two-band model for the conduction electrons of the transition metals and assuming that only the lighter carriers contribute to charge transport the effects of phonon induced and electron-electron interband s-d transitions are investigated. Provided that the total thermopower - not including the phonon-drag contribution - is given by $S_T = \frac{1}{W_T} \sum_i W_i S_i$ we find that interband electron-electron scattering may manifest itself in the total thermopower at low as well as at high temperatures. At lowest temperatures (near $T/\theta_D = 0.03$), depending upon the magnitudes and temperature dependences of electron-electron and electron-phonon scattering contributions, a well defined extremum of the order of $1\mu V/^\circ K$ may appear. At high temperatures the total thermopower, weighted as indicated above, may be dominated by electron-electron scattering effects, and in that event, will exhibit a T^2 temperature dependence. The effect of the impurities are discussed and the theoretical total thermopower is compared with available experimental data.

Part II:

The use of symmetry properties results in a great saving of time and effort in the theoretical study of molecules and crystals and, frequently, the application of group theory leads to valuable qualitative conclusions. A group theoretical method to obtain the appropriate eigenvectors of the dynamical problem (normal modes) is presented in detail and compatibility conditions for the eigenvectors of the subgroups are derived in a number of important cases. As a first example of the practical value of symmetry arguments it is demonstrated that a study of the dependence of the infrared absorption on polarization relative to the crystallographic axes already leads to specific information on the orientation of a polyatomic molecule imbedded in a cubic crystal. In a second example we study the scattering of lattice waves by a stereoscopic defect molecule. We give a survey on the relevant aspects of lattice dynamics and show how the molecular coordinates are removed using the extended Green's function technique. A scattering formalism is developed and a formally exact solution of the scattering problem is given in terms of the T matrix. An expression for the differential cross section is derived. It contains two terms, the direct term and an interference term, which may be of the same order. The resonances in the scattering cross section are given by the resonances in the T matrix and conditions for such resonances to occur are briefly discussed. As a simple model a rigid sphere is coupled to a simple cubic lattice with tangential as well as radial springs. The eigenvalue problems are solved and the T matrix constructed. The form of the matrix

elements gives information on the possible initial and final states and on the acoustical activity of the possible modes. For a specific case we estimate the magnitude of the interference term due to a librational mode and the motion of the center-of-mass. Finally we replace the sphere by a rigid ellipsoid which reduces the symmetry at the defect site. The analysis of this case is restricted to librational modes only. We conclude with a discussion on what we might expect in a more realistic situation.

PART I

EFFECT OF PHONON AND ELECTRON-ELECTRON INDUCED INTERBAND
TRANSITIONS ON THE THERMOPOWER OF THE TRANSITION METALS

PART II

LATTICE DYNAMICS OF CRYSTALS WITH MOLECULAR IMPURITY CENTERS

By

Hans Rudolf Fankhauser

A THESIS

Submitted to
Michigan State University
in partial fulfillment of the requirements
for the degree of

DOCTOR OF PHILOSOPHY

Department of Physics

1969

Meinem unvergesslichen Vater

ACKNOWLEDGMENTS

I wish to express my sincere gratitude to Professor Frank J. Blatt for inviting me to complete my studies here at Michigan State University and for his help and encouragement throughout the course of this work.

The analysis reported in Part I was initiated by the author, who focused his attention on electron-electron scattering processes only, at the ETH, Zurich in 1964. Subsequently he and Dr. L. Colquitt, Jr. collaborated on an extension of this work so as to include phonon induced inter-band transitions. Many valuable and illuminating discussions with Dr. Colquitt are gratefully acknowledged.

Concerning the lattice dynamics aspect of Part II I benefitted to a large extent from many enlightening discussions with Dr. W.M. Hartmann.

For the financial support, I thank the National Science Foundation.

I should also like to thank Mrs. Marie E. Ross for the careful typing of the manuscript.

Last but not least I should like to express my deep appreciation to my dear wife Birgit for all the patience and moral support I got while I was completing this work.

TABLE OF CONTENTS

Part I: Section	Page
I. Introduction	1
II. Phonon Scattering	5
III. Electron-Electron Scattering	10
IV. Total Thermopower	16
V. Discussion	24
Appendix	31
References	35
Part II: Section	
I. Introduction	37
II. Use of group theory to determine the eigenvectors . . .	40
III. Compatibility conditions	57
IV. Application I - Linear Molecules	66
V. Application II - Stereoscopic Molecules	70
Lattice Dynamics	70
Scattering Formalism	74
Spherical Molecules	82
Ellipsoidal Molecules	100
VI. Disussion	109
References	115

TABLES

Table	Page
I. Stable subspaces of the full cubic group O_h , structure A	46
II. Stable subspaces of the subgroup D_{4h} , structure A . .	47
III. Stable subspaces of the subgroup D_{3d} , structure A . .	48
IV. Stable subspaces of the subgroup D_{2h} , structure A . .	49
V. Stable subspaces of the full cubic group O_h , structure B	50
VI. Stable subspaces of the subgroup T_d , structure B . . .	51
VII. Stable subspaces of the subgroup D_{3d} , structure B . .	52
VIII. Stable subspaces of the full cubic group O_h , structure C	53
IX. Stable subspaces of the subgroup D_{2h} , structure C . .	55
X. Compatibility conditions for the subgroup D_{4h} with the 4-fold rotation axis along the z-axis of the cube in case of structure A.	60
XI. Compatibility conditions for the subgroup D_{3d} with the 3-fold rotation axis along the [111]-direction of the cube in case of structure A.	61
XII. Compatibility conditions for the subgroup D_{2h} , with the 2-fold ζ -axis oriented along the [110]-direction of the cube in case of structure A.	62

TABLES (continued)

Table	Page
<p>XIII. Compatibility conditions for the stable subspaces which correspond to the representation according to which the infrared active modes transform in case of structure B and symmetry D_{3d}. The 3-fold rotation axis is oriented along the [111]-direction of the cube</p>	63
<p>XIV. Compatibility conditions for the stable subspaces which correspond to the representation according to which the infrared active modes transform in case of structure C and symmetry D_{2h}. The 2-fold ζ-axis is oriented along the [110]-direction of the cube.</p>	64

FIGURES

Part I:	Page
Figure 1. Theoretical total thermopower in the case of an inverted d-band, $\underline{k}_s < \underline{k}_d$, $m_d/m_s = 10$, for different gap parameter η	18
Figure 2. Theoretical total thermopower in the case of an inverted d-band, $\underline{k}_s < \underline{k}_d$, $m_d/m_s = 10$, $\eta = 0.1$. In the inset, the details of a local maximum - not to be confused with a phonon-drag peak - are shown. This extremum is associated with the exponential decay of phonon induced s-d transitions at very low temperatures.	19
Figure 3. Theoretical total thermopower in the case of an inverted d-band, $\underline{k}_s > \underline{k}_d$, $m_d/m_s = 10$, $\eta = 0.5$. In the inset, the details of a local minimum, due to electron-electron scattering effects, are shown.	21
Figure 4. Theoretical total thermopower in the case where the two bands have the same curvature, $\underline{k}_s < \underline{k}_d$, $\eta = 0.1$, for $m_d/m_s = 3, 10$	22
Figure 5. Experimental thermopower of some of the transition metals taken from N. Cusack and P. Kendall, Ref. 21.	25
Figure 6. Theoretical total thermopower in the case where the two bands have the same curvature $\underline{k}_s > \underline{k}_d$, $m_d/m_s = 3$, $\eta = 0.5$, for different values of the ratio R.	29

FIGURES (continued)

Part II:	Page
Figure 1a). simple cubic structure (A).	
Figure 1b). body-centered cubic structure (B).	
Figure 1c). face-centered cubic structure (C).	
<p>The heavy bonds indicate possible orientations of a linear molecule with the center-of-mass at the origin 41</p>	
Figure 2.	
<p>$1 - \omega^2 \epsilon g(0) ^{-2}$, which enters the scattering cross section of an isotope defect, as a function of the lattice wave frequency in the Debye approx- imation, taken from Thoma and Ludwig [37]. 97</p>	
Figure 3.	
<p>$t(F_{1g}) ^2$, which enters the scattering cross section of the librational mode, as a function of the square modulus of the lattice wave frequency in the Debye approximation, taken from Wagner [25]. 99</p>	

PART I

EFFECT OF PHONON AND ELECTRON-ELECTRON INDUCED INTERBAND
TRANSITIONS ON THE THERMOPOWER OF THE TRANSITION METALS

I. INTRODUCTION

Recently there has been a resurgence of interest in the low temperature resistivities of transition metals¹⁻⁴. Although it has been known for some time⁵ that the electrical resistivity, ρ , of some of the transition metals varies as T^2 at the lowest temperatures, concomitant linear variations in the thermal resistivities, W , have only recently been observed. The origin of the T^2 dependence of ρ is a problem of long standing. Although it was in 1937 that Baber⁶ proposed that electron-electron scattering was the cause for this variation, evidence to establish this proposal as valid has been slow in coming. Two of the major criticisms of Baber's proposal are:

- (a) ρ is observed to vary as T^2 in only a few of the transition metals rather than all of them as might be expected.
- (b) Experimentally it is found that electron-electron scattering contributes a T^2 term to ρ and consequently dominates the total resistivity at lowest temperatures where the contribution from phonon-scattering eventually varies as T^5 . Similarly at the highest temperatures where the lattice resistivity varies linearly with temperature the electron-electron scattering contribution should again be dominant. This latter behavior, however, has not been observed.

In a study on these problems Colquitt⁷ attempted to answer the first objection by a careful analysis of available experimental data. He

was able to show that one could give a consistent theoretical interpretation of the ideal resistivities of the transition metals in terms of a two band model and assuming (in all of the metals) the existence of a T^2 term which may, however, be masked to a greater or lesser degree by phonon scattering in different metals of the series.

Appel⁸ attempted to answer the second objection to electron-electron scattering by appealing to numerical estimates of the two resistivity contributions. He argues that in some metals the T^2 contribution will only "peak-through" the phonon contribution at extremely high temperatures - near or above the melting point.

With increasing evidence for and interest in e-e scattering in transition metals, it seemed appropriate to consider the effect of these scattering processes on another electron transport phenomenon, the thermoelectric power. The calculation has been carried forward within the framework of the two-band model introduced by Mott⁹ many years ago. Although the work assumes the "standard band structure" for the two bands, we have extended Mott's model somewhat by placing no a priori restriction on the curvatures of the bands; i.e., either the "s-band" or the "d-band" may be electron-like or hole-like. We also allow $\underline{k}_s > \underline{k}_d$ as well as $\underline{k}_s < \underline{k}_d$ where \underline{k}_s , \underline{k}_d are the Fermi wave vectors. Hence we consider four different situations, corresponding to two bands of identical or opposite curvature, with $\underline{k}_s > \underline{k}_d$ and $\underline{k}_s < \underline{k}_d$. The subscripts s and d in this paper are used simply to denote a light mass, conduction band and a high mass, narrow band, respectively.

As we shall see, it is not possible to classify the results uniquely in terms of the above-mentioned four possibilities since two other

parameters, the effective mass ratio m_d/m_s and the "momentum gap" η defined by Eq. (6) which was introduced by Colquitt⁷ have a profound effect on the results.

In most situations electron-phonon scattering dominates over electron-electron interband scattering in its effect on the thermopower at all temperatures and the temperature dependence of the thermopower is linear at elevated temperatures ($T/\theta_D > 1$). However, when the momentum gap is not too small, say 0.3 or more, we do find instances where the electron-electron contribution to the thermopower exhibits a well-defined extremum at very low temperatures. We also find conditions under which electron-electron interband scattering may dominate the effect of phonon-induced scattering at high temperatures and manifest itself in a more rapid temperature dependence (roughly T^2) of the total thermopower.

In this investigation phonon-drag was completely neglected. A more severe limitation, however, is the neglect of Umklapp processes which in electron-electron scattering, at any rate, do not occur frequently enough to modify the transport coefficients significantly¹⁰. The reason appears to be that energy conservation severely restricts the possibility of electron-electron Umklapp processes, in contrast to phonon-phonon or phonon-electron Umklapp processes. However, since Umklapp processes depend sensitively on the details of the Fermi surface, it seemed to us that to include these processes in the parabolic band approximation would still not answer the difficult question of their importance in a more realistic situation. The calculation is, thus, in the spirit of a model calculation and we concern ourselves only with general qualitative conclusions.

In sections II and III the effects of electron-phonon and electron-electron scattering on the different intrinsic transport properties are studied. In section IV the temperature dependence and sign of the total thermopower are discussed and figures for some typical cases are shown. In section V the effect of electron-electron scattering on the total thermopower at low and at elevated temperature is discussed and the results are compared with available experimental data.

II. PHONON SCATTERING

The effects of electron-phonon scattering on the electrical and thermal resistivities of the transition metals in terms of a two band model are given by^{11,7}.

$$\rho_{\text{pho}}(T) = \frac{3m_s P_{ss} h^3}{8 \pi (2m_s)^{1/2} e^2 E_F^2} \left(\frac{T}{\theta_D}\right)^3 \left\{ 2^{-1/3} n^{-2/3} \left(\frac{T}{\theta_D}\right)^2 J_5\left(\frac{\theta_D}{T}\right) + \omega_d \frac{m_d}{m_s} \frac{P_{sd}}{P_{ss}} \left[J_3\left(\frac{\theta_D}{T}\right) - J_3\left(\frac{\theta_E}{T}\right) \right] \right\} \quad (1)$$

and

$$W_{\text{pho}}(T) = \frac{27m_s P_{ss} h^3 T}{16\pi^5 (2m_s)^{1/2} E_F^4} \left(\frac{T}{\theta_D}\right)^3 \left(\frac{E_F}{k_B T}\right)^2 \left\{ J_5\left(\frac{\theta_D}{T}\right) + 2^{-1/3} n^{-2/3} \left(\frac{T}{\theta_D}\right)^2 [2/3 \pi^2 J_5\left(\frac{\theta_D}{T}\right) - 1/3 J_7\left(\frac{\theta_D}{T}\right)] + \omega_d \frac{m_d}{m_s} \frac{P_{sd}}{P_{ss}} \left\{ 2/3 [J_5\left(\frac{\theta_D}{T}\right) - J_5\left(\frac{\theta_E}{T}\right)] + 2/3 \pi^2 [J_3\left(\frac{\theta_D}{T}\right) - J_3\left(\frac{\theta_E}{T}\right)] \right\} \right\} \quad (2)$$

Here n is the effective number of the lighter carriers per atom, ω_d is the statistical weight (degeneracy) of the d-states, P_{ss} and P_{sd} are proportional to the square of the matrix elements for phonon-induced s-s and s-d transitions respectively, E_F is the Fermi energy, θ_D the Debye temperature, and $k_B \theta_E$ the minimum energy of phonons that can induce s-d transitions. The transport integrals $J_n(x)$ are defined in Eq. (7).

In an early work Mott⁹ argues that the resistivities (electrical and thermal) due to phonon induced s-d transitions would contain a factor

$N_d(E_F)$, the density of states in the d-band. Wilson¹¹ on the other hand, showed that if not all states on the d-Fermi sphere could be reached from a given s-state by phonon induced transitions, the proportionality factor should be $\omega_d m_d$. In Mott's case, one assumes that the upper limit of the phonon wave vector, $|\underline{q}|$, inducing s-d transitions is equal to $\underline{k}_s + \underline{k}_d$, $\underline{k}_s, \underline{k}_d$ being the Fermi momenta of s- and d-type carriers respectively. In the other case, the upper limit is the Debye wave vector, $|\underline{q}_D|$.

There is little distinction between these two cases when one is computing the magnitudes of the resistivities. However, as pointed out by Wilson, the thermopowers in the two cases are very different. In the first case in which one assumes that the largest momentum transferred is $q_{\max}^I = \underline{k}_s + \underline{k}_d < \underline{q}_D$, a situation which seems hardly realized in nature, the thermopower would be augmented by a factor proportioned to $\partial N_d(\epsilon)/\partial \epsilon$ which always has the same sign. In the second case where the largest momentum transferred is $q_{\max}^{II} = \underline{q}_D < \underline{k}_s + \underline{k}_d$, the thermopower will contain a contribution from $\partial \theta_E/\partial \epsilon$ which may be positive or negative depending on the relative magnitudes of the Fermi momenta and the relative curvatures of the two bands (See Eq. (5)).

We shall restrict ourselves to the latter case so that Wilson's model is the appropriate one. This is the reason that in the Eqs. (1) and (2) θ_D appears in the transport integrals instead of $\hbar \underline{u}(\underline{k}_s + \underline{k}_d)/k_B$, where \underline{u} is the velocity of sound.

We now assume that the following expression, derived by Ziman¹² for low temperatures is valid also when we allow interband as well as intraband transitions

$$S_{\text{pho}} = \frac{\pi^2 k_B^2 T}{3e} \left\{ -\frac{L_T}{L_0} \frac{\partial \ln \rho}{\partial \epsilon} + \left(1 - \frac{L_T}{L_0}\right) \frac{\partial \ln \sigma k_F}{\partial \epsilon} - \frac{3}{2\pi^2 E_F} \left(\frac{\theta_D}{T}\right)^2 \left(\frac{k_F}{q_D}\right)^2 \frac{L_s}{L_0} \right\}_{\epsilon=E_F} \quad (3)$$

We note that in the high temperature limit Eq. (3) reduces to the well-known formula

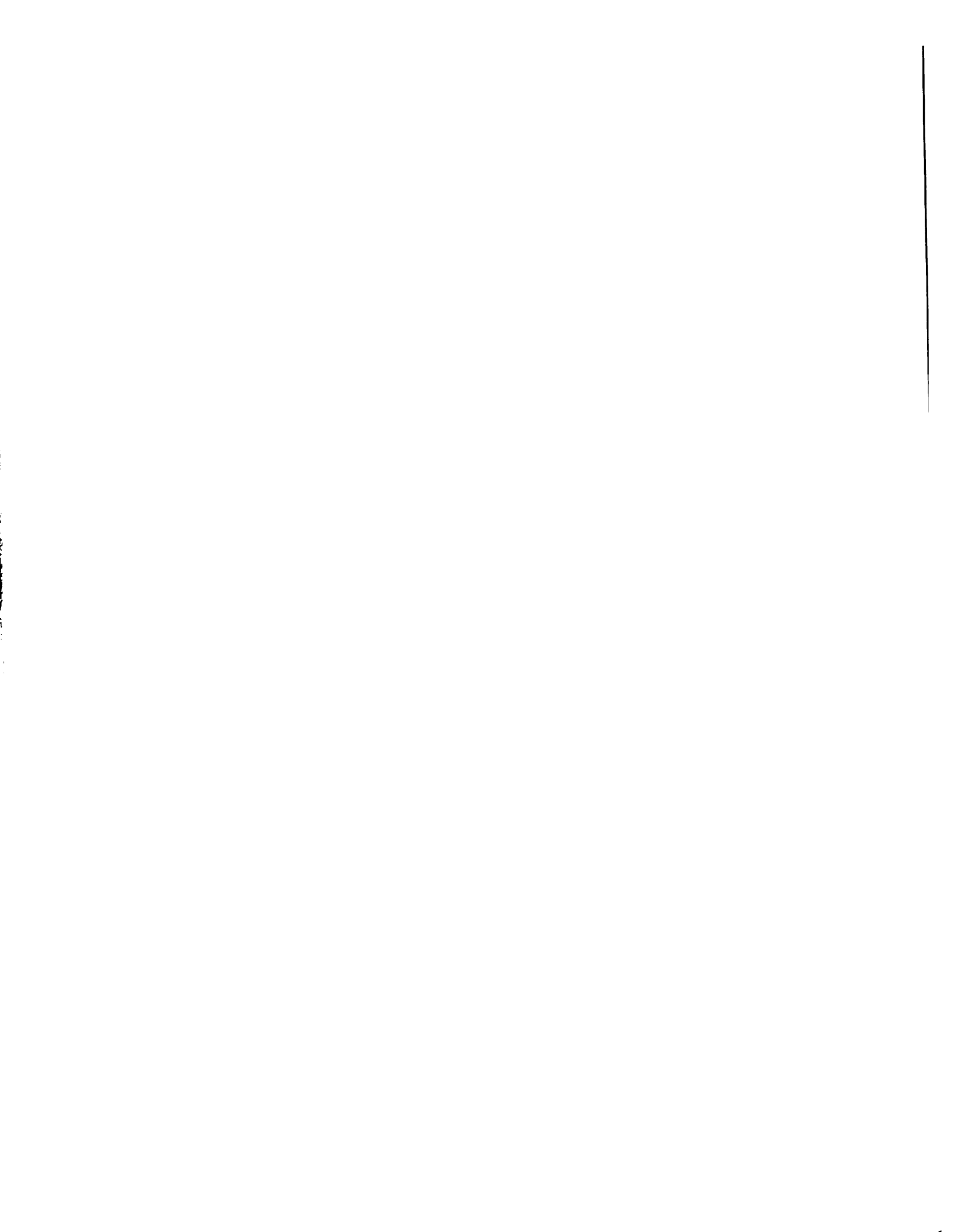
$$S_{\text{pho}} = -\frac{\pi^2 k_B^2 T}{3e E_F} \left\{ E_F \frac{\partial \ln \rho}{\partial \epsilon} \right\}_{\epsilon=E_F} \quad (4)$$

We now substitute the electrical resistivity as given by Eq. (1) into Eq. (3). We assume, of course, that the two scattering processes, intra-band and interband, are independent and contribute additively to the total resistivity. For the Fermi surface, σ , and the Fermi momentum, k_F , we put in the corresponding values of the lighter carriers and obtain

$$S_{\text{pho}} = \frac{\pi^2 k_B^2 T}{3e} \left\{ \frac{L_T}{L_0} \left[\frac{1}{2E_F} + \frac{A \frac{\left(\frac{T}{\theta_D}\right)^2}{m_s E_F} J_5\left(\frac{\theta_D}{T}\right) + \frac{m_d}{q_D h^2} \left(\frac{\theta_D}{T}\right) \left[(-1)^j \frac{m_d}{m_s} k_d^{-1} + k_s^{-1} \right] G(\theta_E/T)}{A \frac{\left(\frac{T}{\theta_D}\right)^2}{m_s E_F} J_5\left(\frac{\theta_D}{T}\right) + \frac{m_d}{m_s} \left[J_3\left(\frac{\theta_D}{T}\right) - J_3\left(\frac{\theta_E}{T}\right) \right]} \right] - \frac{L_s}{L_0} \frac{3}{2\pi^2 E_F} \left(\frac{\theta_D}{T}\right)^2 \left(\frac{k_s}{q_D}\right)^2 \right\} \quad (5)$$

using the relation

$$\eta = \frac{\theta_E}{\theta_D} = \frac{|k_s - k_d|}{q_D} \quad (6)$$



to calculate the derivative $\partial\theta_E/\partial\epsilon$. The following quantities and abbreviations have been introduced

$$J_n(x) = \int_0^x \frac{z^n}{(e^z-1)(1-e^{-z})} dz$$

$$A = \frac{(6\pi^2)^{2/3} h^2 P_{ss}}{4a^2 \omega_d P_{sd}} \quad (7)$$

$$G(\theta_E/T) = \frac{(\theta_E/T)^3}{[e^{(\theta_E/T)} - 1][1 - e^{-(\theta_E/T)}]}$$

where a is the lattice parameter and L_o , L_T , L_s , are the Lorentz numbers defined by

$$L_o = \frac{\pi^2}{3} \left(\frac{k_B}{e}\right)^2$$

$$L_T = \frac{\rho_{ss} + \rho_{sd}}{T(W_{ss} + W_{sd})} \quad (8)$$

$$L_s = \frac{\rho_{ss}}{T W_{ss}}$$

The upper sign in the numerator in Eq. (5) corresponds to the case $\underline{k}_d < \underline{k}_s$, the lower one to $\underline{k}_d > \underline{k}_s$, j is equal to 2 in the case of an inverted d-band, and equal to 1 otherwise.

The sign of e is that of the lighter carriers. In our model we assume only that the carriers described by one band are substantially heavier than those of the other and that the former do not contribute to the charge transport. The dominant charge carriers may be either electrons or holes.

The discussion of the effect on the total thermopower of phonon induced scattering is complicated by the fact, that the intrinsic thermopower must be weighted by the corresponding thermal resistivity. What we expect is that for $T/\theta_D > 1$ the curly bracket in Eq. (5) will be constant and S_{pho} therefore proportional to T . Below this temperature the contribution decreases mainly because the ratio of the Lorentz numbers diminishes. Below θ_E the exponential decay of s-d transitions further reduces the contribution and S_{pho} may even reverse sign.

III. ELECTRON-ELECTRON SCATTERING

If we assume that one can define a relaxation time for these processes, then the change with time of the distribution of the carriers due to collisions is given by¹³,

$$\left. \frac{\partial f(\underline{y}, \underline{x})}{\partial t} \right|_{\text{coll}} = - \frac{f(\underline{y}, \underline{x}) - f^0(\underline{y}, \underline{x})}{\tau(\underline{y}, \underline{x})} \quad (9)$$

If we denote by¹⁴

$$2 \int_{\underline{k}_1}^{\underline{k}'_1} \int_{\underline{k}_2}^{\underline{k}'_2} \underline{dk}_2 \underline{dk}'_1 \underline{dk}'_2 \quad (10)$$

the a priori transition probability that an electron in state \underline{k}_1 collides with an electron in state $(\underline{k}_2, \underline{k}_2 + \underline{dk}_2)$ and that the two particles are scattered into the states $(\underline{k}'_1, \underline{k}'_1 + \underline{dk}'_1)$, $(\underline{k}'_2, \underline{k}'_2 + \underline{dk}'_2)$ respectively, and furthermore assume the electrons to be free, and describe the interaction by a screened Coulomb potential, then we obtain¹⁵

$$\left. \dot{f}_{\underline{k}_1} \right|_{\text{coll}} = - \frac{32 \pi^3 e^4}{\hbar k_B T V^2 v_2 v_3 v_4} \phi_{\underline{k}} \iiint \frac{\delta_{\underline{k}_1 + \underline{k}_2, \underline{k}'_3 + \underline{k}'_4}}{[|\underline{k}_3 - \underline{k}_1|^2 + \underline{g}^2]^2} dA_2 dA_3 dA_4$$

$$\iiint \sigma (\epsilon_1 + \epsilon_2 - \epsilon_3 - \epsilon_4) f_1^0 f_2^0 (1 - f_3^0) (1 - f_4^0) d\epsilon_2 d\epsilon_3 d\epsilon_4 \quad (11)$$

Here the subscripts 1, 2, 3, and 4, stand for \underline{k}_1 , \underline{k}_2 , \underline{k}'_1 , and \underline{k}'_2 , respectively. The \underline{v}_i 's are the corresponding Fermi velocities, V is the volume of the Brillouin zone, $\phi_{\underline{k}}$ stands for $(\phi_1 + \phi_2 - \phi_3 - \phi_4)$ where the ϕ_i 's are defined by

$$f_i = f_i^0 - \phi_i \frac{\partial f_i^0}{\partial \epsilon_i} \quad (12)$$

g is the reciprocal of the screening radius, $\delta_{\underline{k}}$ the Kronecker delta and the surface elements dA_i are defined in the Appendix. For a discussion of the properties of the energy conservation function $\mathcal{O}(\epsilon)$ we refer to Ziman¹⁶.

We should like to mention that implicit in Eq. (11) is the fact that as a result of momentum conservation, Normal intraband transitions provide no relaxation.

For the calculational details, we refer the reader to the Appendix and quote here merely the result

$$\dot{f}_{\underline{k}_1} \Big|_{\text{coll}} = - \frac{128 \pi^5 e^4}{\hbar^4 k_B T^2 v_2 v_3 v_4} [(\pi k_B T)^2 + (\epsilon_1 - E_F)^2] f_i^0(\epsilon_1) [1 - f_i^0(\epsilon_1)] \phi_{\underline{k}} \frac{K_2 K_3 K_4}{|\underline{k}_1|} I(\Delta_{\min}, \Delta_{\max}) \quad (13)$$

where $\beta = 1/k_B T$ and the integral $I(\Delta_{\min}, \Delta_{\max})$ is given by Eqs. (A14) and (A15).

We now use Eqs. (9), (12), (13) and the property

$$\frac{\partial f_i^0}{\partial \epsilon_i} = - \frac{f_i^0 (1 - f_i^0)}{k_B T} \quad (14)$$

to obtain

$$\tau(\underline{k}_1) = \frac{\hbar^7 v^2}{128 \pi^5 e^4} \frac{1}{m_2 m_3 m_4} \frac{|\underline{k}_1|}{I(\Delta_{\min}, \Delta_{\max})} \frac{1}{(\pi k_B T)^2 + (\epsilon_1 - E_F)^2} \quad (15)$$

In the usual framework of the theory of macroscopic transport coefficients, the electrical conductivity is given to first order by

$$\sigma(\epsilon) = \frac{e^2}{12\pi^3 \hbar} \int \underline{v}_1 \tau(k_1) dA_1 \quad (16)$$

Inserting Eq. (15) in Eq. (16) we obtain

$$\sigma(E_F) = \frac{\hbar^8 v^2}{384\pi^9 e^2} \frac{1}{m_1 m_2 m_3 m_4} \frac{1}{(k_B T)^2} \frac{k_1^4}{I(\Delta_{\min}, \Delta_{\max})} \quad (17)$$

From this expression we see that the most effective scattering processes are those in which $(s, d) \rightarrow (d', d'')$. The contribution of this type of process is larger than those of any other electron-electron scattering processes by a factor greater than $N_d(E_F)/N_s(E_F)$. Hereafter we restrict our attention to these processes only and obtain for the electrical resistivity

$$\rho_{e-e} = \frac{384\pi^9 e^2}{\hbar^8 v^2} m_s m_d^3 \frac{I(\Delta_{\min}, \Delta_{\max})}{k_s^+} (k_B T)^2 \quad (18)$$

The lower and upper limits of $I(\Delta_{\min}, \Delta_{\max})$ depend on the relative magnitudes of \underline{k}_s and \underline{k}_d as follows

$$\underline{k}_s < \underline{k}_d : \quad \Delta_{\min} = \underline{k}_d - \underline{k}_s \quad \Delta_{\max} = \underline{k}_d + \underline{k}_s \quad (19a)$$

$$\underline{k}_s > \underline{k}_d : \quad \Delta_{\min} = \underline{k}_s - \underline{k}_d \quad \Delta_{\max} = 2\underline{k}_d \quad (19b)$$

We require, of course, that $\Delta_{\min} < \Delta_{\max}$ and hence in case of $\underline{k}_s > \underline{k}_d$ we

get the condition

$$\underline{k}_s < 3\underline{k}_d$$

If this condition is violated, then there is no way for a scattering process to occur conserving linear momentum. Substituting the appropriate values

for $I(\Delta_{\min}, \Delta_{\max})$ according to Eq. (A15) we finally obtain

for $\underline{k}_s < \underline{k}_d$

$$\rho_{e-e} = A_{e-e} \frac{m_s m_d^3}{k_s^5 k_d} \left\{ \frac{(\chi+1)}{(\chi+1)^2 + \chi^2} - \frac{(1-\chi)}{(1-\chi)^2 + \chi^2} + \frac{1}{\chi} \tan^{-1}(2\chi^2) \right\} T^2 \quad (20a)$$

and for $\underline{k}_s > \underline{k}_d$

$$\rho_{e-e} = A_{e-e} \frac{m_s m_d^3}{k_s^6} \left\{ \frac{2\lambda}{4\lambda^2 + 1} - \frac{(1-\lambda)}{(1-\lambda)^2 + 1} + \tan^{-1} \frac{(3\lambda-1)}{1+2\lambda(1-\lambda)} \right\} T^2 \quad (20b)$$

where $\chi = 1/\lambda = \underline{k}_s/\underline{k}_d$ and we have set $\underline{g} = \underline{k}_s$. The constant factor is

$$A_{e-e} = \frac{192\pi^9 e^2 k_B^2}{\hbar^8 v^2} \quad (21)$$

From Eq. (4) we now find the intrinsic thermopower due to electron-electron scattering

for $\underline{k}_s < \underline{k}_d$

$$S_{e-e} = - \frac{\pi^2 k_B^2 T}{3 e} \frac{m_d}{\hbar^2 k_d^2}$$

$$\left[\left\{ \frac{[\chi^2 - (\chi+1)^2] \left(\frac{m_s}{m_d} \chi^{-1} + 1 \right) [\chi^2 - (1-\chi)^2] \left(\frac{m_s}{m_d} \chi^{-1} + 1 \right) + 2 \frac{m_s}{m_d} \chi^{-1} (2\chi^2 + 1) + 4\chi}{[\chi^2 + (\chi+1)^2]^2} + \frac{[\chi^2 - (1-\chi)^2]^2}{[\chi^2 + (1-\chi)^2]^2} + \frac{2 \frac{m_s}{m_d} \chi^{-1} (2\chi^2 + 1) + 4\chi}{1 + 4\chi^4} \right\} \right. \\ \left. - 4 \frac{m_s}{m_d} \chi^{-2} \right] \quad (22a)$$

and for $\frac{k_s}{m_s} > \frac{k_d}{m_d}$

$$S_{e-e} = - \frac{\pi^2 k_B^2 T}{3 e} \frac{m_d}{\hbar^2 k_s^2}$$

$$\left[\left\{ \frac{+2\lambda^{-1}(4\lambda^2 - 1)}{(4\lambda^2 + 1)^2} - \frac{[1 - (1-\lambda)^2] \left(\frac{m_s}{m_d} + \lambda^{-1} \right)}{[1 + (1-\lambda)^2]^2} - \frac{\frac{m_s}{m_d} (1 + 4\lambda^2) + 6\lambda + 5\lambda^{-1} - 4}{[1 + 2\lambda(1-\lambda)]^2 + (3\lambda - 1)^2} \right. \right. \\ \left. \left. - 4 \frac{m_s}{m_d} \right\} \right] \quad (22b)$$

In Eqs. (22a, b) the upper sign corresponds to the case of an inverted d-band.

The total measured thermopower (discounting phonon-drag) is the sum of the intrinsic thermopowers each weighted by the corresponding thermal resistivity. For electron-electron scattering we have¹⁷

$$W_{e-e} = \frac{\rho_{e-e}}{T(12-\pi^2) \left(\frac{k_B}{e}\right)^2} \quad (23)$$

Since the expressions for S_{e-e} and W_{e-e} are rather complicated, it is difficult to predict the magnitude and sign of this contribution to the total thermopower in the general case. We do expect that if this contribution dominates that associated with electron-phonon scattering at high temperatures, the total thermopower will vary as $\alpha T + \beta T^2$, where the second term arises from electron-electron scattering. This follows from the expression for the total thermopower¹⁸

$$S_T = \frac{W_{pho} S_{pho} + W_{e-e} S_{e-e}}{W_{pho} + W_{e-e}} \quad (24)$$

and the fact that $W_{pho}(\theta_D) \gg W_{e-e}(\theta_D)$. W_{pho} at high temperatures is independent of T whereas W_{e-e} and S_{e-e} are both linear in T . At still higher temperatures W_{e-e} may become comparable to, or greater than, W_{pho} and where this happens, the quadratic contribution in the total thermopower will diminish. In that event, the total thermopower will exhibit a linear temperature dependence even though electron-electron scattering effects dominate over those of electron-phonon scattering. In some cases, this behavior is apparent from the calculated results and also in the data in some of the transition metals (See Sections IV and V).

IV. TOTAL THERMOPOWER

The total thermopower for multiple scattering mechanisms is given by¹⁸

$$S_T = \frac{1}{W_T} \sum_i W_i S_i$$

with

$$W_T = \sum_i W_i$$

(25)

where S_i and W_i are the contributions to the thermopower and thermal resistivities of each mechanism independently. Thus, before we can construct the total thermopower, it is necessary to know the relative magnitudes of W_{e-e} and W_{pho} . As it is difficult to estimate these from first principles, we have resorted to an empirical estimate of the ratio $\rho_{pho}(T)/\rho_{e-e}(T)$ by defining a parameter T_E by

$$\rho_{pho}(T_E) = \rho_{e-e}(T_E) \quad (26)$$

Estimates from experimental data⁵ put T_E in the range from 5°K to 20°K consistent with the evidence that $W_{e-e}(\theta_D) \ll W_{pho}(\theta_D)$. The theoretical total thermopower is plotted in Figures 1, 2, 3, and 4, representing typical cases for different values of the gap parameter, η , different effective mass ratios, m_d/m_s , and possible arrangements of the s- and d-bands.

To aid our discussion we introduce S_{pho}^T and S_{e-e}^T , the weighted contributions of the two scattering processes to the total thermopower. These are defined by

$$S_{\text{pho}}^T = \frac{W_{\text{pho}} S_{\text{pho}}}{W_T} \qquad S_{\text{e-e}}^T = \frac{W_{\text{e-e}} S_{\text{e-e}}}{W_T} \qquad (27)$$

We now consider four distinct situations

Case I: One band inverted relative to the other band.

- a) $\underline{k}_s < \underline{k}_d$: S_{pho}^T is negative at all temperatures¹⁹ and it is dominant at low temperatures. For small and intermediate values of η (≤ 0.5) $S_{\text{e-e}}^T$ is positive. When m_d/m_s is large (10) it dominates S_{pho}^T at higher temperatures. In the case of large η (0.7) $S_{\text{e-e}}^T$ is positive for $m_d/m_s = 10$ only, and it is always smaller than S_{pho}^T throughout the temperature range. These results are shown in Figure 1. If $\eta = 0.1$ and $m_d/m_s = 10$ we find a local extremum of the total thermopower at very low temperatures associated with the freezing out of phonon induced s-d transitions. A typical curve is shown in Figure 2. On the other hand, in the case of $\eta = 0.3$ and the same large ratio m_d/m_s we find (depending upon the magnitude of \underline{k}_s) a local extremum due to electron-electron scattering processes. Both these

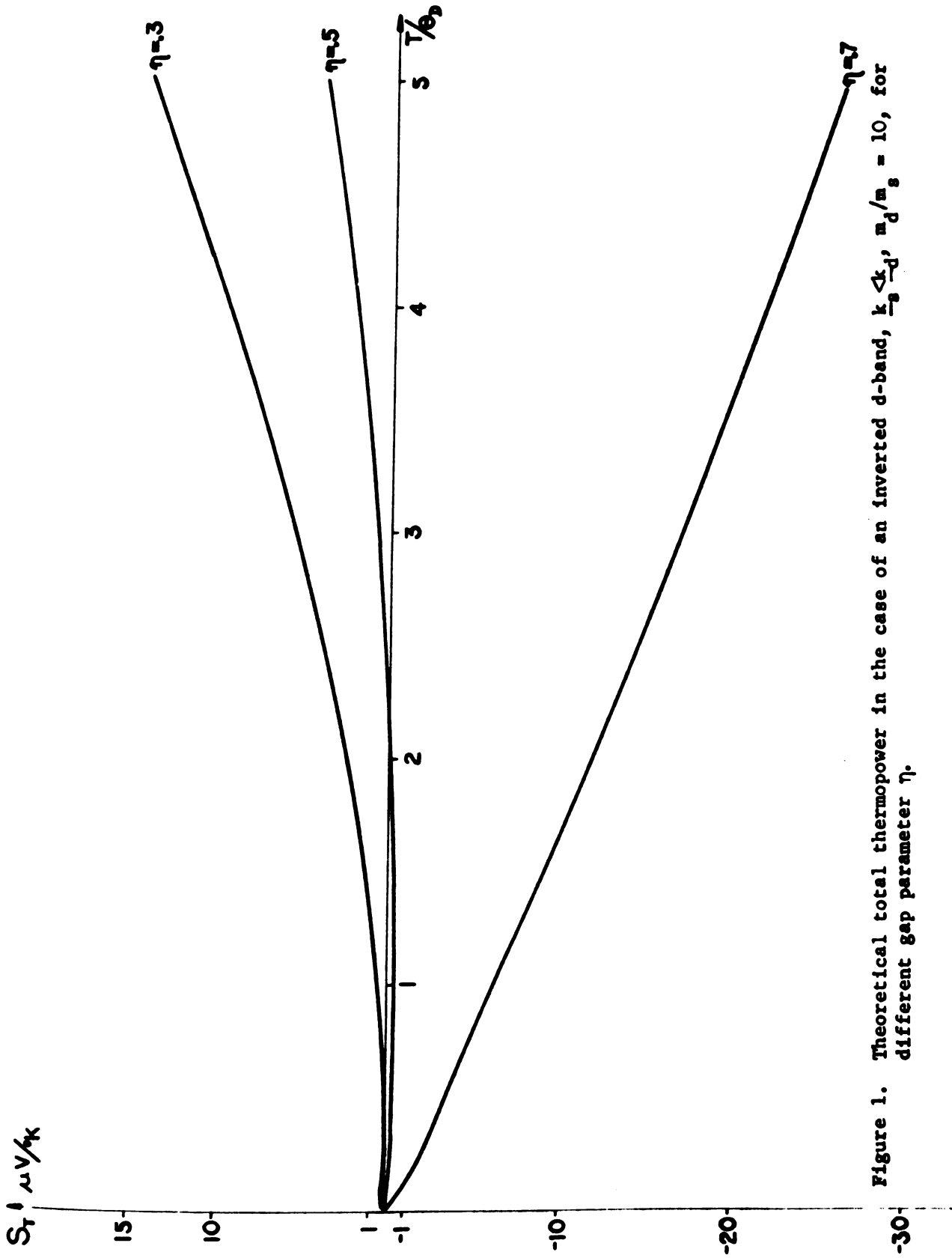


Figure 1. Theoretical total thermopower in the case of an inverted d-band, $k \ll k_d$, $m_d/m_s = 10$, for different gap parameter η .

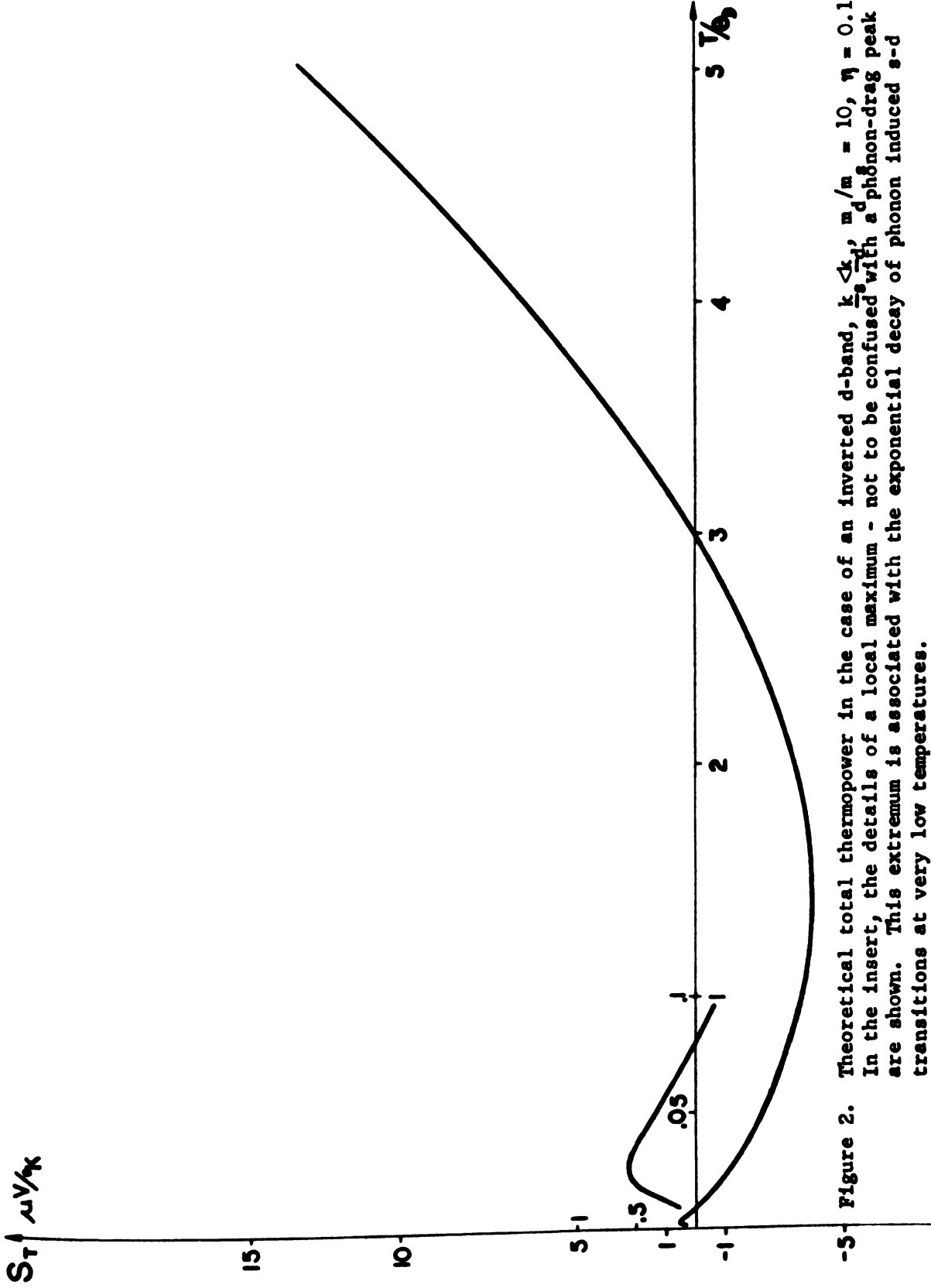


Figure 2. Theoretical total thermopower in the case of an inverted d-band, $\frac{k \langle k \rangle}{m_d/m} = 10$, $\eta = 0.1$. In the insert, the details of a local maximum - not to be confused with a phonon-drag peak - are shown. This extremum is associated with the exponential decay of phonon induced s-d transitions at very low temperatures.

peculiarities will be discussed more in detail below (See section V.).

- b) $\frac{k_s}{k_d} > \frac{k_d}{k_s}$: S_{pho}^T is always negative and it is dominant at low temperatures. S_{e-e}^T is always negative and dominates S_{pho}^T at higher temperatures. Independent of the ratio m_d/m_s we find for $\eta = 0.5$ a strong local extremum associated with electron-electron scattering effects. A representative curve for this behaviour is shown in Figure 3.

Case II: Both bands have curvatures of equal sign.

- a) $\frac{k_s}{k_d} < \frac{k_d}{k_s}$: S_{pho}^T as well as S_{e-e}^T are negative throughout the temperature range. For small and intermediate values of η and for large m_d/m_s S_{e-e}^T dominates at higher temperatures, but this is not the case if m_d/m_s is small (3). This change of the temperature dependence of the total thermopower with the effective mass ratio is shown in Figure 4.
- b) $\frac{k_s}{k_d} > \frac{k_d}{k_s}$: S_{pho}^T is dominant at low temperatures. The sign is negative²⁰ if m_d/m_s is small and η is small or intermediate (≤ 0.3), or if m_d/m_s is large and η is small (0.1). The sign is positive if m_d/m_s is small and η

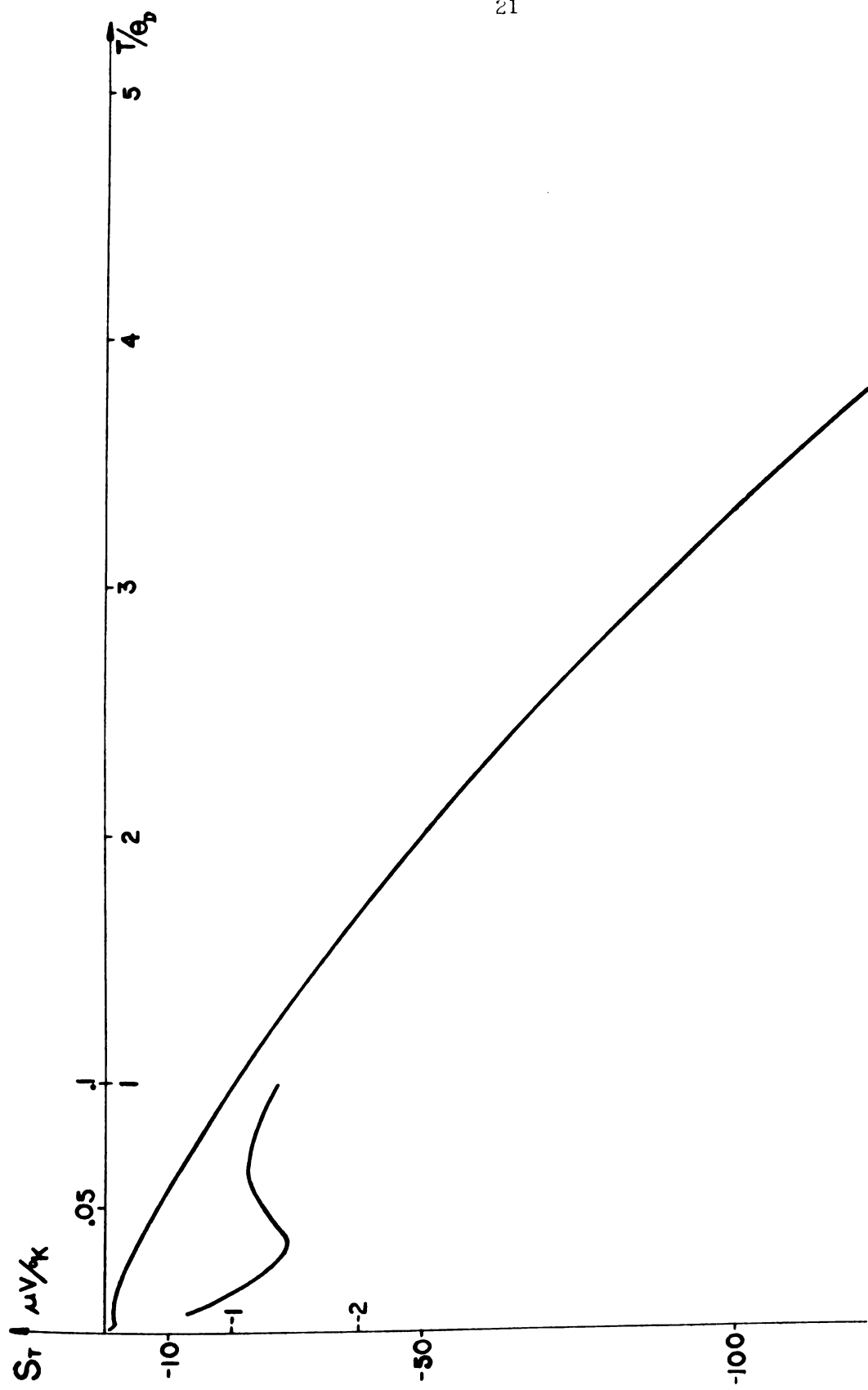


Figure 3. Theoretical total thermopower in the case of an inverted d-band, $k > k_s$, $m_d/m = 10$, $\eta = 0.5$. In the insert, the details of a local minimum, due to electron-electron scattering effects, are shown.

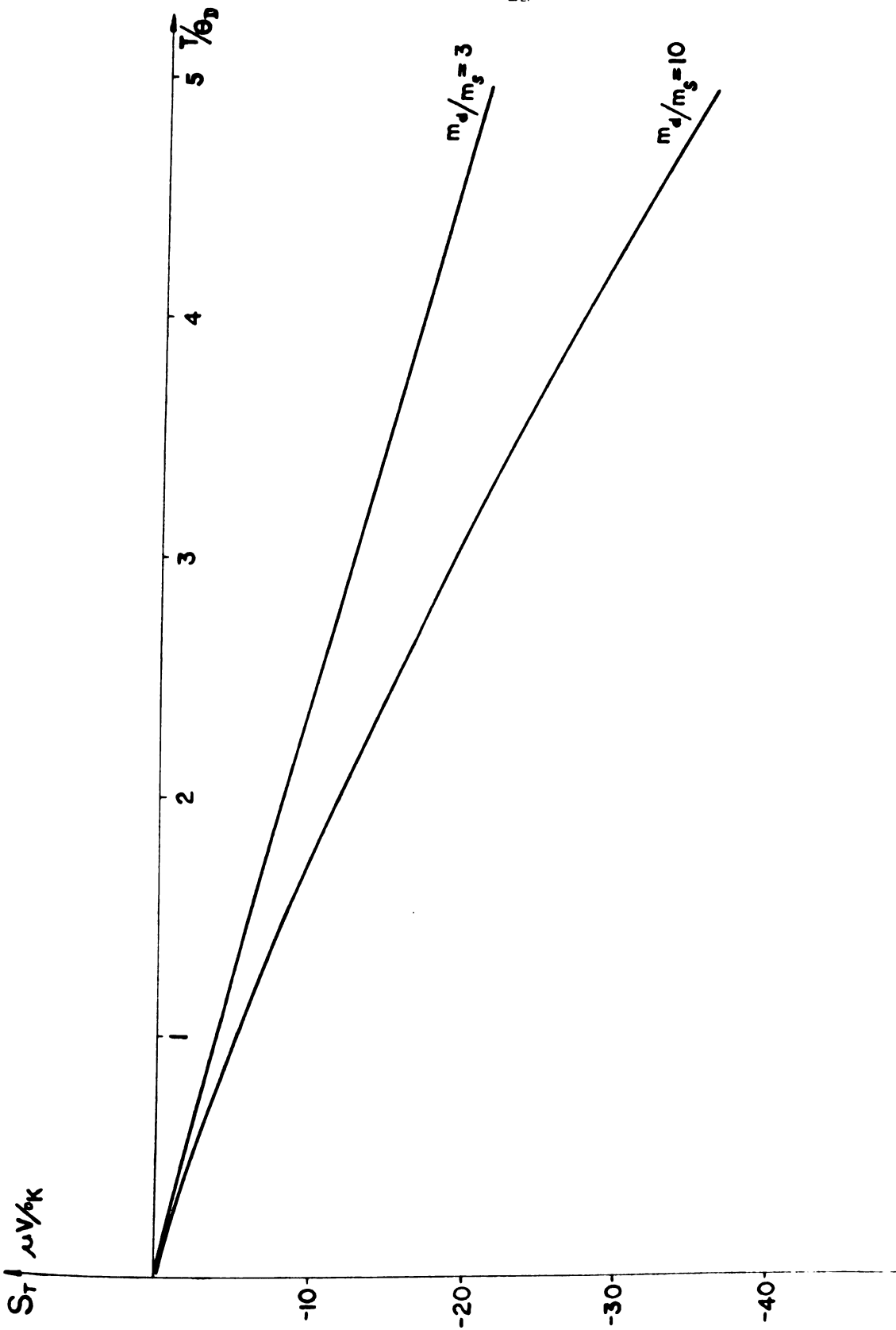


Figure 4. Theoretical total thermopower in the case where the two bands have the same curvature, $k_s < k_d$, $\gamma = 0.1$, for $m_d/m_s = 3, 10$.

is large (≥ 0.5), or if m_d/m_s is large and η is intermediate or large (≥ 0.3). Independent of the effective mass ratio S_{e-e}^T is positive for small and intermediate η (≤ 0.5) and dominates S_{pho}^T at high temperatures. Under the same conditions as in case Ia) we obtain a local extremum characteristic for the exponential decay of the phonon induced s-d transitions at very low temperatures. We also find local extrema due to electron-electron scattering effects which become more pronounced as the gap size increases ($\eta \geq 0.3$) and the ratio m_d/m_s becomes larger.

V. DISCUSSION

There are several important limitations to our calculations which preclude a detailed comparison with the experimental data for each of the transition metals. First, we have used a spherical model for the Fermi surfaces of the conduction electrons in order to simplify the calculations. Although this is an obvious oversimplification of the actual Fermi surfaces in the transition metals, it perhaps suffices to represent the general features of these metals. The magnitudes of the quantities m_d/m_s , a , g_D , k_s , k_d , η and related derivatives with respect to the energy which enter the theory must then, however, be considered as empirical parameters. Secondly, we have omitted considerations of phonon-drag processes. Consequently, a comparison with the experimental data must be restricted to regions where T/θ_D is greater or much less than unity and phonon-drag effects have essentially disappeared. Finally, we neglected Umklapp processes throughout this investigation.

Nonetheless, there are certain general features of the experimental data in these two limiting regions which seem to bear out our model calculation. For comparison we include the figure given by Cusack and Kendall²¹ (Figure 5) and refer also to more recent results²². In the high temperature limit the thermopower for the transition metals is observed^{23,21} to vary from large negative values (e.g. for Pd and Pt) to large positive values (e.g. for W and Mo) at a given temperature as we pass from one metal to another. Although the argument that this variation is due to differences in the slope of the density of states of the d-band is essentially correct (i.e. making no distinction between the Mott and Wilson models), it may be crucial in some cases to include

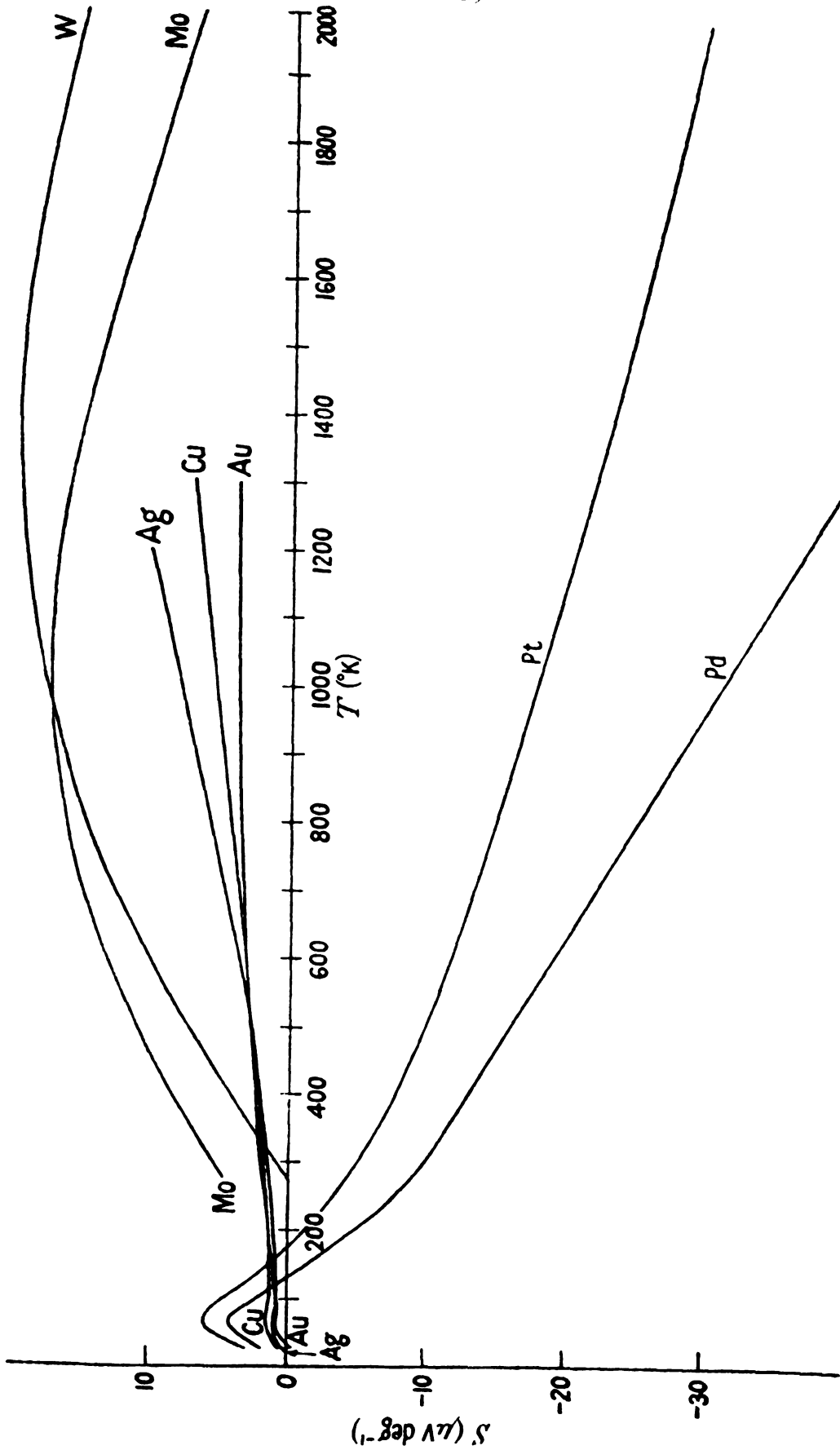


Figure 5. Experimental thermopower of some of the transition metals taken from N. Cusack and P. Kendall, Ref. 21.

the effects of electron-electron scattering. For example, the thermopower of W and Mo above the Debye temperature is given quite closely by

$$S_T = \alpha T - \beta T^2 \quad (28)$$

where the constants are $\alpha \approx 4.5 \cdot 10^{-2} \mu\text{V}/^\circ\text{K}$, $\beta \approx 2 \cdot 10^{-5} \mu\text{V}/(^\circ\text{K})^2$, respectively. The second term may reflect the importance of electron-electron scattering on the thermopower at elevated temperatures. Moreover, in the low temperature region (near 10°K) the experimental data for W²² display a peak of the order of $0.2 \mu\text{V}/^\circ\text{K}$ which may be due to effects of electron-electron interband scattering. To understand this, we must look at the weighted contribution to the total thermopower, since from the linear temperature dependence of the corresponding intrinsic thermopower one would not expect such a behavior. From Eq. (27) we get the following temperature dependence

$$S_{e-e}^T = \frac{AT^2}{BT^n + CT} \quad (29)$$

since we know that S_{e-e} , as well as W_{e-e} , are proportional to the temperature. In the case where we have intraband scattering induced by phonons only (e.g. noble metals), n would be equal to 2. In our case where in the temperature region of interest the probability of phonon induced interband transitions drops exponentially, n will be larger than 2 but to a first approximation (up to the second term in the expansion of the exponential factor) still smaller than 3. We now differentiate with respect to temperature and obtain the following relation for the temperature at which the weighted contribution of electron-electron

effects reaches a local extremum

$$T_{\text{extr}} = \left[\frac{C}{(n-2)B} \right]^{\frac{1}{n-1}} \quad (30)$$

The calculated thermopower exhibits such a local extremum only if T_{extr} lies below the characteristic temperature where effects due to phonon induced interband scattering are diminished exponentially. Otherwise S_{e-e}^T not only diminishes with increasing temperature but the extremum will further be masked by S_{pho}^T which increases rapidly with increasing temperature. In the case of $\underline{k}_s > \underline{k}_d$ the local extremum becomes more pronounced as the ratio $\lambda = \underline{k}_d/\underline{k}_s$ approaches 1/3 for then only large angle scattering events provide relaxation.

If the "momentum gap" is small ($\eta = 0.1$), the phonon induced s-d transitions decay exponentially only at very low temperatures after essentially all contributions from electron-electron scattering effects have diminished considerably. It then is not surprising, considering the complex temperature dependence of S_{pho}^T in this region, that we may find under these circumstances and especially for a large ratio m_d/m_s a local extremum quite similar to the one ascribed to electron-electron scattering effects above.

Thus a local extremum in the case of small η is more likely to be associated with phonon induced scattering effects whereas in case of intermediate or large η it might be due to the influence of electron-electron scattering.

We also might point out that in view of the rather complicated temperature dependence of S_{pho}^T , especially at low temperatures, and the

interplay with S_{e-e}^T we must not be surprised if the general behaviour of the total thermopower in this region is such that the thermopower, though it must surely vanish at absolute zero, does not appear to extrapolate to this value even if measurements are carried out to quite low temperatures, e.g. near 1°K^{24} .

We also should like to mention briefly the influence of effects due to impurities. Since the corresponding thermal resistivity is proportional to T^{-1} and the intrinsic thermopower varies linearly with the temperature, we expect no qualitative change at higher temperature, but only a parallel shift in very impure materials. On the other hand, at low temperature there may arise a substantial change especially in the case where we have a local extremum in the ideal case. This situation is indicated in Figure 6 where we show S versus T for various values of $\rho(293^\circ\text{K})/\rho_{\text{res}} = R$

We should like to point out that Figures 1-4 and 6 were obtained with an almost random choice (within our assumptions) of the parameters involved. In various portions of the temperature scale they qualitatively reflect some of the features of the experimental data shown in Figure 5. A better fit to the experimental results could be obtained by adjusting the lattice constant, $a(3 \cdot 10^{-10} \text{ m})$, the statistical weight of s - d transitions in the case of phonon induced scattering, $\omega_d^P/P_{ss} (2)$, the magnitude of the Fermi vector \underline{k}_s (0.47 to $1.88 \cdot 10^{10} \text{ m}^{-1}$) and the Debye wave vector, $\underline{q}_D(1.6 \cdot 10^{10} \text{ m}^{-1})$. The values in parenthesis indicate our choice and were not changed with temperature.

In view of the various simplifying assumptions of the model calculation, such adjustment of parameters is of questionable value.

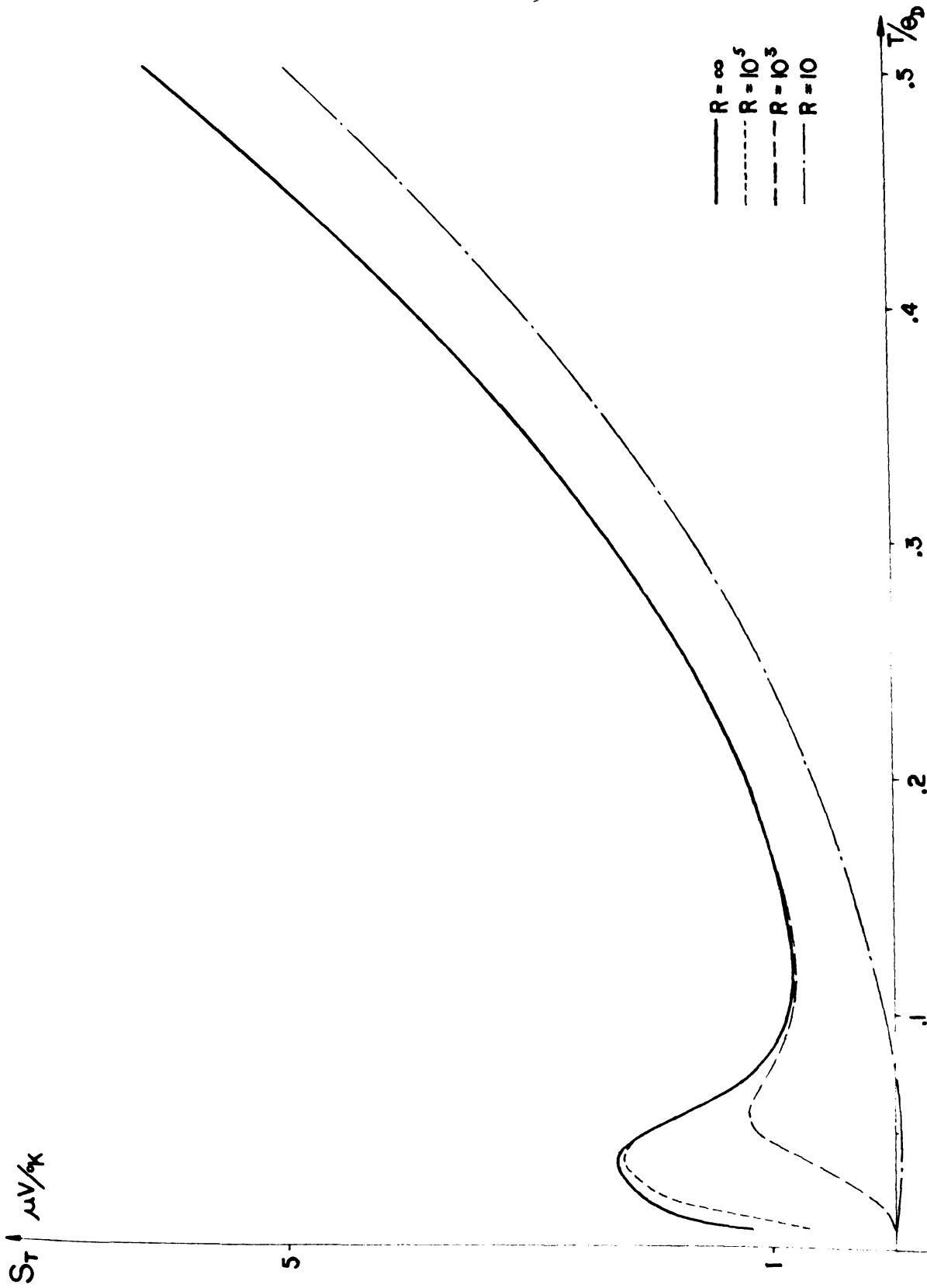


Figure 6. Theoretical total thermopower in the case where the two bands have the same curvature $k_g > k_d$, $m_s/m_d = 3$, $\gamma = 0.5$, for different values of the ratio R .

What we do wish to emphasize is that this simple model is capable of reproducing the general features of the available experimental data.

APPENDIX

APPENDIX

We start with Eq. (11)

$$\dot{f}_{\mathbf{k}_1} \Big|_{\text{coll}} = - \frac{32\pi^3 e^4}{\hbar^4 k_B^4 T^2 v_2 v_3 v_4} \phi_{\mathbf{k}} \iiint \frac{\delta_{\mathbf{k}_1+\mathbf{k}_2, \mathbf{k}_3+\mathbf{k}_4}}{[|\mathbf{k}_3-\mathbf{k}_1|+g]^2} dA_2 dA_3 dA_4$$

$$\iiint \sigma(\epsilon_1+\epsilon_2-\epsilon_3-\epsilon_4) \cdot f_1^0 f_2^0 (1-f_3^0)(1-f_4^0) d\epsilon_2 d\epsilon_3 d\epsilon_4 \quad (\text{A1})$$

and perform first the integration over energy. We made use of the relation

$$1 - f_i^0 = f_i^0 e^{(\epsilon_i - E_F)\beta} \quad (\text{A2})$$

and of the property of $\sigma(\epsilon)$ for large times to reduce the energy dependent part to the form

$$\frac{1}{1+e^{-(\epsilon_1-E_F)\beta}} \int \frac{d\epsilon_3}{e^{(\epsilon_3-E_F)\beta} + 1} \int \frac{e^{(\epsilon_2-E_F)\beta} d\epsilon_2}{(e^{(\epsilon_2-E_F)\beta} + 1) (e^{(\epsilon_1+\epsilon_2-\epsilon_3-E_F)\beta} + 1)} \quad (\text{A3})$$

To evaluate the integral over ϵ_2 we make the substitutions

$$e^{(\epsilon_1-\epsilon_3)\beta} = a \quad \text{and} \quad e^{(\epsilon_2-E_F)\beta} = u \quad (\text{A4})$$

Separation into partial fraction

$$\frac{1}{(u+1)(au+1)} = \frac{1}{1-a} \left[\frac{1}{u+1} - \frac{1}{u+\frac{1}{a}} \right] \quad (\text{A5})$$

gives

$$\frac{1}{(1-a)\beta} \ln \frac{u+1}{u+\frac{1}{a}} \Bigg|_0^\infty = \frac{e^{\epsilon_1-\epsilon_3}}{(e^{\epsilon_1-\epsilon_3})^\beta - 1} \quad (\text{A6})$$

With the further substitutions

$$e^{(\epsilon_1 - E_F)\beta} = b \quad \text{and} \quad (\epsilon_1 - \epsilon_3)\beta = x \quad (\text{A7})$$

we find for the whole energy dependent part of Eq. (A1)²⁵

$$\begin{aligned} \frac{b}{2(b+1)^2\beta} [\pi^2 + (\ln b)^2] &= \frac{(\pi k_B T)^2 + (\epsilon_1 - E_F)^2}{2(e^{(\epsilon_1 - E_F)\beta} + 1)(e^{-(\epsilon_1 - E_F)\beta} + 1)} \\ &= \frac{1}{2} [(\pi k_B T)^2 + (\epsilon_1 - E_F)^2] f^0(\epsilon_1) [1 - f^0(\epsilon_1)] \end{aligned} \quad (\text{A8})$$

This leaves us with the momentum dependent part of Eq. (A1). We now define

$$\Delta_I^2 = |\underline{k}_3 - \underline{k}_1|^2 = \underline{k}_1^2 + \underline{k}_3^2 - 2 \underline{k}_1 \underline{k}_3 \cos \varphi_I \quad (\text{A9})$$

$$\Delta_{II}^2 = |\underline{k}_2 - \underline{k}_4|^2 = \underline{k}_2^2 + \underline{k}_4^2 - 2 \underline{k}_2 \underline{k}_4 \cos \varphi_{II}$$

where the φ 's are the angles between the corresponding k-vectors. First, we keep k_1 and k_3 fixed and vary k_4 only; then

$$dA_4 = 2\pi \underline{k}_4^2 \sin \varphi_{II} d\varphi_{II} = 2\pi \frac{\Delta_{II}}{\underline{k}_2 \underline{k}_4} \underline{k}_4^2 d_{II} \quad (\text{A10})$$

where \underline{K}_i is the radius of the Fermi sphere of carriers of type i.

Similarly

$$dA_2 = \underline{K}_2^2 d\Omega_2 = \frac{\underline{K}_2^2}{\Delta_{II}} dA(\underline{k}_2, \underline{k}_4) \quad (\text{A11})$$

where Ω_2 is the space angle generated by \mathbf{k}_2 (while \mathbf{k}_4 varies) and $A(\mathbf{k}_2 - \mathbf{k}_4)$ is the surface area swept out by the rotation of $\mathbf{k}_2 - \mathbf{k}_4$. Thus, the integrations dA_2 , dA_4 can be evaluated as shown below

$$\begin{aligned}
 2\pi \int \frac{dA_3}{[\Delta_I^2 + \mathbf{g}^2]^2} \iint \frac{\Delta_{II} K_4^2}{k_2 k_4} \frac{K_2^2}{\Delta_{II}} \delta_{\Delta_I, \Delta_{II}} d\Delta_{II} dA(\mathbf{k}_2 - \mathbf{k}_4) \\
 = 2\pi \frac{K_2 K_4}{k_2 k_4} \int \frac{dA_3}{\Delta_I [\Delta_I^2 + \mathbf{g}^2]^2} \quad (A12)
 \end{aligned}$$

In an analogous manner we write

$$dA_3 = 2\pi \frac{K_3^2}{k_1 k_3} \sin \varphi_I d\varphi_I = 2\pi \frac{\Delta_I}{k_1 k_3} \frac{K_3^2}{k_3} d\Delta_I \quad (A13)$$

and find that Eq. (A12) becomes

$$\begin{aligned}
 2\pi \frac{K_2 K_4}{k_2 k_4} \int \frac{dA_3}{\Delta_I [\Delta_I^2 + \mathbf{g}^2]^2} &= 4\pi^2 \frac{K_2 K_3 K_4}{k_1} \int_{\Delta_{\min}}^{\Delta_{\max}} \frac{d\Delta_I}{[\Delta_I^2 + \mathbf{g}^2]^2} \\
 &= 4\pi^2 \frac{K_2 K_3 K_4}{k_1} I(\Delta_{\min}, \Delta_{\max}) \quad (A14)
 \end{aligned}$$

The integral $I(\Delta_{\min}, \Delta_{\max})$ so defined is given by²⁶

$$I(\Delta_{\min}, \Delta_{\max}) = \frac{1}{2\mathbf{g}^2} \left[\frac{\Delta}{\Delta^2 + \mathbf{g}^2} + \frac{1}{\mathbf{g}} \tan^{-1} \frac{\Delta}{\mathbf{g}} \right] \Big|_{\Delta_{\min}}^{\Delta_{\max}} \quad (A15)$$

Combining the above results we obtain finally

$$\dot{f}_{\mathbf{k}_1} \Big|_{\text{coll}} = - \frac{128\pi^5 e^4}{\hbar^4 k_B^4 v_2 v_3 v_4} [(\pi k_B T)^2 + (\epsilon_1 - E_F)^2] f^0(\epsilon_1) [1 - f^0(\epsilon_1)]$$

$$\phi_{\mathbf{k}} \frac{\frac{K_2 K_3 K_4}{|k_1|}}{I(\Delta_{\min}, \Delta_{\max})} \quad (\text{A16})$$

We may point out here if we had not excluded intraband scattering already, their contribution to $\dot{f}_{\mathbf{k}_1} \Big|_{\text{coll}}$ would now be seen to vanish since in that case, particles 1, 2, and 3, 4 are indistinguishable and consequently $\Delta_{\text{I,II}}$ and $d\Delta_{\text{I,II}}$ must vanish ($\phi_{\text{I}} = \phi_{\text{II}} = \pi$ in Eqs. (A9) or (A10), (A13)).

LIST OF REFERENCES

REFERENCES

1. G. K. White and R. J. Tainsh, Phys. Rev. Letters 19, 165 (1967).
2. C. Herring, Phys. Rev. Letters 13, 167, 684 (E) (1967).
3. J. T. Schriempf, Phys. Rev. Letters 19, 1131 (1967).
4. A. C. Anderson, R. E. Peterson, and J. E. Robichaux, Phys. Rev. Letters 20, 459 (1968).
5. G. K. White and S. B. Woods, Phil. Trans. Roy. Soc. (London) A251, 273 (1958).
6. W. G. Baber, Proc. Roy. Soc. (London) A158, 383 (1937).
7. L. Colquitt, Jr., J. Appl. Phys. 36, 2454 (1965).
8. J. Appel, Phil. Mag. 8, 1071 (1963).
9. N. F. Mott, Proc. Roy. Soc. (London) A156, 368 (1936).
10. J. Appel, Phys. Rev. 122, 1760 (1961).
11. A. H. Wilson, Proc. Roy. Soc. (London) A167, 580 (1938).
12. J. Ziman, Electrons and Phonons (Oxford University Press, Oxford 1963) pp. 403.
13. e.g. A. H. Wilson, Theory of Metals (Cambridge University Press, Cambridge 1953) 2nd ed. p. 6.
14. J. Ziman, Ref. 12, pp. 257.
15. J. Ziman, Ref. 12, pp. 412.
16. J. Ziman, Ref. 12, p. 129.
17. F. J. Blatt and H. R. Fankhauser, Phys. kondens. Materie 3, 183 (1965).
18. D. K. C. McDonald, Thermoelectricity (J. Wiley and Sons, New York 1962) p. 107.
19. In a few exceptional situations S_{pho}^T may be slightly positive at extremely low temperatures.
20. Except at very low temperatures where it may undergo one or two sign changes.

2

1

2

2

2

2

REFERENCES (continued)

21. N. Cusack and P. Kendall, Proc. Phys. Soc. (London) 72, 898 (1958).
22. R. L. Carter, A. I. Davidson and P. A. Schroeder, to be published in J. Phys. Chem. Solids.
23. G. Borelius, Handbuch der Metallphysik (Ed. by Prof. Dr. G. Masing, Akademische Verlagsgesellschaft, Leipzig 1935) p. 185.
24. H. J. Trodahl, Rev. Sci. Instrum. 40, 648 (1969). [see particularly Figure 7].
25. D. Bierens de Haan, Nouvelles Tables d'Integrales Définies (Hafner Publishing Company, New York 1939) Ed. of 1867 - corrected, p. 143.
26. H. B. Dwight, Tables of Integrals and other Mathematical Data (The MacMillan Company, New York 1965) 4th ed. p. 30.

PART II

LATTICE DYNAMICS OF CRYSTALS WITH MOLECULAR IMPURITY CENTERS

I. INTRODUCTION

During the past decade there has developed considerable interest in the study of vibrational spectra of imperfect crystals [1]. The reason for pursuing these investigations is two-fold. First, the effect of the impurity is generally to introduce localized or resonance (pseudo localized) modes in the vibrational spectrum of the ideal lattice. These frequently give rise to observable changes in bulk properties, for example, specific heat [2], resistivity [3], and infrared absorption [1], and a detailed study of these modes can provide useful information on interatomic forces between the impurity and host lattice ions. Second, if the impurity has internal degrees of freedom, the impurity - host lattice interaction can affect a change of the normal modes associated with these degrees of freedom. This is a matter of considerable practical importance since one method often employed in infrared and Raman spectroscopy is to introduce the molecule of interest in a suitable matrix, usually an alkali halide crystal. Depending upon the strength of the interaction between this molecule and the surrounding matrix and the orientation of the defect molecule with respect to the crystallographic axes the recorded spectra will not be characteristic of the free molecule [4-8].

It is generally recognized that a great saving in time and effort can be achieved in the theoretical study of these systems by making optimum use of symmetry properties. Not only does the application of group theory expedite detailed calculations but it also frequently leads to valuable qualitative deduction based on symmetry considerations alone. We shall

demonstrate in section II the group theoretical procedure employed in the solution of such problems in detail, giving not only the decomposition into the irreducible representations of the appropriate subgroup [9] but also the corresponding basis vectors in explicit form. Using the symmetry elements themselves to obtain the stable subspaces rather than a projection operator technique has the advantage that one does not need an explicit matrix representation of the symmetry operations and furthermore only a few symmetry elements are needed for the complete reduction of the total space. The stable subspaces as well as instructive compatibility conditions (section III) for a number of important cases are given in tabular form. As a first example, we shall demonstrate in section IV that a study of the dependence of the infrared absorption on polarization relative to the crystallographic axes already leads to specific information on the orientation of a polyatomic molecule imbedded in a cubic crystal. In a second example, in section V, we shall make optimal use of the symmetry properties while studying the scattering of lattice waves by a stereoscopic defect molecule. In a first subsection on lattice dynamics we give a survey of Wagner's treatment [24, 25] which is most suitable to solve this type of problems. The molecular coordinates are removed by means of a Green's function technique and we are left with a problem of the same dimension as in case of a point defect. However, the difference is that in our case the effective disturbance is complimented by a term which has poles at the molecular frequencies. In the next subsection we develop a scattering formalism and give a formally exact solution of the scattering problem in terms of the T matrix. An expression for the differential cross section is derived. It

contains two terms, the direct term and an interference term, which may be of equal importance. From the form of the two terms it is seen that the scattering processes of phonons are far more complicated than the scattering of plane waves by a static potential. Conditions for such resonances to occur are briefly discussed.

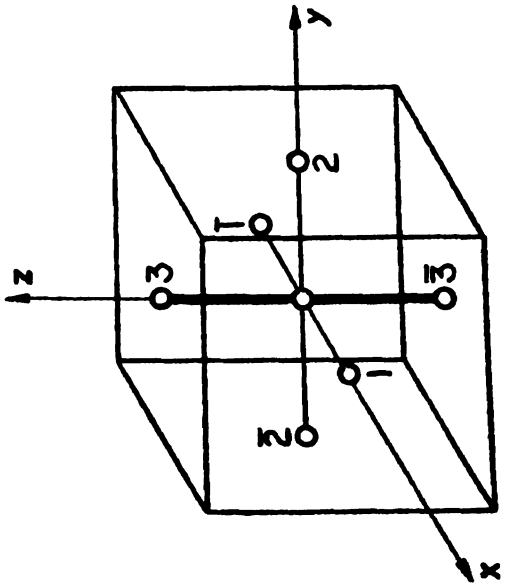
We then consider the following simple model. A rigid sphere is coupled to a simple cubic lattice with tangential as well as radial springs. The eigenvalue problems are solved using the stable subspaces in section II. With this information we construct for each mode the scattering matrix and calculate the matrix elements to obtain the scattering cross section. From the form of these matrix elements we can determine possible initial and final states and decide if the mode is acoustically active. We discuss the conditions under which there may be inband modes but focus our attention to the modes transforming according to the irreducible representations F_{1g} (librational motion) and F_{1u} (motion of the center-of-mass) and estimate the magnitude of the interference term for a specific case. In the next subsection we replace the sphere by a rigid ellipsoid with one moment of inertia different from the other two. In this case the symmetry at the defect site is reduced depending upon the orientation of the molecule. We restrict our analysis to librational modes only. We then conclude with a discussion of some of the details and what we expect in a more realistic situation.

II. USE OF GROUP THEORY TO DETERMINE THE EIGENVECTORS

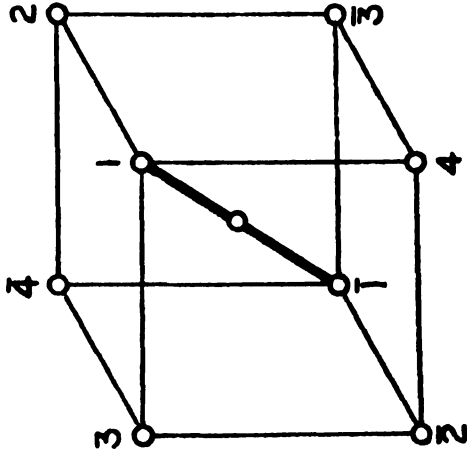
We shall consider the following three basic structures given in Fig. 1.a), b), c). The dimension of the space carrying the total representation S_T is given by the number of points involved. This space is generated by all allowed point group operations as well as translations. For a molecule imbedded in a crystal we must not exclude free rotation operations since these yield the librational modes. The translation of the center-of-mass must be removed, but this is most conveniently done by excluding that set of eigenvectors from the total space which correspond to this motion at the end of the analysis. This results in lowering the dimension by three of the reducible subspace which carries that (those) irreducible representation(s) for which the coordinate axes transform according to the three degrees of freedom of the center-of-mass. With the aid of character tables [9, 10] we decompose the total representation of the symmetry group (or subgroup) G into its irreducible representations and determine their multiplicities m^μ from Frobenius' theorem

$$m^\mu = \frac{1}{g} \sum_{x \in G} \chi(x) \chi^{*\mu}(x) \quad (1)$$

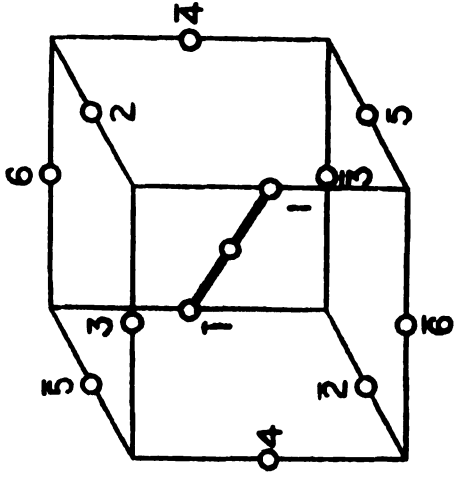
where g is the number of elements in G (order of G) and $\chi^\mu(x)$ is the character of the μ^{th} irreducible representation. From group theoretical theorems [9, 10, 11] we conclude that if the symmetry group involved has c classes then the carrier space of the total representation will decompose into at least c subspaces, the carrier spaces of the row(s) of the c irreducible representations. The dimension d^μ of the μ^{th} irreducible representation gives the degree of its degeneracy due to symmetry, i. e., the number of subspaces with the same eigenvalue. The multiplicity m_T^μ



A



B



C

Figure 1a. Simple cubic structure (A).

Figure 1b. Body-centered cubic structure (B).

Figure 1c. Face-centered cubic structure (C).

The heavy bonds indicate possible orientations of a linear molecule with the center of mass at the origin.

of the μ^{th} irreducible representation in the total representation gives the dimension of the corresponding subspaces which is also the dimension of the eigenvalue problem which we have to solve. These considerations lead, in a natural way, to the correct dynamical eigenvectors which are linear combinations of the vectors which span the stable subspace carrying a particular row of a certain irreducible representation. The idea goes back to some general remarks by Wigner [12] and was also used by Ludwig [13] and Dettmann and Ludwig [14]. The point is that one uses the symmetry elements of the group to decompose the total space S_T into its stable constituents by separating out the subspaces which are spanned by the set of all eigenvectors corresponding either to the eigenvalue +1 or -1 under a specific symmetry operation. The intersection of two spaces obtained in this way is also an invariant subspace. In this manner one gets subspaces, characterized by the eigenvalues of the symmetry operations, by successively operating with commuting group elements and forming intersections until the subspace has the correct dimension. Symmetry elements not used in this procedure can not lead to a further reduction because the multiplicity is determined with consideration of the full symmetry group. This is the reason (and advantage compared to projector technique where one has to have an explicit matrix representation of all the symmetry elements) that one needs only a few of the symmetry elements.

In order to introduce our notation let us consider the operation of the inversion I on the total space corresponding to the structure A

$$S_T^A = \{ \bar{3}_x \bar{3}_y \bar{3}_z \mid \bar{2}_x \bar{2}_y \bar{2}_z \mid \bar{1}_x \bar{1}_y \bar{1}_z \mid 0_x 0_y 0_z \mid 1_x 1_y 1_z \mid 2_x 2_y 2_z \mid 3_x 3_y 3_z \} \quad (2)$$

$$I S_T^A = - \{ 3_x 3_y 3_z \mid 2_x 2_y 2_z \mid 1_x 1_y 1_z \mid 0_x 0_y 0_z \mid \bar{1}_x \bar{1}_y \bar{1}_z \mid \bar{2}_x \bar{2}_y \bar{2}_z \mid \bar{3}_x \bar{3}_y \bar{3}_z \} \quad (3)$$

where the curly bracket is a compact notation for the set of the vectors

spanning the 21-dimensional space. The numbers label the lattice points and x, y, z are the components of the displacements from equilibrium position. In what follows it is important always to bear in mind that whatever stands in the place 3_z , say, as introduced in the curly bracket of Eq. (2) represents the displacement of the point 3 in the z-direction, hence $\dots |aab|00\bar{b}\}$ means that the displacements of the lattice point 2 in the x and y direction are related and equal a , the displacement of point 2 in the z direction is b and is opposite to the z displacement of point 3 which is the only possible motion for the latter point. From Eq. (3) we determine by inspection the two subspaces invariant under inversion, one corresponding to the eigenvalue $+1$, one to -1 , respectively:

$$S_{\bar{I}}^A = \{ \bar{x}_3 \bar{y}_3 \bar{z}_3 | \bar{x}_2 \bar{y}_2 \bar{z}_2 | \bar{x}_1 \bar{y}_1 \bar{z}_1 | 0 \ 0 \ 0 | x_1 y_1 z_1 | x_2 y_2 z_2 | x_3 y_3 z_3 \} \quad (4a)$$

$$S_{\bar{I}}^A = \{ x_3 y_3 z_3 | x_2 y_2 z_2 | x_1 y_1 z_1 | x_0 y_0 z_0 | x_1 y_1 z_1 | x_2 y_2 z_2 | x_3 y_3 z_3 \} \quad (4b)$$

and we note that in case of inversion symmetry the displacements at a point $\underline{\epsilon}^n = (n_x \ n_y \ n_z)$ and that of the inverted point $\bar{n} \ \underline{\epsilon}^{\bar{n}} = (\bar{n}_x \ \bar{n}_y \ \bar{n}_z)$ are related by

$$\underline{\epsilon}_g^n = - \underline{\epsilon}_g^{\bar{n}} \quad (5a)$$

$$\underline{\epsilon}_u^n = \underline{\epsilon}_u^{\bar{n}} \quad (5b)$$

for the eigenvalues $+1$ ($g = \text{gerade}$) and -1 ($u = \text{ungerade}$) respectively.

In order to demonstrate how one obtains the intersection of two stable subspaces we first determine the stable subspace of another symmetry element, σ_z , say, a reflection in the mirror plane perpendicular to the z axis

$$\sigma_z S_I^A = \{3_{x_3 y_3} \bar{z}_3 | \bar{2}_{x_2 y_2} \bar{z}_2 | \bar{1}_{x_1 y_1} \bar{z}_1 | 0_{x_0 y_0} \bar{z}_0 | 1_{x_1 y_1} \bar{z}_1 | 2_{x_2 y_2} \bar{z}_2 | \bar{3}_{x_3 y_3} \bar{z}_3\} \quad (6)$$

with the stable subspaces

$$S_{\sigma_z}^A = \{x_3 y_3 \bar{z}_3 | x_5 y_5^0 | x_4 y_4^0 | x_0 y_0^0 | x_1 y_1^0 | x_2 y_2^0 | x_3 y_3 z_3\} \quad (7a)$$

$$S_{\sigma_z}^A = \{\bar{x}_3 \bar{y}_3 z_3 | 0_{z_5} | 0_{z_4} | 0_{z_0} | 0_{z_1} | 0_{z_2} | x_3 y_3 z_3\} \quad (7b)$$

for the eigenvalues +1 and -1, respectively. The intersection

$$S_{I\sigma_z}^A = S_I^A \cap S_{\sigma_z}^A$$

is then given by the parts of the subspaces which are compatible with one-another, i.e., that subspace which is stable

under inversion, either with eigenvalue +1 or -1, as well as under the

operation σ_z corresponding to a certain eigenvalue. Let us concentrate

on the following two cases

$$S_{I\sigma_z}^{A++} = S_I^{A++} \cap S_{\sigma_z}^{A++} = \{0_{z_3} | \bar{x}_2 \bar{y}_2^0 | \bar{x}_1 \bar{y}_1^0 | 0_{z_0} | x_1 y_1^0 | x_2 y_2^0 | 0_{z_3}\} \quad (8a)$$

$$S_{I\sigma_z}^{A-+} = S_I^{A-+} \cap S_{\sigma_z}^{A-+} = \{x_3 y_3^0 | x_2 y_2^0 | x_1 y_1^0 | x_0 y_0^0 | x_1 y_1^0 | x_2 y_2^0 | x_3 y_3^0\} \quad (8b)$$

and suppose that we are dealing with full cubic (octahedral) symmetry.

Then from the character table for the group O_h we see that the carrier

spaces S^μ for the irreducible representations A_{1g} , A_{2g} , and E_g respective-

ly are subspaces of the intersection $S_{I\sigma_z}^{++}$, i.e., $S^{A_{1g}} \subset S_{I\sigma_z}^{++}$ etc.,

whereas the intersection $S_{I\sigma_z}^{-+}$ contains the stable subspaces carrying

the irreducible representations F_{1u} and F_{2u} respectively, i.e.,

$S^{F_{1u}} \subset S_{I\sigma_z}^{-+}$ and $S^{F_{2u}} \subset S_{I\sigma_z}^{-+}$. The dimensions of the intersections obtained

here are in this case higher than the corresponding multiplicities of the irreducible representations and one has to proceed with other symmetry elements in a similar fashion.

In tables I to IX the stable subspaces, which are not normalized, are listed for a number of important cases. The ones for the full cubic group O_h are given for all three structures shown in Fig. 1. For the structure of type A (Fig. 1a) the decomposition of the 21 dimensional total space into its stable subspaces is presented for the subgroups D_{4h} , D_{3d} and D_{2h} . As examples of structure B the subgroups T_d and D_{3d} are considered. Finally, the 39 dimensional carrier space of the total representation corresponding to the structure C is split into its stable constituents for the subgroup D_{2h} .

In the first column only those irreducible representations of the (sub)group are listed, which are part of the total representation. In the next three columns the multiplicities m_i^μ of the corresponding irreducible representations are given. The first of these is for the case where one allows for vibrations only, the next corresponds to librational (quasi-rotational) motion only; and the last includes all degrees of freedom. Clearly, the difference m_t^μ

$$m_t^\mu = m_T^\mu - (m_v^\mu + m_r^\mu) \quad (9)$$

is associated with the translational degrees of freedom and we now have to exclude translations of the center-of-mass explicitly.

As an example let us consider the 3 dimensional stable subspace carrying the first row of the irreducible representation F_{1u}^1 of O_h (table I.). From the information given in the table we see that we

Table II. Stable subspaces of the subgroup D_{4h} , structure A.

D_{4h}	m_V^μ	m_I^μ	m_T^μ	Stable Subspaces								
				3	Z	I	0	1	2	3		
A_{1g}	2	0	2	$\{0 \ 0 \ z_3 \mid 0 \ x_1 \ 0 \mid x_1 \ 0 \ 0 \mid 0 \ 0 \ 0 \mid \bar{x}_1 \ 0 \ 0 \mid 0 \ \bar{x}_1 \ 0 \mid 0 \ 0 \ z_3\}$								
A_{2g}	0	1	1	$\{0 \ 0 \ 0 \mid \bar{y}_1 \ 0 \ 0 \mid 0 \ y_1 \ 0 \mid$								
B_{1g}	1	0	1	$\{0 \ 0 \ 0 \mid 0 \ \bar{x}_1 \ 0 \mid x_1 \ 0 \ 0 \mid$								
B_{2g}	1	0	1	$\{0 \ 0 \ 0 \mid y_1 \ 0 \ 0 \mid 0 \ y_1 \ 0 \mid$								
E_g^1	1	1	2	$\{x_3 \ 0 \ 0 \mid 0 \ 0 \ 0 \mid 0 \ 0 \ z_1 \mid$								
E_g^2	1	1	2	$\{0 \ y_3 \ 0 \mid 0 \ 0 \ z_2 \mid 0 \ 0 \mid$								
A_{2u}	2	0	3	$\{0 \ 0 \ z_3 \mid 0 \ 0 \ z_1 \mid 0 \ 0 \ z_1 \mid 0 \ 0 \ z_0 \mid 0 \ z_1 \mid 0 \ 0 \ z_1 \mid 0 \ 0 \ z_3\}$								
B_{2u}	1	0	1	$\{0 \ 0 \ 0 \mid 0 \ 0 \ \bar{z}_1 \mid 0 \ 0 \ z_1 \mid 0 \ 0 \mid$								
E_u^1	3	0	4	$\{x_3 \ 0 \ 0 \mid x_2 \ 0 \ 0 \mid x_1 \ 0 \ 0 \mid x_0 \ 0 \ 0 \mid$								
E_u^2	3	0	4	$\{0 \ y_3 \ 0 \mid 0 \ y_2 \ 0 \mid 0 \ y_1 \ 0 \mid 0 \ y_0 \ 0 \mid$								

Table III. Stable subspaces of the subgroup D_{3d} , structure A.

D_{3d}	μ_{m_V}	μ_{m_I}	μ_{m_T}	Stable Subspaces							
				$\bar{3}$	$\bar{2}$	$\bar{1}$	0	1	2	3	
A_{1g}	2	0	2	$\{y_1 y_1 x_1 y_1 x_1 y_1 x_1 y_1 y_1 0\}$	$\{x_1 y_1 y_1 0\}$	$\{\bar{x}_1 \bar{y}_1 \bar{y}_1 \bar{y}_1 \bar{x}_1 \bar{y}_1 \bar{y}_1 \bar{y}_1 \bar{x}_1 \bar{x}_1 \bar{y}_1 \bar{y}_1 \bar{y}_1 \bar{y}_1 \bar{x}_1\}$					
A_{2g}	0	1	1	$\{\bar{y}_1 y_1 0 y_1 0 \bar{y}_1 0 \bar{y}_1 y_1 \}$							
E_g^1	2	1	3	$\{x_3^+ x_3^{+2\bar{x}_1} y_1 x_1 z_1 x_1 y_1 z_1 \}$							
E_g^2	2	1	3	$\{\bar{x}_3^- x_3^- \bar{y}_1 \bar{x}_1 \bar{z}_1 x_1 y_1 z_1 \}$							
A_{1u}	1	0	1	$\{\bar{y}_1 y_1 0 y_1 0 \bar{y}_1 0 \bar{y}_1 y_1 0\}$	$\{0\}$	$\{\bar{y}_1 y_1 y_1 0 \bar{y}_1 y_1 y_1 0\}$					
A_{2u}	2	0	3	$\{y_1 y_1 x_1 y_1 x_1 y_1 x_1 y_1 y_1 x_0 x_0\}$							
E_u^1	3	0	4	$\{x_3^+ x_3^{+2\bar{x}_1} y_1 x_1 z_1 x_1 y_1 z_1 x_0 x_0\}$							
E_u^2	3	0	4	$\{\bar{x}_3^- x_3^- \bar{y}_1 \bar{x}_1 \bar{z}_1 x_1 y_1 z_1 \bar{x}_0 x_0\}$							

$$x_3^\pm = -(z_1 \pm y_1)$$

Table IV. Stable subspaces of the subgroup D_{2h} , structure A.

D_{2h}	m_V^μ	m_I^μ	m_T^μ	Stable Subspaces								
				$\bar{3}$	$\bar{2}$	$\bar{1}$	$\bar{1}$	$\bar{0}$	$\bar{0}$	$\bar{1}$	$\bar{2}$	$\bar{3}$
A_{1g}	3	0	3	$\{0 \ 0 \ z_3 \mid y_1 \ x_1 \ 0 \mid x_1 \ y_1 \ 0 \mid 0 \ 0 \ 0 \mid \bar{x}_1 \ \bar{y}_1 \ 0 \mid \bar{y}_1 \ \bar{x}_1 \ 0 \mid 0 \ 0 \ \bar{z}_3\}$								
B_{1g}	1	1	2	$\{\bar{x}_3 \ x_3 \ 0 \mid 0 \ 0 \ \bar{z}_1 \mid 0 \ 0 \ z_1 \mid$								
B_{2g}	1	1	2	$\{x_3 \ x_3 \ 0 \mid 0 \ 0 \ z_1 \mid 0 \ 0 \ z_1 \mid$								
B_{3g}	1	1	2	$\{0 \ 0 \ 0 \mid \bar{y}_1 \ \bar{x}_1 \ 0 \mid x_1 \ y_1 \ 0 \mid$								
A_{1u}	1	0	1	$\{0 \ 0 \ 0 \mid 0 \ 0 \ \bar{z}_1 \mid 0 \ 0 \ z_1 \mid 0 \ 0 \ 0 \mid 0 \ 0 \ 0 \mid z_1 \mid 0 \ 0 \ \bar{z}_1 \mid 0 \ 0 \ 0\}$								
B_{1u}	3	0	4	$\{x_3 \ x_3 \ 0 \mid y_1 \ x_1 \ 0 \mid x_1 \ y_1 \ 0 \mid x_0 \ x_0 \ 0 \mid$								
B_{2u}	3	0	4	$\{\bar{x}_3 \ x_3 \ 0 \mid \bar{y}_1 \ \bar{x}_1 \ 0 \mid x_1 \ y_1 \ 0 \mid \bar{x}_0 \ x_0 \ 0 \mid$								
B_{3u}	2	0	3	$\{0 \ 0 \ z_3 \mid 0 \ 0 \ z_1 \mid 0 \ 0 \ z_1 \mid 0 \ 0 \ z_0 \mid$								

Table VII. Stable subspaces of the subgroup D_{3d} , structure B.

D_{3d}	m_V^μ	m_I^μ	m_T^μ	Stable Subspaces						
				$\bar{4}$	$\bar{3}$	$\bar{2}$	$\bar{1}$	0	1	2
A_{1g}	3	0	3	$\{y_2 y_2 x_2 y_2 x_2 y_2 x_2 y_2 y_2 x_1 x_1 0 0 0 \bar{x}_1 \bar{x}_1 \bar{x}_2 \bar{y}_2 \bar{y}_2 \bar{x}_2 \bar{y}_2 \bar{y}_2 \bar{y}_2 \bar{x}_2\}$						
A_{2g}^1	0	1	1	$\{\bar{y}_2 y_2 0 y_2 0 \bar{y}_2 0 \bar{y}_2 y_2 0 0 0 $						
E_g^1	3	1	4	$\{x_4^+ x_4^+ 2\bar{x}_2 y_2 x_2 z_2 x_2 y_2 z_2 x_1 x_1 2\bar{x}_1 $						
E_g^2	3	1	4	$\{\bar{x}_4^- x_4^- 0 \bar{y}_2 \bar{x}_2 z_2 \bar{x}_2 y_2 z_2 \bar{x}_1 x_1 0 $						
A_{1u}	1	0	1	$\{\bar{y}_2 y_2 0 y_2 0 \bar{y}_2 0 \bar{y}_2 y_2 0 0 0 0 0 0 0 0 0 \bar{y}_2 y_2 y_2 0 \bar{y}_2 \bar{y}_2 y_2 0\}$						
A_{2u}^1	3	0	4	$\{y_2 y_2 x_2 y_2 x_2 y_2 x_2 y_2 y_2 x_1 x_1 x_0 x_0 $						
E_u^1	4	0	5	$\{x_4^+ x_4^+ 2\bar{x}_2 y_2 x_2 z_2 x_2 y_2 z_2 x_1 x_1 2\bar{x}_1 x_0 x_0 2\bar{x}_0 $						
E_u^2	4	0	5	$\{\bar{x}_4^- x_4^- 0 \bar{y}_2 \bar{x}_2 z_2 \bar{x}_2 y_2 z_2 \bar{x}_1 x_1 0 \bar{x}_0 x_0 0 $						

$$x_4^+ = -(z_2 + y_2)$$

Table VIII. Stable subspaces of the full cubic group O_h , structure C.

O_h	m_V^μ	m_T^μ	m_I^μ	Stable Subspaces												
				$\bar{6}$	$\bar{5}$	$\bar{4}$	$\bar{3}$	$\bar{2}$	$\bar{1}$	0	1	2	3	4	5	6
A_{1g}	1	0	1	$\{\bar{x}_1^0 x_1 0 x_1 \bar{x}_1 x_1 \bar{x}_1^0 x_1^0 x_1 0 x_1 x_1 x_1 x_1^0 0 0 0 \bar{x}_1 \bar{x}_1^0 0 \bar{x}_1 \bar{x}_1^0 \bar{x}_1^0 \bar{x}_1 \bar{x}_1^0 \bar{x}_1 \bar{x}_1^0 \bar{x}_1 0 \bar{x}_1 x_1 0 \bar{x}_1 x_1 x_1^0 \bar{x}_1\}$												
A_{2g}	1	0	1	$\{x_1^0 x_1 0 x_1 x_1 x_1 x_1^0 \bar{x}_1^0 x_1 0 x_1 \bar{x}_1 x_1 \bar{x}_1^0 $												
E_g^1	2	0	2	$\{\bar{y}_2^0 z_2 0 y_2 \bar{z}_2 x_4^+ \bar{x}_4^+ y_2^0 z_2 0 y_2 z_2 x_4^+ x_4^+ $												
E_g^2	2	0	2	$\{y_2^0 \bar{z}_2 0 y_2 \bar{z}_2 x_4^- \bar{x}_4^- \bar{y}_2^0 \bar{z}_2 0 y_2 z_2 x_4^- \bar{x}_4^- $												
E_{1g}	1	1	2	$\{x_3^0 x_3 z_1^0 0 0 0 z_1 x_3^0 \bar{x}_3 \bar{z}_1^0 0 0 0 z_1 $												
F_{1g}^2	1	1	2	$\{0 \bar{z}_1^0 0 \bar{y}_2 \bar{y}_2 0 0 \bar{z}_1 0 \bar{z}_1^0 0 y_2 \bar{y}_2 0 0 z_1 $												
F_{1g}^3	1	1	2	$\{0 x_2^0 x_2^0 0 x_1 x_1^0 0 \bar{x}_2^0 0 x_2^0 x_2^0 0 x_1 \bar{x}_1^0 $												
F_{2g}^1	2	0	2	$\{x_3^0 \bar{x}_3 \bar{z}_1^0 0 0 0 z_1 x_3^0 x_3 z_1^0 0 0 0 z_1 $												
F_{2g}^2	2	0	2	$\{0 z_1^0 0 \bar{y}_2 y_2 0 0 \bar{z}_1 0 z_1^0 0 y_2 y_2 0 0 z_1 $												
F_{2g}^3	2	0	2	$\{0 \bar{x}_2^0 x_2^0 0 \bar{x}_1 x_1^0 0 x_2^0 0 x_2^0 x_2^0 0 x_1 x_1^0 $												
A_{2u}	1	0	1	$\{0 \bar{z}_1^0 \bar{z}_1^0 0 0 0 \bar{z}_1 0 z_1^0 z_1^0 0 0 0 z_1 0 0 0 0 0 z_1 z_1^0 0 0 z_1^0 0 0 \bar{z}_1 \bar{z}_1^0 0 0 \bar{z}_1^0\}$												
E_u^1	1	0	1	$\{0 x_2^0 \bar{x}_2^0 0 0 0 0 0 \bar{x}_2^0 0 x_2^0 x_2^0 0 0 0 0 $												
E_u^2	1	0	1	$\{0 z_1^0 0 0 0 0 0 \bar{z}_1 0 \bar{z}_1^0 0 0 0 0 0 z_1 0 0 0 $												
F_{1u}^1	3	0	4	$\{x_1^0 \bar{y}_1 x_2^0 0 x_1 \bar{y}_1^0 x_1^0 y_1 x_2^0 0 x_1 y_1^0 x_1 y_1^0 x_1^0 0 $												
F_{1u}^2	3	0	4	$\{0 y_3^0 0 y_1 \bar{x}_1 \bar{x}_1 y_1^0 0 y_3^0 0 y_1 x_1 x_1 y_1^0 0 y_3^0 $												
F_{1u}^3	3	0	4	$\{\bar{y}_2^0 z_2 0 \bar{y}_2 z_2 0 0 z_1 y_2^0 z_2 0 y_2 z_2 0 0 z_1 0 0 z_1 $												

Table VIII. (cont'd.)

O_h	m_V^μ	m_T^μ	m_T^μ	Stable Subspaces											
			$\bar{6}$	$\bar{5}$	$\bar{4}$	$\bar{3}$	$\bar{2}$	$\bar{1}$	0	1	2	3	4	5	6
F_{2u}^1	2	0	2	$\{y_2^0 \bar{z}_2^0 0 \bar{y}_2 z_2^0 0 0 0 \bar{y}_2^0 \bar{z}_2^0 0 y_2 z_2^0 0 0 0 0 0 0 $											
F_{2u}^2	2	0	2	$\{\bar{x}_1^0 y_1^0 0 0 0 x_1 \bar{y}_1^0 \bar{x}_1^0 \bar{y}_1^0 0 0 0 x_1 y_1^0 0 0 0 $											
F_{2u}^3	2	0	2	$\{0 0 0 0 \bar{y}_1 x_1 \bar{x}_1 y_1^0 0 0 0 0 0 0 0 \bar{y}_1 \bar{x}_1 x_1 y_1^0 0 0 0 $											

$$x_4^\pm = -(y_2 \pm z_2)$$

Table IX. Stable subspaces of the subgroup D_{2h} , structure C.

D_{2h}	m_v^μ	m_r^μ	m_T^μ	Stable Subspaces						
				$\bar{6}$	5	4	3	2	1	0
A_g	5	0	5	$\{\bar{y}_2 \bar{x}_2 z_2 x_2 y_2 \bar{z}_2 \bar{x}_4 x_4 0 y_2 x_2 z_2 x_2 y_2 z_2 x_1 x_1 0 0 0 0 \bar{x}_1 \bar{x}_1 0 \bar{x}_2 \bar{y}_2 \bar{z}_2 \bar{y}_2 \bar{x}_2 \bar{z}_2 x_4 \bar{x}_4 0 \bar{x}_2 \bar{y}_2 z_2 y_2 x_2 \bar{z}_2\}$						
B_{1g}	3	1	4	$\{\bar{y}_2 \bar{x}_2 z_2 \bar{x}_2 \bar{y}_2 z_2 0 0 z_4 \bar{y}_2 \bar{x}_2 \bar{z}_2 x_2 y_2 z_2 0 0 0 $						
B_{2g}	3	1	4	$\{y_2 x_2 \bar{z}_2 \bar{x}_2 \bar{y}_2 z_2 0 0 0 y_2 x_2 z_2 x_2 y_2 z_2 0 0 z_1 $						
B_{3g}	4	1	5	$\{y_2 x_2 \bar{z}_2 x_2 y_2 \bar{z}_2 x_4 x_4 0 \bar{y}_2 \bar{x}_2 \bar{z}_2 x_2 y_2 z_2 \bar{x}_1 x_1 0 $						
A_u	3	0	3	$\{y_2 x_2 \bar{z}_2 \bar{x}_2 \bar{y}_2 z_2 0 0 0 \bar{y}_2 \bar{x}_2 \bar{z}_2 x_2 y_2 z_2 0 0 0 0 0 0 0 0 0 x_2 y_2 z_2 \bar{y}_2 \bar{x}_2 \bar{z}_2 0 0 0 \bar{x}_2 \bar{y}_2 z_2 y_2 x_2 \bar{z}_2\}$						
B_{1u}	5	0	6	$\{y_2 x_2 \bar{z}_2 x_2 y_2 \bar{z}_2 x_4 x_4 0 y_2 x_2 z_2 x_2 y_2 z_2 x_1 x_1 0 x_0 x_0 0 $						
B_{2u}	5	0	6	$\{\bar{y}_2 \bar{x}_2 z_2 x_2 y_2 \bar{z}_2 \bar{x}_4 x_4 0 \bar{y}_2 \bar{x}_2 \bar{z}_2 x_2 y_2 z_2 \bar{x}_1 x_1 0 \bar{x}_0 x_0 0 $						
B_{3u}	5	0	6	$\{\bar{y}_2 \bar{x}_2 z_2 \bar{x}_2 \bar{y}_2 z_2 0 0 z_4 y_2 x_2 z_2 x_2 y_2 z_2 0 0 z_1 0 0 z_0 $						

ba

po

sa

sa

Th

i

c

H

f

n

i

v

c

s

r

t

u

v

w

x

y

z

have to reduce the dimension of this carrier space by one. If the set of points involved is occupied by atoms of equal mass then the obvious, necessary but not sufficient, condition is that the following equality not be satisfied

$$x_0 = x_1 = x_2 . \quad (10)$$

The necessary and sufficient condition is

$$\sum_n \xi^n = 0, \text{ not all } \xi^n = 0 \quad (11)$$

i.e., that the components of the displacements be linearly dependent. This condition is in the special case which we are considering

$$x_0 + 2x_1 + 4x_2 = 0 . \quad (12)$$

However, the reduction of the dimension of the carrier space in question follows in a more natural way if one looks at the dynamical problem. As mentioned above the multiplicity m_T^μ of the μ^{th} irreducible representation in the total representation gives the dimension of the eigenvalue problem which we have to solve. One of the three roots of the secular equation in our example will be zero and it is that set of eigenvectors, which is associated with this particular eigenvalue, which we have to exclude.

The remaining columns give the components of the displacements which span the m_T^μ dimensional stable subspace associated with the μ^{th} irreducible representation. Frequent use of the relations (5a, b) was made.

III. COMPATIBILITY CONDITIONS

There are two obvious physical situations for which compatibility conditions similar to the compatibility relations derived in band theory of crystals [15] will be useful. First, if one introduces a polyatomic molecule into a crystal lattice then generally the symmetry of the system is reduced. One then wishes to determine first if any of the degenerate representations are split, and secondly, what restrictions are imposed on the corresponding eigenvectors under the new circumstances. The same questions also arise if one applies stress, an external electric or a magnetic field to a crystal. The first part of the problem is answered by the correlation tables for the species of a group and its subgroups given in the literature [9], whereas the answer to the latter part is more difficult since the eigenvectors found in the literature are usually presented in pictorial form [16]. The problem is then to establish a set of linear equations relating the components of the stable subspaces of the full cubic group with those of the carrier spaces of the irreducible representation of the subgroup into which the irreducible representations of the group of higher order decompose according to the correlation table. This is done using the stable subspaces given in section II. This procedure often leads to a reduction of the free parameters of the stable subspaces involved since the stable subspaces of a subgroup frequently have a higher dimension than the corresponding stable subspaces of the group of higher order. As an example, let us consider in the case of structure B the conditions imposed on the modes transforming according to the irreducible representations A_{2u} or E_u

into which a mode transforming according to the first row of the irreducible representation F_{1u}^1 splits if the symmetry of the system is lowered from O_h to D_{3d} . From tables V and VII we use the corresponding stable subspaces.

$$A_{2u} : \{ y_2 \ y_2 \ x_2 | y_2 \ x_2 \ y_2 | x_2 \ y_2 \ y_2 | x_1 \ x_1 \ x_1 | x_0 \ x_0 \ x_0 | \quad (13a)$$

$$E_u^1 : \{ x_4' \ x_4' \ 2\bar{x}_4' | x_2' \ x_2' \ z_2' | x_2' \ x_2' \ z_2' | x_1' \ x_1' \ 2\bar{x}_1' | x_0' \ x_0' \ 2\bar{x}_0' | \quad (13b)$$

$$E_u^2 : \{ \bar{x}_4'' \ x_4'' \ 0 | x_2'' \ \bar{x}_2'' \ \bar{z}_2'' | x_2'' \ \bar{x}_2'' \ z_2'' | \bar{x}_1'' \ x_1'' \ 0 | \bar{x}_0'' \ x_0'' \ 0 | \quad (13c)$$

$$F_{1u}^1 : \{ x_1 \ y_1 \ \bar{y}_1 | x_1 \ \bar{y}_1 \ y_1 | x_1 \ \bar{y}_1 \ \bar{y}_1 | x_1 \ y_1 \ y_1 | x_0 \ 0 \ 0 | \quad (14)$$

We note that the stable subspace carrying the first row of the irreducible representation F_{1u}^1 is 3 dimensional whereas the stable subspaces carrying A_{2u} and E_u , respectively, are 4 and 5 dimensional, respectively. This means that the relations between the components of the stable subspaces corresponding to the lower symmetry may not contain more than 3 free parameters, a, b, c, respectively. These relations and restrictions are what we call the compatibility conditions. The sets of the relevant linear equations are

$$x_0 + x_0' - x_0'' = a \quad (15a)$$

$$x_0 + x_0' + x_0'' = 0 \quad (15b)$$

$$x_0 - 2x_0' = 0 \quad (15c)$$

$$x_1 + x_1' - x_1'' = b \quad (16a)$$

$$x_1 + x_1' - x_1'' = c \quad (16b)$$

$$x_1 - 2x_1' = c \quad (16c)$$

$$x_2 + x_2' + x_2'' = b \quad (17a)$$

$$y_2 + x_2' - x_2'' = -c \quad (17b)$$

$$y_2 + z_2' + z_2'' = -c \quad (17c)$$

$$y_2 + x_2' + x_2'' = b \quad (17d)$$

$$x_2 + x_2' - x_2'' = -c \quad (17e)$$

$$y_2 + z_2' - z_2'' = c \quad (17f)$$

$$y_2 + x_4' - x_4'' = b \quad (18a)$$

$$y_2 + x_4' + x_4'' = c \quad (18b)$$

$$x_2 - 2x_4' = -c \quad (18c)$$

with the solutions

$$x_0 = \frac{1}{3}a, \quad x_0' = \frac{1}{6}a, \quad x_0'' = -\frac{1}{2}a \quad (19 \text{ a, b, c})$$

$$x_1 = \frac{1}{3}(b+2c), \quad x_1' = \frac{1}{6}(b-c), \quad x_1'' = \frac{1}{2}(c-b) \quad (20 \text{ a, b, c})$$

$$x_2 = \frac{1}{3}b, \quad x_2' = \frac{1}{6}(b-3c), \quad x_2'' = \frac{1}{2}(b+c) \quad (21 \text{ a, b, c})$$

$$y_2 = \frac{1}{3}b, \quad z_2' = -\frac{1}{3}b, \quad z_2'' = -c \quad (22 \text{ a, b, c})$$

$$x_4' = \frac{1}{6}(b+3c), \quad x_4'' = \frac{1}{2}(c-b) . \quad (23 \text{ a, b})$$

In tables X to XIV we list these conditions in full for the subgroups D_{4h} , D_{3d} and D_{2h} in case of a structure of type A; for the subgroup D_{3d} with structure B, as well as for the subgroup D_{2h} with structure C we will give the compatibility conditions only for those irreducible representations according to which the infrared active modes transform.

In the first column the irreducible representations of the full cubic group are listed and in the next column the correlation table of the

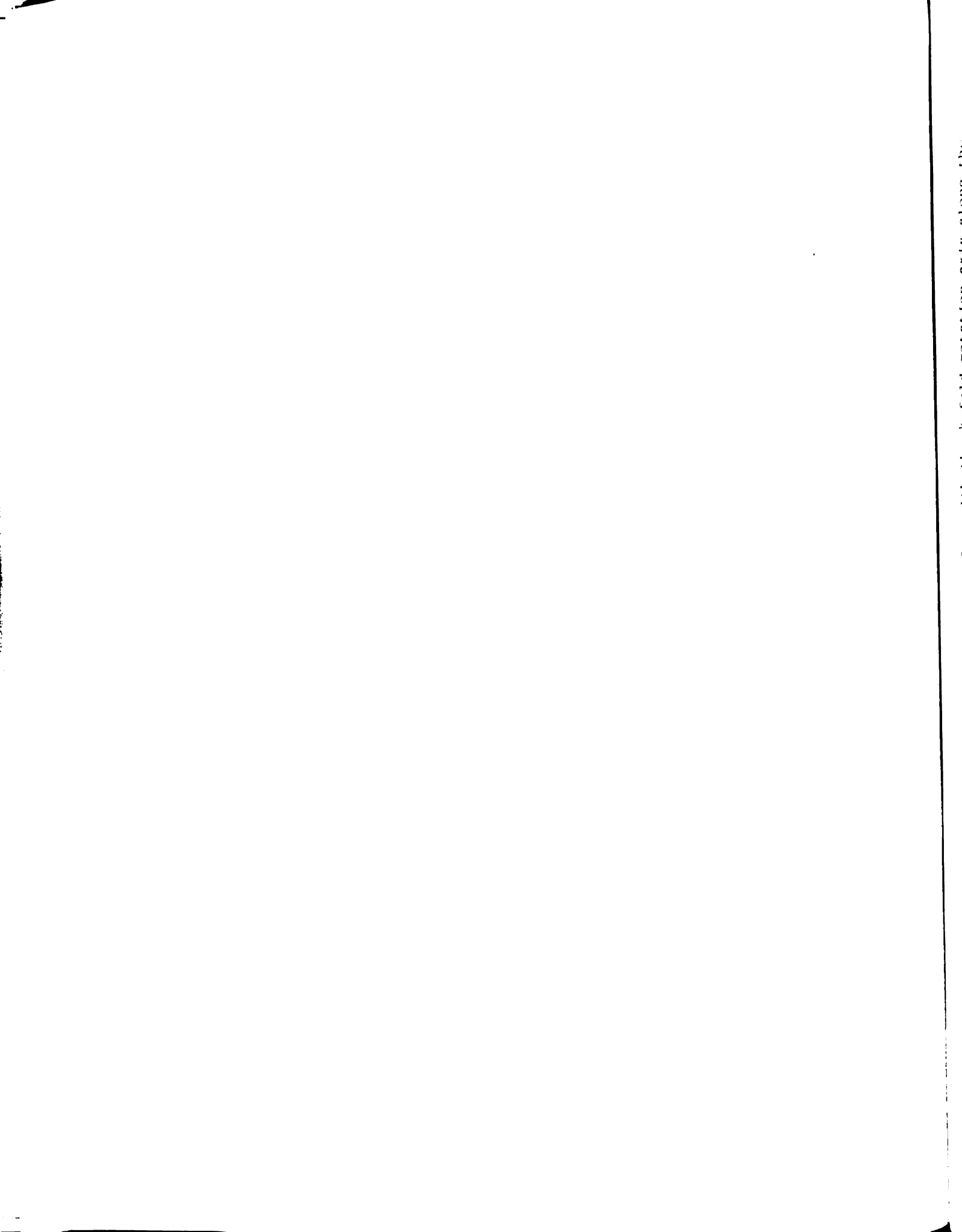


Table XI. Compatibility conditions for the subgroup D_{3d} with the 3-fold rotation axis along the

O_h	D_{3d}	Compatibility Conditions						E_u^2				
		A_{1g} $x_1 y_1$	A_{2g} y_1	E_g^1 $x_1 y_1 z_1$	E_g^2 $x_1 y_1 z_1$	A_{1u} y_1	A_{2u} $x_0 x_1 y_1$		E_u^1 $x_0 x_1 y_1 z_1$			
A_{1g}	A_{1g}	a	0									
E_g^1	E_g	a	0	0	0	$-$	$-$	$-$	$-$	$-$	$-$	$-$
E_g^2		$-$	$-$	a	0	0	0	0	0	0	0	0
F_{1g}^1	$A_{2g} + E_g$	0	0	0	0	$3a$	0	$2\bar{a}$	0	0	0	0
F_{1g}^2		0	0	0	0	$3a$	0	$2a$	0	0	0	0
F_{1g}^3		$-$	$-$	$-$	0	0	0	$2a$	0	0	0	0
F_{2g}^1	$A_{1g} + E_g$	0	$2a$	0	0	$2\bar{a}$	0	0	0	0	0	$3\bar{a}$
F_{2g}^2		0	$2a$	0	0	$2\bar{a}$	0	0	0	0	0	$3a$
F_{2g}^3		0	a	0	0	$2a\bar{a}$	$-$	$-$	$-$	$-$	$-$	$-$
F_{1u}^1	$A_{2u} + E_u$								$2a$	$2b$	$2c$	$3\bar{a}$
F_{1u}^2									$2a$	$2c$	$2b$	$3a$
F_{1u}^3									a	c	b	$-$
F_{2u}^1	$A_{1u} + E_u$							$2a$				0
F_{2u}^2								$2\bar{a}$				0
F_{2u}^3								a				0

Table XII. Compatibility conditions for the subgroup D_{2h} with the 2-fold ζ -axis oriented along the $[110]$ -direction of the cube in case of Structure A.

O_h	D_{2h}	Compatibility Conditions											
		A_{1g} $x_1 y_1 z_3$	B_{1g} $z_1 x_3$	B_{2g} $z_1 x_3$	B_{3g} $x_1 y_1$	A_{1u} z_1	B_{1u} $x_0 x_1 y_1 x_3$	B_{2u} $x_0 x_1 y_1 x_3$	B_{3u} $z_0 z_1 z_3$				
A_{1g}	A_{1g}	a 0 a											
E_g^1	$A_{1g} + B_{3g}$	a 0 $2\bar{a}$			-								
E_g^2		- - -			a 0								
F_{1g}^1	$B_{1g} + B_{2g} + B_{3g}$		\bar{a} a	a \bar{a}	-								
F_{1g}^2		a a	a \bar{a}	a \bar{a}	-								
F_{1g}^3		- - -	-	-	0 a								
F_{2g}^1	$A_{1g} + B_{1g} + B_{2g}$	- - -	\bar{a} a	a a									
F_{2g}^2		- - -	a \bar{a}	a a									
F_{2g}^3		0 a 0	-	-	-								
F_{1u}^1	$B_{1u} + B_{2u} + B_{3u}$						a b c c	\bar{a} b c c	\bar{c}	-	-	-	-
F_{1u}^2							a c b b	a \bar{c} b b	b	-	-	-	-
F_{1u}^3							- - -	- - -	-	-	a b c		
F_{2u}^1	$A_{1u} + B_{1u} + B_{2u}$					-	0 0 a \bar{a}	0 0 \bar{a} a	\bar{a} a				
F_{2u}^2						-	0 0 a \bar{a}	0 0 \bar{a} a	\bar{a}				
F_{2u}^3						a	- - -	- - -	-	-	-	-	-

Table XIII. Compatibility conditions for the stable subspaces which correspond to the representation according to which the infrared active modes transform in case of structure B and symmetry D_{3d} . The 3-fold rotation axis is oriented along the $[111]$ -direction of the cube.

O_h	D_{3d}	Compatibility Conditions														
		A_{2u}			E_u^1			E_u^2								
		x_0	x_1	x_2	y_2	z_2	x_0	x_1	x_2	y_2	z_2	x_0	x_1	x_2	y_2	z_2
F_{1u}^1 F_{1u}^2 F_{1u}^3	$A_{2u} + E_u$	2a	$2e^+$	$2e^-$	2b	2b	a	d^-	d^+	g	$2\bar{b}$	$3\bar{a}$	$3\bar{d}^-$	$3d^+$	$3\bar{d}^+$	$6\bar{c}$
		2a	$2f^+$	$2\bar{f}^-$	2c	2c	a	\bar{d}^-	d^+	\bar{h}	$2\bar{c}$	3a	$3\bar{d}^-$	$3\bar{d}^+$	$3d^+$	$6b$
		a	f^+	\bar{f}^-	c	c	\bar{a}	d^-	\bar{d}^+	h	2c	-	-	-	-	-
		$d^{\pm} = b \pm c, \quad e^{\pm} = b \pm 2c, \quad f^{\pm} = 2b \pm c, \quad g = b - 3c, \quad h = 3b - c$														

Table XIV. Compatibility conditions for the stable subspaces which correspond to the representation according to which the infrared active modes transform in case of structure C and symmetry D_{2h} . The 2-fold ξ -axis is oriented along the $[110]$ -direction of the cube.

O_h	D_{2h}	Compatibility Conditions																	
		B_{1u}				B_{2u}				B_{3u}									
		x_0	x_1	x_2	z_2	x_4	x_0	x_1	x_2	y_2	z_2	x_4	z_0	z_1	x_2	y_2	z_2	z_4	
F_{1u}^1	$B_{1u} + B_{2u} + B_{3u}$	a	e^+	b	c	d	e^-	\bar{a}	\bar{e}^-	b	\bar{c}	\bar{d}	\bar{e}^+	-	-	-	-	-	
F_{1u}^2		a	e^+	b	c	d	e^-	a	e^-	\bar{b}	c	d	e^+	-	-	-	-	-	
F_{1u}^3		-	-	-	-	-	-	-	-	-	-	-	-	-	a	b	0	c	d
		$e^{\pm} = c \mp d$																	

respective subgroup is reproduced. For all components of the stable subspaces of the subgroup the relations imposed by the group of higher symmetry are tabulated under the appropriate heading. A bar (-) means that the particular stable subspace is not contained in the subspace carrying a certain row of the irreducible representation given at the left even though it is contained in the union of the stable subspaces carrying the different rows of the same irreducible representation in agreement with the correlation table.

Since the stable subspaces are given in explicit form in section III it should not be difficult for the reader to establish the missing compatibility relations for the cubic group or derive them for the case when the group of highest symmetry is not the full cubic group.

IV. APPLICATION I - LINEAR MOLECULES

We now apply the results to the case of a linear triatomic molecule in a cubic crystal. If the molecule is aligned along one of the cubic axes, the z-axis, say, then the appropriate symmetry group (subgroup of O_h) is D_{4h} and the applicable structure is of type A. On the other hand, if the molecule is oriented along a body diagonal, the $[111]$ -direction, the symmetry of the system is reduced to D_{3d} and the associated structure is of type B. The third case which we shall consider is the molecule oriented parallel to a face diagonal which leads to the symmetry D_{2h} and belongs to structure C. Let us concentrate on the infrared active modes Σ_u^+ and π_u (in the group $D_{\infty h}$ they transform according to the irreducible representations A_{2u} and E_u , respectively) of this molecule. In case of full cubic symmetry (O_h) the infrared active modes transform according to one of the rows of the 3 dimensional irreducible representation F_{1u} , and, therefore are 3-fold degenerate. Clearly, if we introduce this molecule into a cubic crystal then its infrared active modes have to have the same transformation properties and hence form a base for the irreducible representation F_{1u} . This feature makes it unnecessary to derive compatibility relations especially for $D_{\infty h}$ and its subgroups D_{4h} , D_{3d} and D_{2h} respectively, and we can use the ones derived above (tables X, XIII and XIV, respectively).

In the first case the total space is spanned by

$\{\bar{3}_x \bar{3}_y \bar{3}_z | 0_x 0_y 0_z | 3_x 3_y 3_z\}$. Imposing the compatibility conditions given in table X on the stable subspaces listed in table II we are left with the following

$$D_{4h} : S^{A_{2u}} = \{00b|00a|00b\}, a + 2b = 0 : \text{stretching in z-direction} \quad (24a)$$

$$S^{E_u^1} = \{b00|a00|b00\}, a + 2b = 0 : \text{bending in } (010)\text{-plane} \quad (24b)$$

$$S^{E_u^2} = \{0b0|0a0|0b0\}, a + 2b = 0 : \text{bending in } (100)\text{-plane} \quad (24c)$$

Similarly for the other two cases where the total space is spanned by

$$\left\{ \begin{matrix} \Gamma_x & \Gamma_y & \Gamma_z \\ | & | & | \\ 0_x & 0_y & 0_z \end{matrix} \middle| \begin{matrix} 1_x & 1_y & 1_z \end{matrix} \right\} \quad \text{we find}$$

$$D_{3d} : S^{A_{2u}} = \{bbb|aaa|bbb\}, a + 2b = 0 : \text{stretching in} \\ [111]\text{-direction} \quad (25a)$$

$$S^{E_u^1} = \{bb2b|aa2a|bb2b\}, a + 2b = 0 : \text{bending in } (1\bar{1}0)\text{-plane} \quad (25b)$$

$$S^{E_u^2} = \{bb\ 0|aa\ 0|bb\ 0\}, a + 2b = 0 : \text{bending in } (11\bar{1})\text{-plane} \quad (25c)$$

$$D_{2h} : S^{B_{1u}} = \{bb\ 0|aa\ 0|bb\ 0\}, 2b + a = 0 : \text{stretching in} \\ [110] \text{ direction.} \quad (26a)$$

$$S^{B_{2u}} = \{bb\ 0|aa\ 0|bb\ 0\}, 2b + a = 0 : \text{bending in } (001)\text{-plane} \quad (26b)$$

$$S^{B_{3u}} = \{0\ 0b|0\ 0a|0\ 0b\}, 2b + a = 0 : \text{bending in } (1\bar{1}0)\text{-plane} \quad (26c)$$

The condition $a + 2b = 0$ represents the exclusion of the translation of the center-of-mass. In the first two cases the degenerate mode (π_u) does not split whereas in the third case the appropriate symmetry group has one dimensional (non-degenerate) representations only, and, therefore, the previously degenerate mode must split. We are not surprised to find in each case a stretching mode with the same orientation as the molecule and this fact may, in many cases, be sufficient to determine the orientation of the molecule. Experimentally we would detect this by an absorption maximum if the exciting radiation is polarized parallel to the orientation of the molecule. We must remember, however, that group theory can only

supply the necessary condition that a particular mode be infrared active, and the above mentioned stretching mode need not be active, or if it is, could be so weak to be experimentally unobservable. Then, in our idealized case, we can still extract enough information from the bending modes to uniquely determine the orientation of the molecule. The simplest case to detect, of course, is the splitting of the degenerate bending mode if the molecule is oriented along the face diagonal of the cube.

The other two possibilities are easily resolved by the following experiment. We use light polarized linearly in a plane perpendicular to one of the cubic axes. If the molecule happens to be oriented along this particular axis then the absorption is a maximum and independent of a rotation of the system about this axis. If we repeat the same experiment along one of the two other 4-fold axes we should find a sinusoidal dependence of the absorption upon rotation.

If the molecule is oriented along the $[111]$ -direction a rotation of the polarization vector in the (100) -plane would again give a uniform absorption. However, if one rotates the polarization vector in the $(1\bar{1}0)$ -plane the minimum will appear in this case when the polarization vector is along $[111]$ as contrasted with the previous situation when the minimum appeared along the $[001]$ -direction.

Clearly, the above arguments for the ideal case, where we assumed that all the molecules have the same orientation, does not apply to a real situation where the molecules will be distributed at random among all possible equivalent orientations. This random distribution has the effect that we observe an average absorption for any orientation

of the polarization vector, even for the stretching modes. Consequently, we cannot, in the realistic case, distinguish between molecules oriented randomly along $\langle 111 \rangle$ and $\langle 100 \rangle$ directions, respectively. Of course, the splitting of the bending modes for the $\langle 110 \rangle$ orientation does provide a means for establishing this orientation.

V. APPLICATION II - STEREOSCOPIC MOLECULES

Lattice Dynamics

The Green's function formalism introduced by Lifshitz [17] and others [18 - 23] for the calculation of lattice vibrations in impure crystals is restricted to disturbed lattices with an unchanged number of particles (monatomic impurity centers), i.e., to cases where there are neither new degrees of freedom nor a change in symmetry at this particular lattice site. Wagner [24, 25] extended this method to molecular impurity centers and in this subsection we shall give a survey of this work.

If a molecule of $s+1$ masses m replaces a regular lattice atom at $n = 0$, we may transform the molecular variables to a new set $(x_0^i, \xi_1^i, \dots, \xi_s^i)$ where x_0^i gives the position of the center-of-mass of the molecule. The ξ_ν^i may be chosen rather arbitrarily, but they must diagonalize the kinetic energy, with an associated effective mass m_ν^* . The three center-of-mass coordinates, x_0^i , and the total mass of the molecule, $M_0 = m_1 + m_2 \dots m_{s+1}$, are added to the other lattice coordinates x_n^i and masses M_n^0 ($M_n^0 =$ ideal masses), establishing a $3N$ -dimensional system as in the ideal case. Then, there is a natural way of looking at the problem:

- (a) The "lattice system" is characterized by a $3N \times 3N$ matrix
- $$H_{nm}^{ij} = H_{nm}^{0ij} + H_{nm}^{1ij}, \text{ where } H_{nm}^{0ij} \text{ describes the unperturbed lattice.}$$
- (b) The "molecular system" is characterized by a $3s \times 3s$ matrix
- $$h_{\nu\mu}^{ij}.$$
- (c) The interaction between the two systems is defined by a $3N \times 3s$ matrix $R_{n\nu}^{ij}$.

- (d) The disturbance is assumed to extend only to a small number r of lattice sites n around the origin, which implies that H_{nm}^{1ij} and $R_{n\nu}^{ij}$ are essentially zero outside this region.

We introduce the substitutions

$$z_n^i = (M_n^0)^{1/2} x_n^i$$

$$\zeta_\nu^i = (m_\nu^*)^{1/2} \xi_\nu^i$$

$$L_{nm}^{ij} = (M_n^0 M_m^0)^{-1/2} H_{nm}^{0ij} \quad (27)$$

$$\alpha_{\nu\mu}^{ij} = (m_\nu^* m_\mu^*)^{-1/2} h_{\nu\mu}^{ij}$$

$$B_{n\nu}^{ij} = (M_n^0 m_\nu^*)^{-1/2} R_{n\nu}^{ij}$$

$$A_{nm}^{ij}(\omega^2) = \omega^2 \left(1 - \frac{M_n^0}{M_n^0}\right) \delta_{nm} \delta_{on} \delta_{ij} + (M_n^0 M_m^0)^{-1/2} H_{nm}^{1ij}$$

With this, the eigenvalue equations of the two connected systems are

$$(L + A(\omega^2) - \omega^2 I) \cdot z + B \cdot \zeta = 0 \quad (3N \text{ equations}) \quad (28a)$$

$$(\alpha - \omega^2 I) \cdot \zeta + \tilde{B} \cdot z = 0 \quad (3s \text{ equations}) \quad (28b)$$

Without the perturbation A and the coupling B each of the two systems defines a Green's function

$$G(\omega^2) = (L - \omega^2 I)^{-1} = \sum_{k\lambda} \frac{\eta(k\lambda) \eta^\dagger(k\lambda)}{\omega_{k\lambda}^2 - \omega^2} \quad (29a)$$

$$\gamma(\omega^2) = (\alpha - \omega^2 \mathbf{I})^{-1} = \sum_{\mathbf{k}} \frac{\boldsymbol{\zeta}(\mathbf{k}) \boldsymbol{\zeta}^\dagger(\mathbf{k})}{\omega^2(\mathbf{k}) - \omega^2} \quad (29b)$$

where $\eta(\mathbf{k}\lambda)$, $\boldsymbol{\zeta}(\mathbf{k})$ denote the normalized eigenvectors, $\omega^2(\mathbf{k}\lambda)$, $\omega^2(\mathbf{k})$ the eigenfrequencies of the matrices \mathbf{L} and α , respectively. The solution for the ideal lattice

$$\mathbf{L} \cdot \eta(\mathbf{k}\lambda) = \omega^2(\mathbf{k}\lambda) \eta(\mathbf{k}\lambda) \quad (30)$$

we also shall use in the form

$$\eta_{\mathbf{n}}^i(\mathbf{k}\lambda) = N^{-1/2} \epsilon^i(\mathbf{k}\lambda) e^{i\mathbf{k} \cdot \mathbf{n}} \quad (31)$$

where \mathbf{k} is the wave vector and λ the polarization of the phonon. It is easily verified that the total Green's function for the combined system (28a) - (28b) is given by the individual Green's functions Eqs. (29a,b) in the simple way:

$$G_{\mathbf{T}}(\omega^2) = \begin{pmatrix} G(\omega^2) & 0 \\ 0 & \gamma(\omega^2) \end{pmatrix} \quad (32)$$

It is not necessary, however, to use this $(3N + 3s) \times (3N + 3s)$ matrix, because the special structure of the system (28a) - (28b) allows the molecular coordinates $\boldsymbol{\zeta}$ to be excluded. Using Eq. (29b) we can write Eq. (28b) in the form,

$$\boldsymbol{\zeta} = -\gamma(\omega^2) \tilde{\mathbf{B}} \cdot \mathbf{z} \quad (33)$$

Introducing this expression for $\boldsymbol{\zeta}$ in Eq. (28a) and multiplying from the left by $G(\omega^2)$, Eq. (28a) takes the form,

$$\mathbf{z} = -G(\omega^2) [\mathbf{A}(\omega^2) - \mathbf{B} \gamma(\omega^2) \tilde{\mathbf{B}}] \cdot \mathbf{z} \quad (34)$$

and the molecular coordinates are thus removed. Now \mathbf{A} and \mathbf{B} can be written as

$$A = \begin{pmatrix} a & 0 \\ 0 & 0 \end{pmatrix}, \quad B = (b, 0) \quad (35)$$

where a is $3r \times 3r$ and b a $3r \times 3s$ matrix, both extending only over the r lattice sites involved around the molecular defect. Hence, the eigenvalue equation, extracted from the system (34), reads:

$$D(\omega^2) = \text{Det}(I + g(\omega^2) [a - b \gamma(\omega^2) \tilde{b}]) = 0 \quad (36)$$

which is a determinant of rank $3r$. $g(\omega^2)$ is the $3r \times 3r$ matrix of $G(\omega^2)$ which belongs to the r involved lattice points. It is seen that the Lifshitz matrix $I + g(\omega^2) a$ is supplemented by the matrix $-g(\omega^2) b \gamma(\omega^2) \tilde{b}$, written more explicitly

$$g(\omega^2) b \gamma(\omega^2) \tilde{b} = \sum_{1\nu\mu} g_{n1} b_{1\nu} \gamma_{\nu\mu} b_{\mu m} \quad \begin{matrix} 1, n, m = 1, 2, \dots, 3r \\ \nu, \mu = 1, 2, \dots, 3s \end{matrix} \quad (37)$$

In this formulation the eigenvalue determinant is of the same rank $3r$ as in the Lifshitz problem and $-b \gamma(\omega^2) \tilde{b}$ may be considered as an additional disturbance in the "lattice system". The effective disturbance,

$$v = a(\omega^2) - b \gamma(\omega^2) \tilde{b} \quad (38)$$

within the system of lattice coordinates contains, apart from the rather smooth function $a(\omega^2)$ (associated with the motion of the center-of-mass of the molecular defect), the additional molecular term $-b \gamma(\omega^2) \tilde{b}$ which has poles at the molecular frequencies $\omega(\kappa)$. Thus v cannot be treated as a perturbation near the $\omega(\kappa)$ frequencies, however small the coupling b may be.

The $3N + 3s$ roots of Eq. (36) are the eigensolutions of the fundamental equations of motion (28a,b). Considering for the moment the

factor $g(\omega^2)$ only, we see from the definition (29a) of the lattice Green's function that $g(\omega^2)$ jumps from $-\infty$ to $+\infty$ between two consecutive $\omega^2(k\lambda)$ values. This means that there must be a solution of Eq. (36) between two adjacent $\omega(k\lambda)$ values. Thus we have a spectrum of solutions in the same region and with the same density as in the ideal case. Eventually there are one or a few solutions outside the ideal band(s); these are the localized modes. The factor $a(\omega^2)$ is of little influence as it is not a strongly varying function of ω^2 . There are some new features if we take into account the factor $b \gamma(\omega^2) \tilde{b}$. This term has additional poles at the molecular frequencies $\omega^2(\kappa)$, and gives rise to $3s$ new solutions distributed outside and inside the ideal band(s). But the more important fact is that the Lifshitz solutions, associated with the matrix $g(\omega^2) a(\omega^2)$, are strongly disturbed in the neighborhood of those molecular frequencies $\omega^2(\kappa)$ lying inside the band(s). This has a great influence on phonon scattering and yields resonances in the scattering amplitude.

The Scattering Formalism

The theory of the scattering of lattice waves was first worked out rigorously by Lifshitz [26]. This theory has subsequently been developed further by Klein [27,28], Takeno [29], Krumhansl [30] and Callaway [31].

We have indicated in the last subsection that the spectrum of solutions for the disturbed lattice occupies the same regions as in the ideal lattice, apart from the singular solutions outside the band(s) which we shall not consider here. As the distribution is very dense, we ask for solutions of the form

$$z_{\mathfrak{N}}^i(\underline{k}\lambda) = \eta_{\mathfrak{N}}^i(\underline{k}\lambda) + w_{\mathfrak{N}}^i(\underline{k}\lambda) \quad (39)$$

the frequency of which lies very near to $\omega(\underline{k}\lambda)$. In this case $\eta_{\mathfrak{N}}^i(\underline{k}\lambda)$ represents the incident phonon and $w_{\mathfrak{N}}^i(\underline{k}\lambda)$ the scattered wave. The asymptotic expression for the latter is

$$\lim_{|\mathfrak{N}| \rightarrow \infty} w_{\mathfrak{N}}^i(\underline{k}\lambda) = N^{-1/2} \frac{e^{i|\underline{k}| \cdot |\mathfrak{N}|}}{|\mathfrak{N}|} f^i(\underline{k}\lambda, \underline{k}'\lambda') \quad (40)$$

which defines the scattering amplitude $f^i(\underline{k}\lambda, \underline{k}'\lambda')$. As in the quantum mechanical theory of scattering the differential scattering cross section and the scattering amplitude are related by

$$\sigma(\underline{k}\lambda, \underline{k}') = |\bar{f}(\underline{k}\lambda, \underline{k}'\lambda')|^2 \quad (41)$$

where the bar reminds us that later on we shall have to sum over the possible polarizations λ' of the final states. However, the proof of an optical theorem does not carry over directly to phonon scattering [28], because when changes in mass are involved, there is also a change in the "effective metric tensor".

The spectrum of both the ideal and the disturbed solutions is discrete but very dense. It is convenient, therefore, to go to the continuum by replacing summations in k space by integrations

$$N^{-1} \sum_{\underline{k}\lambda} \dots = \left(\frac{a}{2\pi}\right)^3 \sum_{\lambda} \int \dots d^3k \quad (42)$$

where $V_a = a^3$ is the volume of the primitive unit cell, a the lattice spacing. Then the Green's function $G(\omega^2)$ is no longer defined. In order to avoid the improper integral we redefine $G(\omega^2)$ according to standard

scattering theory as

$$G_+(\omega^2) = (L - I (\omega^2 + i\epsilon))^{-1} = \sum_{\underline{k}\lambda} \frac{\eta(\underline{k}\lambda) \eta^+(\underline{k}\lambda)}{\omega^2(\underline{k}\lambda) - (\omega^2 + i\epsilon)} \quad (43)$$

which is the Green's function for the "outgoing" wave solution as long as the group velocity at the stationary points is an outward normal to the frequency surface. For a detailed discussion on this matter we refer to Maradudin [32] and Ludwig [13].

Substituting Eq. (39) and using Eq. (30) we obtain

$$w_+(\underline{k}\lambda) = - G_+(\omega^2) V(\omega^2) \eta(\underline{k}\lambda) - G_+(\omega^2) V(\omega^2) w_+(\underline{k}\lambda) \quad (44)$$

where V denotes the effective disturbance v in the total space. We can solve this equation by iteration

$$w_+ = - G_+ V \eta + G_+ V G_+ V \eta - G_+ V G_+ V G_+ V \eta \pm \dots \quad (45)$$

If we stop with the first term on the right side of this expansion we have a solution which is equivalent to the first Born approximation of ordinary scattering theory. The succeeding terms represent the second, third, Born approximations to the scattered wave. We can write a formally exact solution to Eq. (45) in terms of the so-called association or scattering matrix T

$$w_+(\underline{k}\lambda) = - G_+(\omega^2) T_+(\omega^2) \eta(\underline{k}\lambda) \quad (46)$$

where T is the solution of the equations

$$T = V - V G T = V - T G V \quad (47)$$

This is a convenient form to calculate the scattered wave, because the rank of the matrix T is equal to the number of degrees of freedom in the crystal affected by the introduction of the defect. If we partition T in the following manner

$$T = \begin{pmatrix} t & t_{12} \\ t_{21} & t_{22} \end{pmatrix} \quad (48)$$

where t is defined in the defect space (space of v), and where, according to Eq. (46), $t_{21} = t_{12}$, then substitution of Eq. (48) into Eq. (47) yields the result that the matrices t_{12} , t_{21} and t_{22} are null matrices, and that the matrix t satisfies the following equation in the defect space

$$\begin{aligned} t &= \dot{v} - vgt = \dot{v} - tgv \\ &= v(I + gv)^{-1} \end{aligned} \quad (49)$$

which is a $3r \times 3r$ matrix.

According to Eqs. (43) and (46) the scattered wave can be written as

$$w_+(k\lambda) = - \sum_{k'\lambda'} \frac{\langle k'\lambda' | t | k\lambda \rangle}{\omega^2(k'\lambda') - (\omega^2 + i\epsilon)} \eta(k'\lambda') \quad (50)$$

where in the scalar product we have introduced the short notation $|k\lambda\rangle$ to label a plane wave state $\eta(k\lambda)$.

Because of the low rank $3r$, it is in general very easy to diagonalize the denominator of the t matrix (Eq. (49)) by symmetry considerations. Let us assume that we know the eigensolutions of the matrix $g_+ v$:

$$g_+ \mathbf{v} \cdot \mathbf{e}(\nu) = u(\nu) \mathbf{e}(\nu) \quad (51)$$

where $\mathbf{e}(\nu)$ is a column vector and ν labels the row of the irreducible representation according to which the eigenvectors transform. Thus we can write the t matrix in the form

$$t = \nu \sum_{\nu} \frac{\mathbf{e}(\nu) \tilde{\mathbf{e}}(\nu)}{1 + u(\nu)} \quad (52)$$

Very often the appropriate symmetry group of the defect is a proper or improper subgroup of the symmetry group of the host lattice, and in this case \mathbf{v} has the same eigenvectors as $g_+ \mathbf{v}$:

$$\mathbf{v} \cdot \mathbf{e}(\nu) = v(\nu) \mathbf{e}(\nu) \quad (53)$$

and the t matrix can be brought to the form

$$t = \sum_{\nu} \frac{v(\nu)}{1 + u(\nu)} \mathbf{e}(\nu) \tilde{\mathbf{e}}(\nu) = \sum_{\nu} t(\nu) T(\nu) \quad (54)$$

where

$$t(\nu) = \frac{v(\nu)}{1 + u(\nu)} \quad (55)$$

and the matrices $T(\nu)$ are given by the outer product of $\mathbf{e}(\nu)$, $\tilde{\mathbf{e}}(\nu)$, respectively.

Let us now turn back to the scattering problem. We start from a relation between the scattering matrix and the scattering amplitude which was derived by Ludwig [13] from an asymptotic expression for the scattered wave. If we make the acoustic approximation

$$\omega(\mathbf{k}\lambda) = c(\lambda) |\mathbf{k}| \quad (56)$$

then in our notation the scattering amplitude has the form

$$f(\underline{k}\lambda, \underline{k}'\lambda') = \frac{ia^3}{4\pi} \frac{1}{c^2(\lambda')} \langle \underline{k}'\lambda' | t | \underline{k}\lambda \rangle \dots \quad (57)$$

As indicated below Eq. (41) we need to sum over all branches of the final states

$$\bar{f}_i(\underline{k}\lambda, \underline{k}'\lambda') = \frac{ia^3}{4\pi} \sum_{\lambda'} \frac{\epsilon_i(\underline{k}'\lambda')}{c^2(\lambda')} \langle \underline{k}'\lambda' | t | \underline{k}\lambda \rangle \quad (58)$$

The resulting differential scattering cross section is

$$\begin{aligned} \sigma(\underline{k}\lambda, \underline{k}') &= |\bar{f}(\underline{k}\lambda, \underline{k}')|^2 = \sum_i |\bar{f}_i(\underline{k}\lambda, \underline{k}')|^2 \\ &= \frac{a^6}{16\pi^2} \sum_{\lambda'} \sum_{\lambda''} \sum_i \frac{1}{c^4(\lambda')} \epsilon_i^*(\underline{k}'\lambda') \epsilon_i(\underline{k}''\lambda'') \langle \underline{k}\lambda | t | \underline{k}'\lambda' \rangle \\ &\quad \langle \underline{k}''\lambda'' | t | \underline{k}\lambda \rangle \quad (59) \end{aligned}$$

We now use the orthogonality relation

$$\sum_i \epsilon_i^*(\underline{k}'\lambda') \epsilon_i(\underline{k}''\lambda'') = \delta_{\lambda'\lambda''}$$

to simplify Eq. (59) and, at the same time, decompose the scattering matrix according to Eq. (56) with the result

$$\begin{aligned} \sigma(\underline{k}\lambda, \underline{k}') &= \frac{a^6}{16\pi^2} \sum_{\lambda'} \sum_{\mu} \sum_{\nu} \frac{1}{c^4(\lambda')} t^*(\mu)t(\nu) \langle \underline{k}'\lambda' | T(\mu) | \underline{k}\lambda \rangle \\ &\quad \cdot \langle \underline{k}'\lambda' | T(\nu) | \underline{k}\lambda \rangle \quad (61) \end{aligned}$$

Using the fact that the matrix elements in Eq. (61) are real we put it in

final form

$$\sigma(\mathbf{k}\lambda, \mathbf{k}'\lambda') = \frac{a^6}{16\pi^2} \sum_{\lambda'} \frac{1}{c^4(\lambda')} \left\{ \sum_{\mu} |t(\mu)|^2 \langle \underline{\mathbf{k}}'\lambda' | T(\mu) | \underline{\mathbf{k}}\lambda \rangle^2 + \right. \\ \left. 2 \sum_{\mu > \nu} \text{Re} (t(\mu) t(\nu)) \langle \underline{\mathbf{k}}'\lambda' | T(\mu) | \underline{\mathbf{k}}\lambda \rangle \langle \underline{\mathbf{k}}'\lambda' | T(\nu) | \underline{\mathbf{k}}\lambda \rangle \right\} \quad (62)$$

From this expression we see clearly that the resonances of the scattering cross section are given by the resonances in the t matrix. Furthermore, we realize that the scattering of lattice waves by an impurity is much more complicated than the scattering of plane waves by a static potential in quantum theory. The equation $\omega^2(\mathbf{k}\lambda) = \omega^2$, which determines the stationary points, can have solutions in several branches of the function $\omega^2(\mathbf{k}\lambda)$. This has the consequence that although the incoming wave is in a definite branch of $\omega^2(\mathbf{k}\lambda)$, there can be several scattered waves propagating in different directions with the same frequency but with different group velocities and polarizations.

In the rest of this subsection we review briefly a discussion by Klein [27] and also Wagner [25]. The expressions (52) or (59) show that there is a resonance in the scattering amplitude if the real part of one of the denominators $1 + u(\nu)$ becomes zero. Hence, the resonance condition is

$$1 + \text{Re} u(\nu)(\omega^2) = 0 \quad (63)$$

and the resonance frequency we shall denote by ω_{ν} . If this resonance is sufficiently strong, then the ν^{th} term may exceed all other terms in the neighborhood of $\omega = \omega_{\nu}$ and we can approximate the matrix t by expanding

the denominator around $\omega = \omega_\nu$

$$t \simeq \nu(\omega_\nu^2) \frac{e(\nu) \tilde{e}(\nu)}{(\omega^2 - \omega_\nu^2)R_\nu + iI_\nu}, \quad \text{for } \omega \simeq \omega_\nu \quad (64)$$

with

$$R_\nu = \frac{d}{d\omega^2} \operatorname{Re} u(\nu)(\omega^2) \Big|_{\omega = \omega_\nu} \quad (65)$$

and

$$I_\nu = \operatorname{Im} u(\nu)(\omega_\nu^2)$$

As the denominator of Eq. (64) enters with its absolute square into the first term for the differential cross section (Eq. (62)), the half-width of the resonance in this term is given by

$$\frac{\omega_\nu^2 \left(\frac{1}{2}\right) - \omega_\nu^2}{\omega_\nu^2} = \frac{I_\nu}{\omega_\nu^2 R_\nu} \quad (66)$$

and there is a sharp resonance if this expression is much smaller than unity.

In his analysis Wagner [25] ignored the possibility for the second term (interference term) in Eq (62) to occur. Even though it is not likely that a resonance in that term would be as pronounced as one in the first term, there exists still the potentiality that the two terms might be of equal importance since the cross term does not enter through a perturbation calculation. If two modes, which transform according to rows of different irreducible representations, have eigenfrequencies in the same

range then they might contribute appreciably to the scattering cross section. This possibility exists for instance in the combination of an inband librational mode and the motion of the center-of-mass of the molecular defect.

From the special form of the disturbance (Eq. (38)) we can see that some of the $u(\nu)$'s (at least one) must contain the poles of the molecular Green's function γ . Since these vary over a wide range, they are very likely to give a solution of the resonance condition Eq. (63). On the other hand, there may be some of the $v(\nu)$'s which do not contain the molecular poles for which there also exist a solution of the resonance condition.

To calculate the structure and spectral position of the resonances explicitly, we have to establish a specific model for both the lattice and the molecular defect.

What we do expect, however, is that the shape and magnitude of the resonances have the same dependence on the density of the frequency spectrum of the host lattice at the position where these pseudolocalized modes would like to appear as in the case of a point defect. The analysis of Dawber and Elliott [33] shows that the resonances due to a monatomic impurity is more pronounced the lower the density of the frequency distribution of the ideal lattice at this particular frequency.

Spherical Molecules

We know that the internal binding in a molecule is often much stronger than the binding to the host lattice and it is practically unchanged when the molecule is brought into the lattice.

If we assume such strong internal binding, we can distinguish

three types of motion for the molecular defect:

- (a) The internal vibrations, which are practically the same as for the free molecule. Some of their frequencies may lie far above the phonon band(s) and are not likely to be excited by phonon scattering. On the other hand, there also might be low frequency modes below the maximum frequency of the host lattice. Such modes usually are associated with the stretching motion involving heavy atoms or bending modes. Bending vibrations have substantially lower frequencies than stretching modes of the same bonds (approximately $1/3$ or even less [16, 34, 35]). The reason for this is that bending motions primarily change angles in the configuration of the participating points which do not call for the same kind of restoring force (electrostatic repulsion) as in the case of stretching modes where the bond length changes.
- (b) The translational vibrations of the whole molecule, which are essentially the same as if the molecule was a single mass. The dynamical behavior of point defects is quite well understood [13, 32]. Also, the scattering problem for this case has been treated already [13, 27, 29, 30, 36, 37] and we can take over the relevant results from there.
- (c) The rotational vibrations (quasi-rotations, librations) of the whole molecule, for which the molecule acts as a

rigid body with three moments of inertia. The coupling of this type of motion to the host lattice will normally be weak and the associated frequency is likely to be found within the phonon band(s).

In the following study we shall concentrate on the scattering of phonons by molecular impurity centers. In many practical examples the frequencies associated with motions of type (a) lie above the frequencies propagated by the host crystal and will not affect the scattering cross section. Furthermore, it would not be possible to set up a general model which accounts for this type of motion and its coupling to the host lattice. Almost every possible molecular defect (or at least each class of molecule) would require a special treatment and since we are more interested in possible general conclusions we shall restrict our attention on the latter two types (types (b) and (c)). There is, however, no justification for also neglecting the motion of the center-of-mass of the defect molecule as was done by Wagner [25]. First, modes associated with this motion are most likely to be inband modes. It is well known [13, 23, 38] that a heavier isotopic mass or the weakening of the force constants around a point defect give rise to resonance (pseudo-localized) modes. Then to be consistent with our model, where the center-of-mass of the molecular defect belongs to the lattice system, and with the assumption that the defect molecule be only weakly bound to the host crystal, we have to expect that the force constants describing the links between the molecular center-of-mass and the neighboring atoms are weaker than in the ideal lattice. Second, as already mentioned in the discussion of the differential cross section, Eq. (62), this mode might not only contribute

directly to the scattering cross section but also appreciably through the interference term.

Let us now consider the rather simple model. As host lattice we choose a monatomic (mass M) lattice of simple cubic structure with radial force constants α and tangential force constants β . The interaction among the lattice points we restrict to nearest neighbors only. This crystal is elastically stable as long as [39]

$$0 < 2\beta < \alpha \quad (67)$$

and the highest frequency propagated is

$$\omega_{\max}^2 = \frac{4(\alpha + 2\beta)}{M} \quad (68)$$

We represent the molecular defect by a rigid sphere of a single moment of inertia θ and mass M' which might be different from that of the atom replaced by the molecule. The sphere is coupled to the six nearest lattice atoms by tangential springs with constants f and radial springs with constants k . Then the three remaining molecular coordinates are degenerate and conveniently taken as the rotations ψ_x, ψ_y, ψ_z around the three cubic axes. It is easy enough to see that this model allows motions of type (b) as well as of type (c).

For this model the molecular Green's function is given by

$$\gamma(\omega^2) = \frac{1}{\omega^2(\mathbf{k}) - \omega^2} \mathbf{I} \quad (3 \text{ dimensional}) \quad (69)$$

where

$$\omega^2(\mathbf{k}) = \frac{4f}{\theta/a^2} \quad (70)$$

There are 21 lattice coordinates involved in the disturbance, namely, those to which the spherical molecule is coupled complemented by the three coordinates of the center-of-mass. Our dynamical problem as well as the matrix t are defined in this 21 dimensional defect space (matrix v). However, group theory provides a powerful tool for reducing the calculational effort, and we do not have to work in this high dimensional space. From the information given in Table I we see that the most that we must do is to solve a 3×3 secular determinant for the modes transforming according to the irreducible representation F_{1u} . It is also easy to see that only modes transforming either according to the irreducible representation F_{1g} or according to F_{1u} can induce dynamical effects in our model where we have replaced the molecular defect by a rigid sphere. The former yield the librational motion and the latter are connected with the motion of the center-of-mass. The symmetry of the other modes is such that they provide no coupling which could lead to a net force or torque.

If we denote by $|s\rangle$ the set of vectors which span the defect space, then the matrices a , b , $\gamma(\omega^2)$, \tilde{b} and g_+ are defined by their Hermite forms in this space:

$$\begin{aligned}
\langle s|a|s\rangle = & \frac{1}{M} (k - \alpha) \left\{ s^2(A_{1g}) + s^2(E_g^1) + s^2(E_g^2) \right\} \\
& + \frac{1}{M} (f - \beta) \left\{ s^2(F_{1g}^1) + s^2(F_{1g}^2) + s^2(F_{1g}^3) + s^2(F_{2g}^1) + s^2(F_{2g}^2) + s^2(F_{2g}^3) \right. \\
& \quad \left. + s^2(F_{2u}^1) + s^2(F_{2u}^2) + s^2(F_{2u}^3) \right\} \\
& + F(M, M', \alpha, \beta, k, f) \left\{ s^2(F_{1u}^1) + s^2(F_{1u}^2) + s^2(F_{1u}^3) \right\} \quad (71)
\end{aligned}$$

$$\langle s | b \gamma(\omega^2) \tilde{b} | s \rangle = \frac{f}{M} \frac{\omega^2(\kappa)}{\omega^2(\kappa) - \omega^2} \left\{ s^2(F_{1g}^1) + s^2(F_{1g}^2) + s^2(F_{1g}^3) \right\} \quad (72)$$

$$\begin{aligned} \langle s | g_+(\omega^2) | s \rangle = & (\hat{A} - \hat{C}) \left\{ s^2(A_{1g}) + s^2(E_g^1) + s^2(E_g^2) + s^2(F_{1g}^1) + s^2(F_{1g}^2) + s^2(F_{1g}^3) \right. \\ & \left. + s^2(F_{2g}^1) + s^2(F_{2g}^2) + s^2(F_{2g}^3) \right\} \\ & + (\hat{A} + \hat{C} - 2\hat{B}) \left\{ s^2(F_{2u}^1) + s^2(F_{2u}^2) + s^2(F_{2u}^3) \right\} \\ & + F(\hat{A}, \hat{B}, \hat{C}) \left\{ s^2(F_{1u}^1) + s^2(F_{1u}^2) + s^2(F_{1u}^3) \right\} \end{aligned} \quad (73)$$

where, assuming that we can define a longitudinal and two transversal branches, the Green's function $\hat{A}, \hat{B}, \hat{C}$ are given by

$$\hat{A}(\omega^2) = \hat{A}_1 + \hat{A}_t = \frac{1}{3N} \left\{ \sum_{\underline{k}} \frac{1}{\omega^2(\underline{k}1) - (\omega^2 + i\epsilon)} + 2\sum_{\underline{k}} \frac{1}{\omega^2(\underline{k}t) - (\omega^2 + i\epsilon)} \right\} \quad (74a)$$

$$\hat{B}(\omega^2) = \hat{B}_1 + \hat{B}_t = \frac{1}{3N} \left\{ \sum_{\underline{k}} \frac{e^{ia(k_x + k_y)}}{\omega^2(\underline{k}1) - (\omega^2 + i\epsilon)} + 2\sum_{\underline{k}} \frac{e^{ia(k_x + k_y)}}{\omega^2(\underline{k}t) - (\omega^2 + i\epsilon)} \right\} \quad (74b)$$

$$\hat{C}(\omega^2) = \hat{C}_1 + \hat{C}_t = \frac{1}{3N} \left\{ \sum_{\underline{k}} \frac{e^{i2ak_x}}{\omega^2(\underline{k}1) - (\omega^2 + i\epsilon)} + 2\sum_{\underline{k}} \frac{e^{i2ak_x}}{\omega^2(\underline{k}t) - (\omega^2 + i\epsilon)} \right\} \quad (74c)$$

The reason that the Hermite forms (71), (73) are determined only up to factors $F(M, M', \alpha, \beta, k, f)$, $F(\hat{A}, \hat{B}, \hat{C})$, respectively, is the following. As we see, they are associated with that part of the defect space which is

spanned by vectors transforming according to the irreducible representation F_{1u} . This stable subspace is three dimensional, and solving the dynamical problem (Lifshitz problem: Eq. (28a), $B = 0$) we would obtain three equations to determine the three free parameters (secular determinant). These results then would enable us to give the factors above in explicit form. The solution of this problem involves Green's functions of the same type as $\hat{A}, \hat{B}, \hat{C}$, respectively, and we know that they cannot be expressed analytically. A good approximation is [23]

$$G_+(\underline{m}) = (-1)^n \int_0^\infty \frac{\sin}{\cos} (M\omega^2 - 2 \sum_{i=1}^3 \gamma_i) t J_{m_1}(2\gamma_1 t) J_{m_2}(2\gamma_2 t) J_{m_3}(2\gamma_3 t) dt \quad \begin{array}{l} \sum_i m_i = 2n \\ \sum_i m_i = 2n + 1 \end{array} \quad (75)$$

where \underline{m} is the vector connecting the two points involved, the γ_i 's denote the force constants, and $J_K(x)$ is the Bessel function of order K . Evaluation of Eq. (75) involves lengthy numerical computation for each $|\underline{m}|$, ω^2 , and combination of α , β . We shall return to this problem later on.

With Eqs. (71), (72) and (73) we find the eigen values $u(v)$ and $v(v)$ to be:

$$u(A_{1g}) = (\hat{A} - \hat{C}) \frac{1}{M} (k - \alpha) \quad \begin{array}{l} \text{degeneracy} \\ (1) \end{array} \quad (76a)$$

$$u(E_g) = (\hat{A} - \hat{C}) \frac{1}{M} (k - \alpha) \quad (2) \quad (76b)$$

$$u(F_{1g}) = (\hat{A} - \hat{C}) \frac{1}{M} \left[f \left(1 - \frac{\omega^2(k)}{\omega^2(k) - \omega^2} \right) - \beta \right] \quad (3) \quad (76c)$$

$$u(F_{2g}) = (\hat{A} - \hat{C}) \frac{1}{M} (f - \beta) \quad (3) \quad (76d)$$

	degeneracy	
$u(F_{1u}) = F(\hat{A}, \hat{B}, \hat{C}) F(M, M', \alpha, \beta, k, f)$	(3)	(76e)
$u(F_{2u}) = (\hat{A} + \hat{C} - 2\hat{B}) \frac{1}{M} (f - \beta)$	(3)	(76f)
$v(A_{1g}) = \frac{1}{M} (k - \alpha)$	(1)	(77a)
$v(E_g) = \frac{1}{M} (k - \alpha)$	(2)	(77b)
$v(F_{1g}) = \frac{1}{M} [f(1 - \frac{\omega^2(\kappa)}{\omega^2(\kappa) - \omega^2}) - \beta]$	(3)	(77c)
$v(F_{2g}) = \frac{1}{M} (f - \beta)$	(3)	(77d)
$v(F_{1u}) = F(M, M', \beta, \beta, k, f)$	(3)	(77e)
$v(F_{2u}) = \frac{1}{M} (f - \beta)$	(3)	(77f)

where we have also indicated the degeneracy of the respective eigenvalue.

Before using the results obtained so far to discuss the effect of the individual modes on the scattering cross section we pause to consider the effect of the requirement [40] that the potential energy be invariant against infinitesimal rigid body rotations of the crystal. In our case of a simple cubic crystal we find that the condition imposed on the tangential force constants is

$$f = \beta ; \quad (78)$$

there is no restriction on the radial force constants. This has the consequence that the eigenvalues corresponding to the modes F_{2g} and F_{2u} vanish and we have to exclude them as possible eigenstates, since otherwise

this basic physical principle would be violated and the lattice would become unstable. On the other hand, there are good reasons to relax this condition. In a more realistic model we would also have to take into account next nearest (and more distant) neighbors resulting in less severe restriction of f , and, furthermore, we would also have to account for the change in structure around the defect which might also affect these conditions.

In order to calculate the individual contributions to the scattering cross section (Eq. (62)) we need, besides the ratios $v(\nu)/(1+u(\nu))$, also matrix elements of the form $\langle \underline{k}'\lambda' | T(\nu) | \underline{k}\lambda \rangle$. From the stable subspaces given in Table I it is not difficult to construct the matrices $T(\nu)$ (the vector spanning the stable subspaces have to be normalized first) and the nonvanishing matrix elements for each row of the different irreducible representations are found to be:

$$\begin{aligned} \langle (k'00) 1 | T(A_{1g}) | (k00) 1 \rangle &= \langle (k'00) 1 | T(A_{1g}) | (0k0) 2 \rangle = \langle (k'00) 1 | T(A_{1g}) | (00k) 3 \rangle \\ &= \frac{2}{9} \sin(\underline{k}'\hat{x}a) \sin ka \end{aligned} \quad (79a)$$

$$\begin{aligned} \langle (0k'0) 2 | T(A_{1g}) | (k00) 1 \rangle &= \langle 0k'0) 2 | T(A_{1g}) | (0k0) 2 \rangle = \langle (0k'0) 2 | T(A_{1g}) | (00k) 3 \rangle \\ &= \frac{2}{9} \sin(\underline{k}'\hat{y}a) \sin ka \end{aligned} \quad (79b)$$

$$\begin{aligned} \langle (00k') 3 | T(A_{1g}) | (k00) 1 \rangle &= \langle (00k') 3 | T(A_{1g}) | (0k0) 2 \rangle = \langle (00k') 3 | T(A_{1g}) | (00k) 3 \rangle \\ &= \frac{2}{9} \sin(\underline{k}'\hat{z}a) \sin ka \end{aligned} \quad (79c)$$

$$\begin{aligned}
\langle (k'00) 1 | T(E_g^1) | (k00) 1 \rangle &= \langle (k'00) 1 | T(E_g^1) | (0k0) 2 \rangle = -\frac{1}{2} \langle (k'00) 1 | T(E_g^1) | (00k) 3 \rangle \\
&= \frac{1}{9} \sin(\underline{k\hat{x}}a) \sin ka \quad (80a)
\end{aligned}$$

$$\begin{aligned}
\langle (0k'0) 2 | T(E_g^1) | (k00) 1 \rangle &= \langle (0k'0) 2 | T(E_g^1) | (0k0) 2 \rangle = -\frac{1}{2} \langle (0k'0) 2 | T(E_g^1) | (00k) 3 \rangle \\
&= \frac{1}{9} \sin(\underline{k\hat{y}}a) \sin ka \quad (80b)
\end{aligned}$$

$$\begin{aligned}
\langle (00k') 3 | T(E_g^1) | (k00) 1 \rangle &= \langle (00k') 3 | T(E_g^1) | (0k0) 2 \rangle = -\frac{1}{2} \langle (00k') 3 | T(E_g^1) | (00k) 3 \rangle \\
&= -\frac{2}{9} \sin(\underline{k\hat{z}}a) \sin ka \quad (80c)
\end{aligned}$$

$$\begin{aligned}
\langle (k'00) 1 | T(E_g^2) | (k00) 1 \rangle &= -\langle (k'00) 1 | T(E_g^2) | (0k0) 2 \rangle \\
&= \frac{1}{3} \sin(\underline{k\hat{x}}a) \sin ka \quad (81a)
\end{aligned}$$

$$\begin{aligned}
\langle (0k'0) 2 | T(E_g^2) | (k00) 1 \rangle &= -\langle (0k'0) 2 | T(E_g^2) | (0k0) 2 \rangle \\
&= -\frac{1}{3} \sin(\underline{k\hat{y}}a) \sin ka \quad (81b)
\end{aligned}$$

$$\begin{aligned}
\langle (00k') 2 | T(F_{1g}^1) | (00k) 2 \rangle &= -\langle (00k') 2 | T(F_{1g}^1) | (0k0) 3 \rangle \\
&= \frac{1}{3} \sin(\underline{k\hat{z}}a) \sin ka \quad (82a)
\end{aligned}$$

$$\begin{aligned}
\langle (0k'0) 3 | T(F_{1g}^1) | (00k) 2 \rangle &= -\langle (0k'0) 3 | T(F_{1g}^1) | (0k0) 3 \rangle \\
&= -\frac{1}{3} \sin(\underline{k\hat{y}}a) \sin ka \quad (82b)
\end{aligned}$$

$$\begin{aligned}
\langle (00k') \ 1 | T(F_{1g}^2) | (00k) \ 1 \rangle &= - \langle (00k') \ 1 | T(F_{1g}^2) | (k00) \ 3 \rangle \\
&= \frac{1}{3} \sin(\underline{k'z}a) \sin ka
\end{aligned} \tag{83a}$$

$$\begin{aligned}
\langle (k'00) \ 3 | T(F_{1g}^2) | (00k) \ 1 \rangle &= - \langle (k'00) \ 3 | T(F_{1g}^2) | (k00) \ 3 \rangle \\
&= - \frac{1}{3} \sin(\underline{k'z}a) \sin ka
\end{aligned} \tag{83b}$$

$$\begin{aligned}
\langle (0k'0) \ 1 | T(F_{1g}^3) | (0k0) \ 1 \rangle &= - \langle (0k'0) \ 1 | T(F_{1g}^3) | (k00) \ 2 \rangle \\
&= \frac{1}{3} \sin(\underline{k'y}a) \sin ka
\end{aligned} \tag{84a}$$

$$\begin{aligned}
\langle (k'00) \ 2 | T(F_{1g}^3) | (0k0) \ 1 \rangle &= - \langle (k'00) \ 2 | T(F_{1g}^3) | (k00) \ 2 \rangle \\
&= - \frac{1}{3} \sin(\underline{k'z}a) \sin ka
\end{aligned} \tag{84b}$$

$$\begin{aligned}
\langle (00k') \ 2 | T(F_{2g}^1) | (00k) \ 2 \rangle &= \langle (00k') \ 2 | T(F_{2g}^1) | (0k0) \ 3 \rangle \\
&= \frac{1}{3} \sin(\underline{k'z}a) \sin ka
\end{aligned} \tag{85a}$$

$$\begin{aligned}
\langle (0k'0) \ 3 | T(F_{2g}^1) | (00k) \ 2 \rangle &= \langle (0k'0) \ 3 | T(F_{2g}^1) | (0k0) \ 3 \rangle \\
&= \frac{1}{3} \sin(\underline{k'y}a) \sin ka
\end{aligned} \tag{85b}$$

$$\begin{aligned}
\langle (00k') \ 1 | T(F_{2g}^2) | (00k) \ 1 \rangle &= \langle (00k') \ 1 | T(F_{2g}^2) | (k00) \ 3 \rangle \\
&= \frac{1}{3} \sin(\underline{k'z}a) \sin ka
\end{aligned} \tag{86a}$$

$$\begin{aligned}
\langle (k'00) \ 3 | T(F_{2g}^2) | (00k) \ 1 \rangle &= \langle (k'00) \ 3 | T(F_{2g}^2) | (k00) \ 3 \rangle \\
&= \frac{1}{3} \sin(\underline{k'z}a) \sin ka
\end{aligned} \tag{86b}$$

$$\begin{aligned} \langle (0k'0) \ 1 | T(F_{2g}^3) | (0k0) \ 1 \rangle &= \langle (0k'0) \ 1 | T(F_{2g}^3) | (k00) \ 2 \rangle \\ &= \frac{1}{3} \sin(\underline{k}'\hat{y}a) \sin ka \end{aligned} \quad (87a)$$

$$\begin{aligned} \langle (k'00) \ 2 | T(F_{2g}^3) | (0k0) \ 1 \rangle &= \langle (k'00) \ 2 | T(F_{2g}^3) | (k00) \ 2 \rangle \\ &= \frac{1}{3} \sin(\underline{k}'\hat{x}a) \sin ka \end{aligned} \quad (87b)$$

$$\langle \underline{k}'1 | T(F_{1u}^1) | (k00) \ 1 \rangle, \quad \langle \underline{k}'1 | T(F_{1u}^1) | (0k0) \ 1 \rangle, \quad \langle \underline{k}'1 | T(F_{1u}^1) | (00k) \ 1 \rangle \quad (88)$$

$$\langle \underline{k}'2 | T(F_{1u}^2) | (k00) \ 2 \rangle, \quad \langle \underline{k}'2 | T(F_{1u}^2) | (0k0) \ 2 \rangle, \quad \langle \underline{k}'2 | T(F_{1u}^2) | (00k) \ 2 \rangle \quad (89)$$

$$\langle \underline{k}'3 | T(F_{1u}^3) | (k00) \ 3 \rangle, \quad \langle \underline{k}'3 | T(F_{1u}^3) | (0k0) \ 3 \rangle, \quad \langle \underline{k}'3 | T(F_{1u}^3) | (00k) \ 3 \rangle \quad (90)$$

$$\begin{aligned} \langle (0k'k') \ 1 | T(F_{2u}^1) | (00k) \ 1 \rangle &= - \langle (0k'k') \ 1 | T(F_{2u}^1) | (0k0) \ 1 \rangle \\ &= \frac{4}{3} [\cos(\underline{k}'\hat{z}a) - \cos(\underline{k}'\hat{y}a)] (\cos ka - 1) \end{aligned} \quad (91)$$

$$\begin{aligned} \langle (k'0k') \ 2 | T(F_{2u}^2) | (00k) \ 2 \rangle &= - \langle (k'0k') \ 2 | T(F_{2u}^2) | (k00) \ 2 \rangle \\ &= \frac{4}{3} [\cos(\underline{k}'\hat{z}a) - \cos(\underline{k}'\hat{x}a)] (\cos ka - 1) \end{aligned} \quad (92)$$

$$\begin{aligned} \langle (k'k'0) \ 3 | T(F_{2u}^3) | (0k0) \ 3 \rangle &= - \langle (k'k'0) \ 3 | T(F_{2u}^3) | (k00) \ 3 \rangle \\ &= \frac{4}{3} [\cos(\underline{k}'\hat{y}a) - \cos(\underline{k}'\hat{x}a)] (\cos ka - 1) \end{aligned} \quad (93)$$

From these matrix elements we can learn a great deal about the possible scattering processes

- A_{1g} : This mode scatters longitudinally polarized phonons. It is acoustically active in the sense that the scattered acoustic wave may be either longitudinally or transverse polarized.
- E_g : This mode also scatters longitudinally polarized phonons only and is acoustically active.
- F_{1g} : This mode scatters transverse polarized phonons only and the acoustical activity is restricted to transverse polarized final states.
- F_{2g} : This mode also scatters transverse polarized phonons only and has the same restricted acoustical activity as F_{1g} .
- F_{1u} : This mode scatters any incident phonon regardless of the polarization but does not change the polarization.
- F_{2u} : This mode scatters transverse polarized phonons only and maintains the polarization.

From these results it is quite clear that, for example, the combination of modes which transform according to the irreducible representations F_{1g} , F_{1u} , respectively, can give rise to a nonvanishing interference term in Eq. (62).

We now ask under what conditions we might expect that one of the modes contributes to the scattering cross section. One of the requirements, of course, is that the associated frequency be inside the band(s) of the ideal crystal. This information can be deduced from the results in the detailed study of localized modes by Lengeler and Ludwig [39]. Under all the conditions where they do not find a local mode outside the ideal band, there must be a resonance (pseudolocalized) mode inside the band. An

exception are the modes transforming according to the irreducible representation F_{1u} where we have two modes either both localized, one localized and one inband or both inside the ideal band. If one allows for a change in mass only (isotope defect) then the solution of the dynamical problem is rather simple. The 3×3 secular determinant reduces to just one equation involving one Green's function $g(m = 0)$ only:

$$\omega^2 \epsilon g(0) - 1 = 0 \quad (94)$$

where $\epsilon = (M' - M)/M$. For frequencies above the ideal band(s) $\omega^2 > \omega^2(k\lambda)$ the Green's function above is negative definite and hence the condition to find a localized mode is simply $\epsilon < 0$ or $M' < M$. For frequencies within the ideal band(s) the Green's function may be either positive or negative definite and we may find solutions for $\epsilon > 0$ as well as for $\epsilon < 0$. On the other hand, we know that the problem has to have at least one solution and since there is no solution outside the ideal band(s) for $\epsilon > 0$ we are bound to find at least one solution inside the spectrum of the ideal lattice for $M' > M$.

Let us consider this particular situation of a mass defect only in more detail. Working within the acoustic approximation Maradudin [36] has derived the following expression for the total scattering cross section:

$$\sigma_T = \frac{a^6 \epsilon^2 \omega^4}{12\pi |D(\omega^2)|^2} \left(\frac{1}{c^4(1)} + \frac{2}{c^4(t)} \right), \quad 0 < \omega < \omega_t \quad (95a)$$

$$= \frac{a^6 \epsilon^2 \omega^4}{12\pi |D(\omega^2)|^2} \frac{1}{c^4(1)}, \quad \omega_t < \omega < \omega_1 \quad (95b)$$

where $C(1)$, $C(t)$ are the propagation velocities of the phonons in the longitudinal branch and in the transversal branch, respectively, ω_l and ω_t are the corresponding Debye cutoff frequencies (ω_D) and $D(\omega^2)$ is essentially the secular determinant of the dynamical problem.

We notice that in the long wavelength limit, i.e., ω small, the total cross section is proportional to ω^4 . This result is the well known Rayleigh scattering cross section. Of more interest, however, is the behavior of the cross section at somewhat higher frequencies. Here the frequency dependence of the total cross section is determined largely by the factor $|D(\omega^2)|^{-2}$.

Thoma and Ludwig [37] have plotted the term $|D(\omega^2)|^{-2}$ for a number of different values of ϵ (Figure 2). They find a very strong resonance peak for $M' = 6M$ in the region of $\omega/\omega_D = 0.2$ and a smaller one for $M' = 2M$ at $\omega/\omega_D = 0.45$. To this result we shall return later on.

We turn now to the contribution due to the librational motion of the defect molecule. For an incident phonon $|(00k) 1\rangle$ we find with Eqs. (83a, b) the first term in Eq. (62) to be

$$\sigma^1((00k) 1, \underline{k}') = \frac{a^6}{16\pi^2} \frac{1}{C^4(t)} |t(F_{1g})|^2 \frac{\sin^2 ka}{9} [\sin^2(\underline{k}'a) + \sin^2(\underline{k}a)] \quad (96)$$

and in the long wavelength limit the contribution to the total cross section is

$$\sigma_T^1((00k) 1) = \frac{1}{54\pi} \left(\frac{a}{C(t)}\right)^4 a^2 (ka)^4 |t(F_{1g})|^2 \quad \omega \ll \omega_D \quad (97)$$

We see that also in this case the Rayleigh scattering term ($\sim k^4$) is modified,

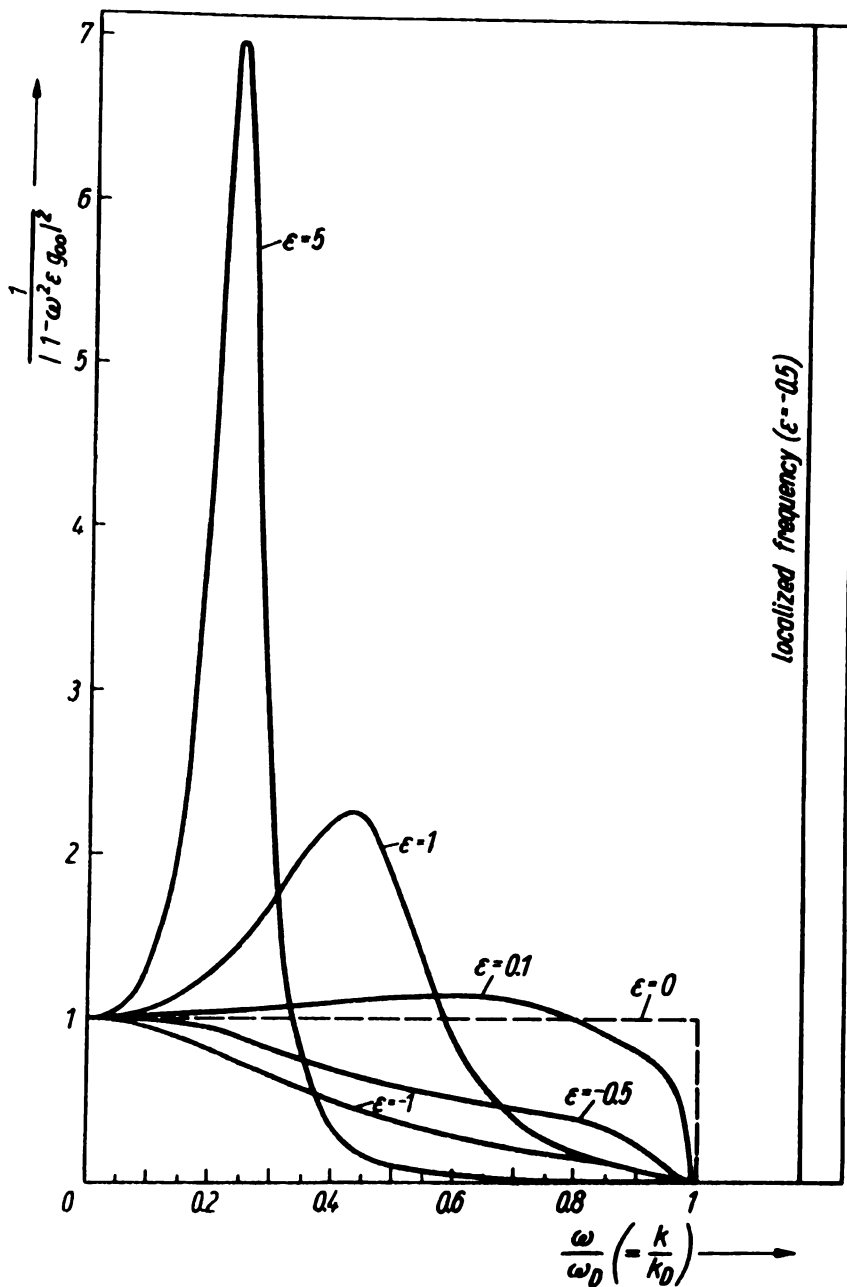


Figure 2. $|1 - \omega^2 \epsilon g(0)|^{-2}$, which enters the scattering cross section of an isotope defect, as a function of the lattice wave frequency in the Debye approximation, taken from Thoma and Ludwig [37].

namely by the functional form of $|t(F_{1g})|^2$. The last expression can be brought into the form

$$\sigma_T^1 ((00k) 1) = \frac{1}{12\pi} \left(\frac{a}{C(t)}\right)^4 a^2 \omega^4 \frac{32\pi^4}{9} \frac{|t(F_{1g})|^2}{C} \quad (98)$$

where $C = 16 (\pi/6)^{4/3} \omega_D$. Wagner [25] has plotted the term $|t(F_{1g})|^2/C$ as a function of $(\omega/\omega_D)^2$ (Figure 3) and, assuming $\omega^2(\kappa) = 0.2 \omega_D^2$, found a very strong resonance peak just below the molecular frequency $\omega(\kappa)$.

If we put the two figures (Figures 2, 3) on the same scales then we note that the resonance peak for $\epsilon = 1$ (due to a heavy mass defect: $M' = 2M$) occurs in the same region ($\omega/\omega_D = 0.45 \rightarrow (\omega/\omega_D)^2 \approx 0.2$) as the molecular resonance of the librational mode and the ratio of the peak heights is approximately 2.3/17.3. From this information we may make a reasonable estimate about the magnitude of the interference term. We assume that the two matrix elements (83) and (88) do not differ greatly and consider the product of the two factors $t^*(F_{1g})$ and $t(F_{1u})$ only. Its real part we express near the resonance as

$$\text{Re} \frac{1}{\epsilon_r - i\epsilon_i} \cdot \frac{1}{\eta_r + i\eta_i} = \frac{\epsilon_r \eta_r + \epsilon_i \eta_i}{(\epsilon_r^2 + \epsilon_i^2)(\eta_r^2 + \eta_i^2)} \quad (99)$$

at the resonance we make the approximation

$$\text{Re}(t^*(F_{1g}) t(F_{1u})) \simeq \frac{\epsilon_i \eta_i}{\epsilon_i^2 \eta_i^2} \quad (100)$$

with this we get for the factor of the interference term

$$2 \text{Re} (t^*(F_{1g}) t(F_{1u})) \simeq 2 (2.3 \cdot 17.3)^{1/2} = 12.6 \quad (101)$$

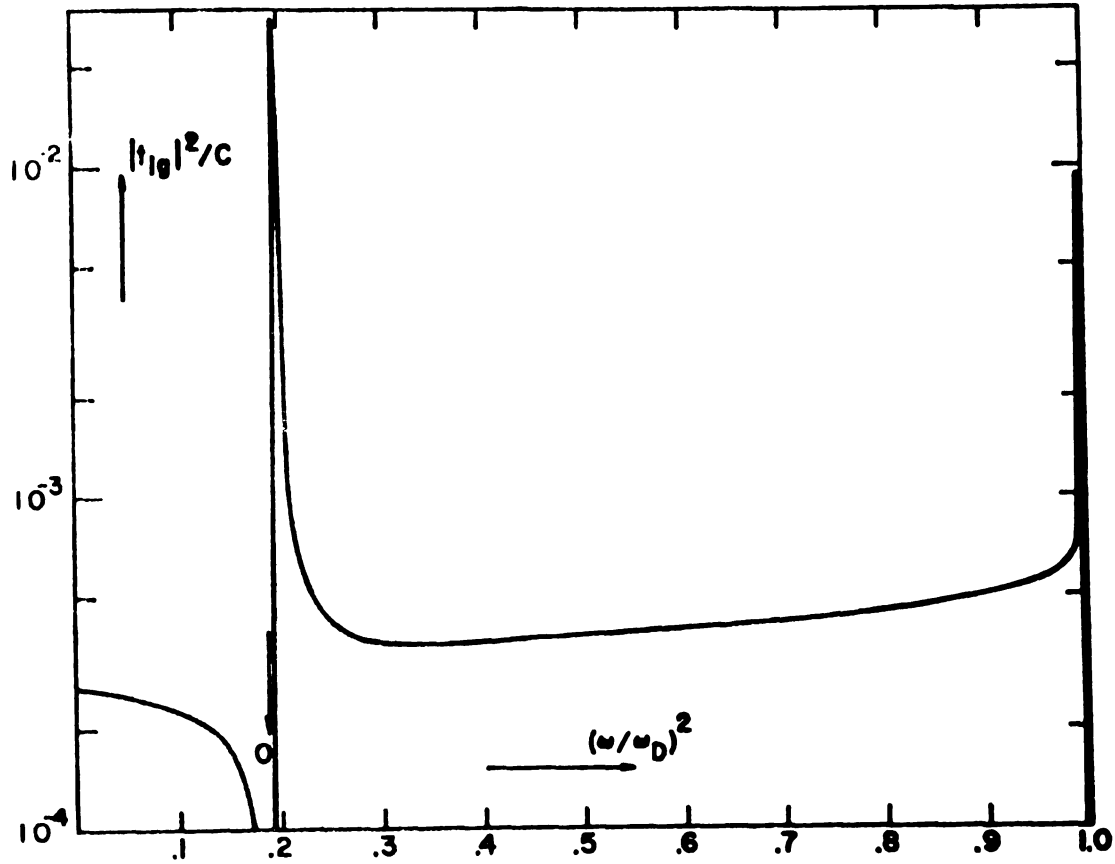


Figure 3. $|t(F_{lg})|^2$, which enters the scattering cross section of the librational mode, as a function of the square modulus of the lattice wave frequency in the Debye approximation, taken from Wagner [25].

From this consideration we see that the interference term can be of the same order as the larger of the two direct terms and its contribution to the scattering cross section is certainly not negligible.

Ellipsoidal Molecules

We now replace in our model the rigid sphere by a rigid ellipsoid of which two moments of inertia are equal but different from that with respect to the body ζ -axis. As we shall be mostly interested in the dynamical behavior of the librational modes in this case of an ellipsoidal defect molecule, we assume the coupling to the lattice to be the same as in the spherical case. Introducing this particular defect into the host lattice results in a lower symmetry at the defect site depending upon the orientation of the molecule with respect to the crystallographic axes. We shall consider the following three situations. The defect molecule is oriented along one of the axes of the cube. In this case the symmetry of the dynamical problem is D_{4h} . If the molecular defect is oriented along a body diagonal then we are dealing with the symmetry group D_{3d} . The appropriate symmetry group for the molecule with its ζ -axis parallel to one of the face diagonals is D_{2h} .

We are primarily interested to see if there are associated with the librational motion any new scattering mechanism (different initial and final states) introduced by the non-spherical defect molecule which is conveniently done by looking at the elements of the scattering matrix.

First we consider the situation where the ellipsoid is oriented

along a main axis. The necessary information to construct the corresponding $T(\nu)$ matrices is contained in Tables II and X. The matrix elements different from zero are:

$$\begin{aligned} \langle (0k'0) \ 1 | T(A_{2g}) | (0k0) \ 1 \rangle &= - \langle (0k'0) \ 1 | T(A_{2g}) | (k00) \ 2 \rangle \\ &= \frac{1}{3} \sin(\hat{k}_y a) \sin ka \end{aligned} \quad (102a)$$

$$\begin{aligned} \langle (k'00) \ 2 | T(A_{2g}) | (0k0) \ 1 \rangle &= - \langle (k'00) \ 2 | T(A_{2g}) | (k00) \ 2 \rangle \\ &= - \frac{1}{3} \sin(\hat{k}_x a) \sin ka \end{aligned} \quad (102b)$$

$$\begin{aligned} \langle (00k') \ 1 | T(E_g^1) | (00k) \ 1 \rangle &= - \langle (00k') \ 1 | T(E_g^1) | (k00) \ 3 \rangle \\ &= \frac{1}{3} \sin(\hat{k}_z a) \sin ka \end{aligned} \quad (103a)$$

$$\begin{aligned} \langle (k'00) \ 3 | T(E_g^1) | (00k) \ 1 \rangle &= - \langle (k'00) \ 3 | T(E_g^1) | (k00) \ 3 \rangle \\ &= - \frac{1}{3} \sin(\hat{k}_x a) \sin ka \end{aligned} \quad (103b)$$

$$\begin{aligned} \langle (00k') \ 2 | T(E_g^2) | (00k) \ 2 \rangle &= - \langle (00k') \ 2 | T(E_g^2) | (0k0) \ 3 \rangle \\ &= \frac{1}{3} \sin(\hat{k}_z a) \sin ka \end{aligned} \quad (104a)$$

$$\begin{aligned} \langle (0k'0) \ 3 | T(E_g^2) | (00k) \ 2 \rangle &= - \langle (0k'0) \ 3 | T(E_g^2) | (0k0) \ 3 \rangle \\ &= - \frac{1}{3} \sin(\hat{k}_y a) \sin ka \end{aligned} \quad (104b)$$

We notice that, except for the different nomenclature and the fact that the mode transforming according to the irreducible representation A_{2g} is associated with the different moment of inertia, the matrix elements are exactly the same as in the spherical case (Eqs. (82), (83) and (84)). However, the non-degenerate mode interacts with phonons whose direction of incidence is perpendicular to the defect axis only.

For the orientation along the body diagonal we find the stable subspaces listed in Table III and the compatibility conditions are given in Table XI. The following matrix elements are found to be different from zero:

$$\begin{aligned}
 \langle (Ok'k')_1 | T(A_{2g}) | (Ok0)_1 \rangle &= -\langle (Ok'k')_1 | T(A_{2g}) | (00k)_1 \rangle \\
 &= -\langle (Ok'k')_1 | T(A_{2g}) | (k00)_2 \rangle = \langle (Ok'k')_1 | T(A_{2g}) | (00k)_2 \rangle \\
 &= \langle (Ok'k')_1 | T(A_{2g}) | (k00)_3 \rangle = -\langle (Ok'k')_1 | T(A_{2g}) | (Ok0)_3 \rangle \\
 &= \frac{1}{9} [\sin(\underline{k}'_y a) - \sin(\underline{k}'_z a)] \sin ka \quad (104a)
 \end{aligned}$$

$$\begin{aligned}
 \langle (k'Ok')_2 | T(A_{2g}) | (Ok0)_1 \rangle &= -\langle (k'Ok')_2 | T(A_{2g}) | (00k)_1 \rangle \\
 &= -\langle (k'Ok')_2 | T(A_{2g}) | (k00)_2 \rangle = \langle (k'Ok')_2 | T(A_{2g}) | (00k)_2 \rangle \\
 &= \langle (k'Ok')_2 | T(A_{2g}) | (k00)_3 \rangle = -\langle (k'Ok')_2 | T(A_{2g}) | (Ok0)_3 \rangle \\
 &= -\frac{1}{9} [\sin(\underline{k}'_x a) - \sin(\underline{k}'_z a)] \sin ka \quad (104b)
 \end{aligned}$$

$$\begin{aligned}
\langle (k'k'0)_3 | T(A_{2g}) | (0k0)_1 \rangle &= - \langle (k'k'0)_3 | T(A_{2g}) | (00k)_1 \rangle \\
&= - \langle (k'k'0)_3 | T(A_{2g}) | (k00)_2 \rangle = \langle (k'k'0)_3 | T(A_{2g}) | (00k)_2 \rangle \\
&= \langle (k'k'0)_3 | T(A_{2g}) | (k00)_3 \rangle = - \langle (k'k'0)_3 | T(A_{2g}) | (0k0)_3 \rangle \\
&= \frac{1}{9} [\sin(\hat{k}_x a) - \sin(\hat{k}_y a)] \sin ka \quad (104c)
\end{aligned}$$

$$\begin{aligned}
\langle (00k')_1 | T(E_g^1) | (00k)_1 \rangle &= \langle (00k')_1 | T(E_g^1) | (00k)_2 \rangle \\
&= - \langle (00k')_1 | T(E_g^1) | (k00)_3 \rangle = - \langle (00k')_1 | T(E_g^1) | (0k0)_3 \rangle \\
&= \frac{1}{6} \sin(\hat{k}_z a) \sin ka \quad (105a)
\end{aligned}$$

$$\begin{aligned}
\langle (00k')_2 | T(E_g^1) | (00k)_1 \rangle &= \langle (00k')_2 | T(E_g^1) | (00k)_2 \rangle \\
&= - \langle (00k')_2 | T(E_g^1) | (k00)_3 \rangle = - \langle (00k')_2 | T(E_g^1) | (0k0)_3 \rangle \\
&= \frac{1}{6} \sin(\hat{k}_z a) \sin ka \quad (105b)
\end{aligned}$$

$$\begin{aligned}
\langle (k'k'0)_3 | T(E_g^1) | (00k)_1 \rangle &= \langle (k'k'0)_3 | T(E_g^1) | (00k)_2 \rangle \\
&= - \langle (k'k'0)_3 | T(E_g^1) | (k00)_3 \rangle = - \langle (k'k'0)_3 | T(E_g^1) | (0k0)_3 \rangle \\
&= - \frac{1}{6} [\sin(\hat{k}_x a) + \sin(\hat{k}_y a)] \sin ka \quad (105c)
\end{aligned}$$

$$\begin{aligned}
\langle (0k'k')_1 | T(E_g^2) | (0k0)_1 \rangle &= 2 \langle (0k'k')_1 | T(E_g^2) | (00k)_1 \rangle \\
&= - \langle (0k'k')_1 | T(E_g^2) | (k00)_2 \rangle = -2 \langle (0k'k')_1 | T(E_g^2) | (00k)_2 \rangle \\
&= -2 \langle (0k'k')_1 | T(E_g^2) | (k00)_3 \rangle = 2 \langle (0k'k')_1 | T(E_g^2) | (0k0)_3 \rangle \\
&= \frac{1}{9} [\sin(\underline{k}'_z a) + 2 \sin(\underline{k}'_y a)] \sin ka \quad (106a)
\end{aligned}$$

$$\begin{aligned}
\langle (k'0k')_2 | T(E_g^2) | (0k0)_1 \rangle &= 2 \langle (k'0k')_2 | T(E_g^2) | (00k)_1 \rangle \\
&= - \langle (k'0k')_2 | T(E_g^2) | (k00)_2 \rangle = -2 \langle (k'0k')_2 | T(E_g^2) | (00k)_2 \rangle \\
&= -2 \langle (k'0k')_2 | T(E_g^2) | (k00)_3 \rangle = 2 \langle (k'0k')_2 | T(E_g^2) | (0k0)_3 \rangle \\
&= -\frac{1}{9} [\sin(\underline{k}'_z a) + 2 \sin(\underline{k}'_x a)] \sin ka \quad (106b)
\end{aligned}$$

$$\begin{aligned}
\langle (k'k'0)_3 | T(E_g^2) | (0k0)_1 \rangle &= 2 \langle (k'k'0)_3 | T(E_g^2) | (00k)_1 \rangle \\
&= - \langle (k'k'0)_3 | T(E_g^2) | (k00)_2 \rangle = -2 \langle (k'k'0)_3 | T(E_g^2) | (00k)_2 \rangle \\
&= -2 \langle (k'k'0)_3 | T(E_g^2) | (k00)_3 \rangle = 2 \langle (k'k'0)_3 | T(E_g^2) | (0k0)_3 \rangle \\
&= -\frac{1}{9} [\sin(\underline{k}'_x a) - \sin(\underline{k}'_y a)] \sin ka \quad (106c)
\end{aligned}$$

In this case we notice a considerable increase in the number of matrix elements, but basically there is the same feature as for the spherical defect, namely, that only transverse polarized phonons are scattered into transverse polarized final states. It is also not difficult to see (e.g. by looking at the first

and second matrix element in Eq. (104a): $\langle (0k'k') \ 1 | T(A_{2g}) | (0k0) \ 1 \rangle = -\langle (0k'k') \ 1 | T(A_{2g}) | (00k) \ 1 \rangle$ and remembering that matrix elements of the form $\langle \underline{k}' \lambda' | T(A_{2g}) | (k00) \ 1 \rangle$ are zero) that phonons incident parallel to the axis of the defect are not scattered at all if their frequency corresponds to the mode A_{2g} . In the limit when the ellipsoid degenerates into a sphere, of course, the corresponding matrix elements have to become equal. We demonstrate this with the following example. We concentrate on the first matrix elements in Eqs. (104a) and (106a)

$$\langle (0k'k') \ 1 | T(A_{2g}) | (0k0) \ 1 \rangle = \frac{1}{9} [\sin(\underline{k}'\hat{y}a) - \sin(\underline{k}'\hat{z}a)] \sin ka$$

$$\langle (0k'k') \ 1 | T(E_g^2) | (0k0) \ 1 \rangle = \frac{1}{9} [\sin(\underline{k}'\hat{z}a) + 2 \sin(\underline{k}'\hat{y}a)] \sin ka$$

In the limiting case as mentioned above the two modes A_{2g} and E_g^2 become degenerate and the two matrix elements appear in Eq. (62) (scattering cross section) with the same factor. Therefore, we might add them to get the combined contribution

$$\langle (0k'k') \ 1 | T(A_{2g}) + T(E_g^2) | (0k0) \ 1 \rangle = \frac{1}{3} \sin(\underline{k}'\hat{y}a) \sin ka \quad (107)$$

This value corresponds to the first matrix element in Eq. (84a),

$\langle (0k'0) \ 1 | T(F_{1g}^3) | (0k0) \ 1 \rangle$, in agreement with the correlation table given in Table XI according to which the mode F_{1g}^3 splits into A_{2g} and E_g^2 as the symmetry is lowered from O_h to D_{3d} .

For the molecule with its ζ -axis parallel to one of the face diagonals of the cube we find all the necessary information in Tables IV and

XII. The nonvanishing matrix elements are:

$$\begin{aligned}
 \langle (00k')_1 | T(B_{1g}) | (00k)_1 \rangle &= - \langle (00k')_1 | T(B_{1g}) | (00k)_2 \rangle \\
 &= - \langle (00k')_1 | T(B_{1g}) | (k00)_3 \rangle = \langle (00k')_1 | T(B_{1g}) | (0k0)_3 \rangle \\
 &= \frac{1}{6} \sin(\underline{k'_2}a) \sin ka \quad (108a)
 \end{aligned}$$

$$\begin{aligned}
 \langle (00k')_2 | T(B_{1g}) | (00k)_1 \rangle &= - \langle (00k')_2 | T(B_{1g}) | (00k)_2 \rangle \\
 &= - \langle (00k')_2 | T(B_{1g}) | (k00)_3 \rangle = \langle (00k')_2 | T(B_{1g}) | (0k0)_3 \rangle \\
 &= -\frac{1}{6} \sin(\underline{k'_2}a) \sin ka \quad (108b)
 \end{aligned}$$

$$\begin{aligned}
 \langle (k'k'0)_3 | T(B_{1g}) | (00k)_1 \rangle &= - \langle (k'k'0)_3 | T(B_{1g}) | (00k)_2 \rangle \\
 &= - \langle (k'k'0)_3 | T(B_{1g}) | (k00)_3 \rangle = \langle (k'k'0)_3 | T(B_{1g}) | (0k0)_3 \rangle \\
 &= -\frac{1}{6} [\sin(\underline{k'_2}a) - \sin(\underline{k'_1}a)] \sin ka \quad (108c)
 \end{aligned}$$

$$\begin{aligned}
 \langle (00k')_1 | T(B_{2g}) | (00k)_1 \rangle &= \langle (00k')_1 | T(B_{2g}) | (00k)_2 \rangle \\
 &= - \langle (00k')_1 | T(B_{2g}) | (k00)_3 \rangle = - \langle (00k')_1 | T(B_{2g}) | (0k0)_3 \rangle \\
 &= \frac{1}{6} \sin(\underline{k'_2}a) \sin ka \quad (109a)
 \end{aligned}$$

$$\begin{aligned}
\langle (00k')_2 | T(B_{2g}) | (00k)_1 \rangle &= \langle (00k')_2 | T(B_{2g}) | (00k)_2 \rangle \\
&= - \langle (00k')_2 | T(B_{2g}) | (k00)_3 \rangle = - \langle (00k')_2 | T(B_{2g}) | (0k0)_3 \rangle \\
&= \frac{1}{6} \sin(\hat{k}_z a) \sin ka \quad (109b)
\end{aligned}$$

$$\begin{aligned}
\langle (k'k'0)_3 | T(B_{2g}) | (00k)_1 \rangle &= \langle (k'k'0)_3 | T(B_{2g}) | (00k)_2 \rangle \\
&= - \langle (k'k'0)_3 | T(B_{2g}) | (k00)_3 \rangle = - \langle (k'k'0)_3 | T(B_{2g}) | (0k0)_3 \rangle \\
&= - \frac{1}{6} [\sin(\hat{k}_x a) + \sin(\hat{k}_y a)] \sin ka \quad (109c)
\end{aligned}$$

$$\begin{aligned}
\langle (0k'0)_1 | T(B_{3g}) | (0k0)_1 \rangle &= - \langle (0k'0)_1 | T(B_{3g}) | (k00)_2 \rangle \\
&= \frac{1}{3} \sin(\hat{k}_y a) \sin ka \quad (110a)
\end{aligned}$$

$$\begin{aligned}
\langle (k'00)_2 | T(B_{3g}) | (0k0)_1 \rangle &= - \langle (k'00)_2 | T(B_{3g}) | (k00)_2 \rangle \\
&= - \frac{1}{3} \sin(\hat{k}_x a) \sin ka \quad (110b)
\end{aligned}$$

As in the first two cases here the results also show that only transverse polarized phonons are scattered by the librational motion and the acoustic activity is restricted to transverse polarized final states. In our calculations we assumed the ellipsoidal defect to be oriented along the [110]-direction. From the third and fourth matrix element in Eq. (108a),

$$\langle (00k')_1 | T(B_{1g}) | (k00)_3 \rangle = - \langle (00k')_1 | T(B_{1g}) | (0k0)_3 \rangle$$

we see that phonons propagating parallel to the orientation of the molecule are not affected by the librational mode B_{1g} which is associated with the different moment of inertia. In our model where we did not allow for any changes in the force constants the modes B_{2g} and B_{3g} are degenerate.

VI. DISCUSSION

The group theoretical method presented in section II enabled us to determine the stable subspaces which are spanned by eigenvectors corresponding to a certain eigenvalue for given symmetry operations. These stable subspaces are listed for the three basic cubic structures in the case of full cubic symmetry and some of the subgroups of O_h . We then went on to derive in section III compatibility relations for the components of the stable subspaces of some of the subgroups. As first example, these results were used in section IV to analyze the polarizations of the infrared active modes of a linear molecule imbedded in a cubic crystal, and it was shown that in an ideal situation the direction of polarization, with respect to the crystallographic axes, already determines uniquely the orientation of the molecule within the crystal. As a second example we studied in section V the scattering of lattice waves by a stereoscopic defect molecule in a simple cubic crystal in some detail. To do so we started with a survey on a treatment most suitable to deal with this type of defects as presented by Wagner [24, 25]. This Green's function technique enabled us to remove the molecular coordinates and limit the defect space to the same dimension as in the Lifshitz problem. The difference between this problem and the point defect problem is that in this case the effective disturbance contains an additional term which has poles at the molecular frequencies. In the neighborhood of these frequencies the effective disturbance cannot be treated as a perturbation. If one of the molecular frequencies lies inside the ideal band(s) then we may find a resonance in the scattering amplitude of lattice waves. In the next subsection we developed

a scattering formalism in terms of a T matrix and we were able to obtain a formally exact solution of the scattering problem. We then derived an expression for the differential scattering cross section which contained two terms of equal importance. It was pointed out that there exists the possibility that the interference term which had been neglected in the work of Wagner may be of the same order of magnitude as the direct term. From the form of the two terms in the scattering cross section it was realized that the scattering of lattice waves by an impurity is much more complicated than the scattering of plane waves by a static potential in quantum theory. The equation which determines the stationary points can have solutions in several branches of the function $\omega^2(\mathbf{k}\lambda)$ with the consequence that although the incoming wave is in a definite branch of $\omega^2(\mathbf{k}\lambda)$, there can be several scattered waves propagating in different directions with the same frequency but with different group velocities and polarizations. From the expression for the scattering cross section it was also seen that its resonances are given by the resonances in the T matrix. We briefly discussed the conditions for such resonances to occur and found that modes for which the eigenvalues of the dynamical problem contain the poles of the molecular Green's function are likely to satisfy the resonance condition. Assuming that the internal binding in a molecule is much stronger than the binding to the host lattice, one can distinguish three types of motion for the molecular defect: (a) the internal vibrations, (b) the translational vibrations of the molecule as a whole, (c) the rotational vibrations of the whole molecule. As it is not possible to describe motions of type (a) by a general model we restricted our attention to motions of type (b) and (c). We

pointed out that it would not be reasonable to also exclude motions of type (b) especially in view of the possibility that in combination with a librational mode they may give rise to a strong interference term in the scattering cross section. First we considered the simple model of a rigid sphere coupled to a simple cubic lattice with tangential as well as radial springs. The stable subspaces which we determined at the beginning of this study simplified the solution of the eigenvalue problems to a large extent since we were able to define the relevant matrices by their Hermite forms in the defect space. Imposing the condition resulting from the requirement that the potential energy be invariant against infinitesimal rigid body rotations of the crystal has the consequence that modes transforming according to the irreducible representations F_{2g} and F_{2u} have to be excluded as possible eigenstates, since they would lead to a local instability of the lattice. Two reasons are given suggesting that we can relax this condition in a more realistic situation. Then the matrix elements in the expression for the differential cross section were calculated and from their particular form we could draw the following conclusions:

1. Modes A_{1g} and E_g interact with longitudinally polarized phonons only and are acoustically active.
 2. Modes F_{1g} and F_{2g} scatter transverse polarized waves only and their acoustical activity is restricted to transverse polarized final states.
 3. The mode F_{1u} scatters any incident phonon regardless of the polarization but does not change the polarization.
 4. The mode F_{2u} scatters transverse polarized phonons only, without changing their polarization.
- We then studied the conditions under which we expect that one or the other of the modes lies within the ideal band and

focused our attention on the situation of a mass defect motion of the symmetry F_{1u} and the librational motion of a spherical molecule (symmetry F_{1g}). In particular we considered the contribution to the scattering cross section. In both instances we found a Rayleigh scattering term ($\sim k^4$) modified in the first case by a term depending upon the solution of the secular determinant and in the latter case by the square modulus of the eigenvalue of the T matrix corresponding to the mode F_{1g} . We used the results obtained by Thoma and Ludwig [37] and Wagner [25] to get a reasonable estimate about the magnitude of the interference term for the case where the resonances due to the mode F_{1u} and F_{1g} occur at about the same frequency. We demonstrated that under this circumstances the interference term is of the same order as the larger of the two direct terms. In the next subsection we replaced the rigid sphere by a rigid ellipsoid with two equal moments of inertia, but different from the third one. We restricted our attention to the librational modes only and also assumed the coupling to the lattice to be the same as for the spherical molecule. Depending upon the orientation of the ellipsoid the symmetry at the defect site is reduced either to D_{4h} (orientation along one of the principal axes of the cube), D_{3d} (orientation along one of the body diagonals) or D_{2h} (orientation parallel to one of the face diagonals). With aid of the appropriate stable subspaces and compatibility conditions we constructed the relevant matrix elements. In all three cases we found basically the same matrix elements as for the spherical defect molecule with the properties that only transverse polarized lattice waves are scattered and the acoustical activity is restricted to transverse polarized final states. It was noted that the mode corresponding

to the different moment of inertia did not interact with phonons propagating parallel to the orientation of the defect molecule.

We start the discussion of more realistic situations with the question, what happens if we let $M' = M$, $k = \alpha$ and $f = \beta$, which, in case of a point defect, corresponds to an ideal crystal. Therefore all the eigenvalues of the defect dynamical problem have to vanish since the translational symmetry of the lattice is no longer destroyed by a defect site and acceptable solutions must have the proper point symmetry as well as translational symmetry. We note (Eqs. (76) and (77)) that all the eigenvalues except those associated with the mode transforming according to the irreducible representation F_{1g} fulfill this requirement. The reason for this deviation is the following. The mode F_{1g} corresponds to the librational motion of the defect molecule, which is a consequence of the additional degrees of freedom. The extended Green's function technique, although it allowed us to exclude the molecular coordinates from our calculations, yet the additional degrees of freedom must remain even when we change the parameters back to the ideal situation. We are thus dealing with a totally different situation in the case of the "molecular defect" and we must then exclude the mode F_{1g} explicitly (Eqs. (76 c) and (77 c)).

Our expression for the scattering cross section (Eq. (62)) was based on an acoustic approximation (we allowed, however, the propagation velocity to be different in each branch). The correct form would have contained second derivatives of the surfaces of constant square modulus of the frequency in \mathbf{k} -space, which we subsequently would have replaced by $2c^2(\lambda)$ anyway in order to use the results of Thoma and Ludwig [37] and Wagner [25]. There are certainly limitations in the assumption of a Debye spectrum

especially when Green's functions are involved. Calculating the Green's functions at any given frequency we get contributions from the entire range of the spectrum and the unrealistic singularity at the cutoff may reflect itself in an unfavorable manner. However, the form of the matrix elements is dependent on the symmetry of the defect problem alone, and a more realistic spectrum would affect the eigenvalues of the T matrix only. This means that we would get exactly the same initial and final states but the resonances might be shifted and their magnitudes altered.

Studying the librational motion of an elliptical molecule we assumed that the force constants are the same as in the case of a spherical defect. We now drop this assumption and ask if we could now couple to longitudinally polarized lattice waves under this circumstance. The necessary but not sufficient condition is that in the decomposition of the modes A_{1g} , E_g and F_{1g} due to the lower symmetry (correlation table) there must be at least one irreducible representation in common to F_{1g} and A_{1g} or E_g . This is the case for the symmetries D_{3d} (Table XI, E_g) and D_{2h} (Table XII, B_{3g}). As mentioned above this condition is not sufficient and from the compatibility conditions we see that the corresponding stable subspaces are in fact mutually exclusive. There might be reasons to relax these compatibility conditions, for example, if the defect is no longer assumed to be rigid. Then there exists the possibility that the neighboring atoms might follow (energetic favorable) the internal motion of lower symmetry of the defect, and are no longer governed by the over all cubic symmetry of the crystal.

All calculations were performed within the harmonic approximation. If the amplitude of any of the modes becomes too large to justify this approximation all the obtained results become invalid as well.

LIST OF REFERENCES

REFERENCES

- [1] R. F. Wallis, editor, Localized Excitations in Solids (Plenum Press, Inc., New York, 1968) and references given there.
- [2] M. Wagner, Phys. Rev. 131, 1443 (1963).
- [3] G. Kh. Panov et al., Sov. Phys. - JETP 26, 283 (1968).
- [4] J. A. A. Ketelaar et al., J. Chem. Phys. 24, 624 (1956).
- [5] J. A. A. Ketelaar et al., Spectrochim. Acta 13, 336 (1959).
- [6] J. A. A. Ketelaar and C. J. H. Schutte, Spectrochim. Acta 17, 1240 (1961).
- [7] J. I. Bryant and G. C. Turrell, J. Chem. Phys. 37, 1069 (1962).
- [8] A. Cabana et al., J. Chem. Phys. 39, 2942 (1963).
- [9] E. B. Wilson, Jr., J. C. Decius, and P. C. Cross, Molecular Vibrations (McGraw-Hill Book Company, Inc., New York, 1955).
- [10] H. Eyring, J. Walter, and G. E. Kimball, Quantum Chemistry (John Wiley and Sons, Inc., New York, 1944).
- [11] L. Jansen and M. Boon, Theory of Finite Groups, Applications in Physics (North-Holland Publishing Company, Amsterdam, 1967).
- [12] E. Wigner, Gruppentheorie und ihre Anwendung auf die Quantenmechanik der Atomspektren (Friedr. Vieweg and Sohn Akt.-Ges., Braunschweig, 1931) pp. 226.
- [13] W. Ludwig, Ergeb. Exakt. Naturw. 35, 1 (1963).
- [14] K. Dettmann and W. Ludwig, Phys. Kondens. Materie 2, 241 (1964).
- [15] H. Jones, The Theory of Brillouin Zones and Electronic States in Crystals (North-Holland Publishing Company, Amsterdam, 1960) pp. 108.
- [16] G. Herzberg, Infrared and Raman Spectra of Polyatomic Molecules (D. Van Nostrand Company, Inc., New York, 1945).

- [17] I. M. Lifshitz, *Nuovo Cimento* 3, Suppl., 716 (1956) and references to earlier work given there.
- [18] E. W. Montroll and R. B. Potts, *Phys. Rev.* 100, 525 (1955).
- [19] E. W. Montroll and R. B. Potts, *Phys. Rev.* 102, 72 (1956).
- [20] E. W. Montroll et al., Proceedings of the Many-Body Conference (Interscience Publishers Inc., New York 1958).
- [21] A. A. Maradudin et al., *Revs. Modern Phys.* 30, 175 (1958).
- [22] J. A. Krumhansl, *J. Appl. Phys.* 33, Suppl., 307 (1962).
- [23] A. A. Maradudin et al., Theory of Lattice Dynamics in the Harmonic Approximation (Academic Press, New York 1963).
- [24] M. Wagner, *Phys. Rev.* 131, 2520 (1963).
- [25] M. Wagner, *Phys. Rev.* 133, A750 (1963).
- [26] I. M. Lifshitz, *Zh. Eksperim. i Teor. Fiz.* 18, 293 (1948).
- [27] M. V. Klein, *Phys. Rev.* 131, 1500 (1963).
- [28] M. V. Klein, *Phys. Rev.* 141, 716 (1966).
- [29] S. Takeno, *Prog. Theor. Phys., Japan*, 29, 191 (1963).
- [30] J. A. Krumhansl, Proc. Int. Conf. on Lattice Dynamics, Copenhagen 1963 (Ed. R. F. Wallis, Pergamon Press, New York 1965) p. 523.
- [31] J. Callaway, *J. Math. Phys.* 5, 783 (1964).
- [32] A. A. Maradudin. *Rept. Progr. Phys.* 28, 331 (1965); this is a review article with more complete references.
- [33] P. G. Dawber and R. J. Elliott, *Proc. Roy. Soc. A*, 273, 222 (1963)
- [34] N. B. Colthup, *J. Opt. Soc. Am.* 40, 397 (1950).
- [35] P. T. Manoharan and H. B. Gray, *Inorg. Chem.* 5, 823 (1966).

- [36] A. A. Maradudin, Phonons and Phonon Interactions (Ed. T. A. Bak, Benjamin, New York 1964) p. 424.
- [37] K. Thoma and W. Ludwig, *Phys. Stat. Solidi*, 8, 487 (1965).
- [38] A. A. Maradudin, Astrophysics and the Many-Body Problem (Benjamin, New York, 1963) p. 109.
- [39] B. Lengeler and W. Ludwig, *Z. Physik.* 171, 273 (1963).
- [40] G. Leibfried, Gittertheorie der mechanischen und thermischen Eigenschaften der Kristalle. Handbuch der Physik, Bd. VII/1 (Springer, Berlin-Göttingen - Heidelberg 1955) p. 104.

MICHIGAN STATE UNIV. LIBRARIES



31293010096273